Safety Benefit Evaluation of a Forward Collision Warning System: Final Report

REPORT DOCUMENTATION PAGE

Form Approved
OMB No. 0704-0188

1. AGENCY USE ONLY (Leave blank)	2. REPORT DATE February 2008	3. REPORT TYPE AND DATES COVERED Final Report September 2006 – February 2008

4. TITLE AND SUBTITLE
Safety Benefit Evaluation of a Forward Collision Warning System

5. FUNDING NUMBERS
DTNH22-05-D-01019

6. AUTHOR(S)
Gregory M. Fitch, Hesham A. Rakha, Mazen Arafeh, Myra Blanco, Santosh K. Gupta, Richard P. Zimmermann, and Richard J. Hanowski.

7. PERFORMING ORGANIZATION NAME(S) AND ADDRESS(ES)
Center for Truck and Bus Safety
Virginia Tech Transportation Institute
3500 Transportation Research Plaza (0536)
Blacksburg, VA 24061

8. PERFORMING ORGANIZATION REPORT NUMBER

9. SPONSORING/MONITORING AGENCY NAME(S) AND ADDRESS(ES)
U.S. Department of Transportation
National Highway Traffic Safety Administration
1200 New Jersey Avenue SE.
Washington, DC 20590

10. SPONSORING/MONITORING AGENCY REPORT NUMBER
DOT HS 810 910

11. SUPPLEMENTARY NOTES

12a. DISTRIBUTION/AVAILABILITY STATEMENT
This document is available to the public through the National Technical Information Service, Springfield, Virginia 22161.

12b. DISTRIBUTION CODE

13. ABSTRACT (Maximum 200 words)
This report presents the work completed for the research study Safety Benefit Evaluation of a Forward Collision Warning System (FCW) under Contract DTNH22-05-D-01019, Task Order # 13. The purpose of this study was to estimate the safety benefits that may be obtained by deploying an FCW system in heavy vehicles. The approach involved simulating driver collision avoidance behavior, with and without FCW alarms, in response to rear-end (RE) conflicts recorded in a previous naturalistic driving study. The naturalistic driving dataset used was produced by a heavy-vehicle field operational test (FOT) that was conducted by the Virginia Tech Transportation Institute (VTTI). RE conflicts were identified using methods that were based on Volvo's Intelligent Vehicle Initiative Field Operation Test (Volvo, 2005), which observed heavy vehicles operating with an FCW system for one year. The algorithms used by the Eaton VORAD (Vehicle On-Board Radar) FCW system were applied to the identified RE conflict data. The auditory alarm severity and timing of the FCW alarms (that would have occurred had an FCW system been installed) were computed. Drivers' actual alarm perception-response times and braking-levels that were measured during the Volvo (2005) FOT were then used to simulate driver response behavior to the theoretical FCW alarms using a Monte Carlo approach. An assumption was made that drivers made the best decision when receiving FCW alarms, allowing them to apply the brakes sooner and possibly avoid a crash. Enhancing the approach used in Battelle (2006), the number of conflicts avoided, as well as the additional response time available prior to encountering a crash, were both used to compute a prevention ration (PR) and exposure ratio (ER). The PR and ER were then combined to compute an overall crash reduction estimate. This simulation determined that a nationwide deployment of FCW systems in heavy vehicles could reduce the number of RE crashes by 21 percent ($p < 0.001$).

14. SUBJECT TERMS
alarm, alert, collision avoidance, collision warning system, forward collision warning, RE conflict, VORAD.

15. NUMBER OF PAGES
113

16. PRICE CODE

17. SECURITY CLASSIFICATION OF REPORT Unclassified	18. SECURITY CLASSIFICATION OF THIS PAGE Unclassified	19. SECURITY CLASSIFICATION OF ABSTRACT Unclassified	20. LIMITATION OF ABSTRACT

i

EXECUTIVE SUMMARY

This report presents the work completed for the research study titled *Safety Benefit Evaluation of a Forward Collision Warning System* under Contract DTNH22-05-D-01019, Task Order 13. The objective of this study was to estimate the safety benefits that may be obtained by deploying a forward collision warning (FCW) system for heavy vehicles.

FCW systems are designed to alert drivers to an impending rear-end (RE) crash. This is accomplished by using radar to track the position of vehicles in the forward pathway (termed leading vehicles, LVs) and algorithms to assess their crash threat. Drivers can be warned of threatening objects by visual, auditory, and tactile (touch) alarms. It is expected that this timely feedback will allow drivers to respond to the crash threat sooner, thus reducing their impact speed, or allow them to avoid the crash altogether.

The Intelligent Vehicle Initiative (IVI) program, sponsored by the U.S. Department of Transportation, assessed the performance of a commercially available FCW system (Volvo, 2005). This investigation consisted of performing a field operational test (FOT) on 100 tractors, 50 of which had an Eaton VORAD (vehicle on-board radar) FCW system as well as other safety features including adaptive cruise control and an electronically controlled braking system. This FCW system provided 10 grades of alarms, which were presented both visually and aurally, as an aid to the driver. Data acquisition systems (DAS) recorded driving behavior for three years. An independent evaluation performed by Battelle (2006) found that, on average, drivers using the FCW system adopted following distances 4.6 m (15 ft) longer than drivers without FCW systems. By calculating the overall safety benefits, the study also determined that the FCW system was the main contributor in reducing RE crash likelihood by 21 percent.

Around the same time, the U.S. DOT sponsored an FOT of a drowsy-driver warning system (DDWS) conducted by the Virginia Tech Transportation Institute (VTTI). Naturalistic driving data was collected between May 2004 and September 2005 from 103 volunteer commercial driver participants (Hanowski et al., in press). A database consisting of approximately 46,000 hours of driving data spanning 3.7 million km (2.3 million mi) (equivalent to almost 96 trips around the world or 770 coast-to-coast trips across the United States) was produced. Additionally, all trucks collected kinematic driving data using the Eaton VORAD radar. Since both video and parametric driving data were continuously collected, the DDWS dataset offers a repository that can be mined to investigate other driving phenomena.

Since components of the same FCW system were used in both the Volvo and DDWS FOTs, this project was initiated with the purpose of calculating potential safety benefits using the DDWS data by following the methodology the Battelle study performed on the Volvo FOT data. Figure ES-1 provides an overview of the steps performed in this study. The rectangles represent processes, while the parallelograms represent data output. The diamonds are decision points. The arrows denote the flow of data from one task to the next. A description of the major steps taken is presented below it.
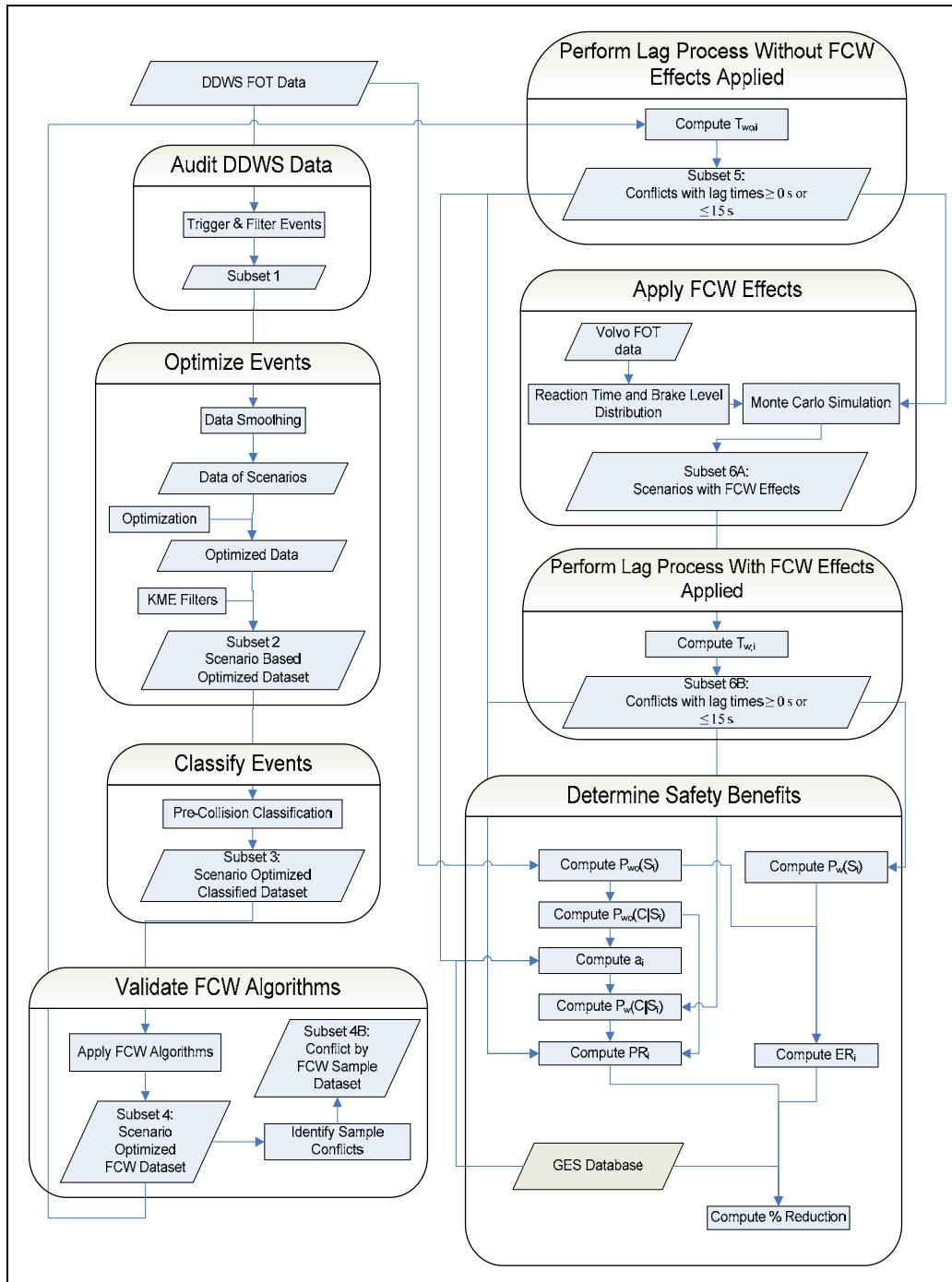
Figure ES-1. Data Flow for Safety Benefits Analysis

RE events involving a following vehicle (FV) rapidly approaching an LV were parametrically identified using a modification of the logic formulated in Volvo (2005) (see Table ES-5 for a list of the modifications). This involved first triggering potential RE events when: (1) an FV decelerated more than 0.25 *g* in 1.5 s behind an LV (Kinematic Motion Event [KME] trigger), (2) an FV had a time-to-collision (TTC) to an LV less than 4 s, and (3) an FV's following interval (FI) to an LV was less than 0.5 s (see Chapter 3 for an explanation of these trigger conditions). Non-

threatening RE events identified through this process were removed using parametric filters. A total of 76,546 RE events remained and comprised Subset 1.

Since video data was available, a sample of 60 RE events from Subset 1 were visually inspected to validate the performance of the filter logic. Approximately 67 percent of the sampled RE events were found to be invalid. Examples of invalid events include events generated by benign targets such as bridges, as well as LVs located outside of the FV's lane. Additional filtration was thus performed on the RE events in Subset 1. Table ES-5 at the end of this executive summary lists the criteria added to the filter logic.

The remaining RE events were optimized to generate idealized conflict parameters. Hypothetical RE crashes (termed *conflicts*) were identified by applying KME filters (not to be confused with the KME trigger previously discussed) to these RE events (see Chapter 3 for an explanation). Here, conflicts were said to exist when an FV decelerated more than 3 m/s^2 (10 ft/s^2) to avoid an LV traveling in the same lane. Conflict identification was made under the assumption that drivers did not input a manual response after the onset of braking. A total of 7,155 conflicts were identified and comprised Subset 2.

These conflicts were then classified into one of five pre-collision conflict types developed in Volvo (2005) and consolidated into three conflict categories specified in Battelle (2006). Conflicts that did not meet these classification schemes were discarded. The 6,456 conflicts that remained formulated Subset 3.

The Eaton VORAD FCW algorithms were then applied to the conflicts in Subset 3. The timing and severity of the FCW alarms were determined. Conflicts in which an alarm was not generated were discarded. The remaining 6,274 conflicts comprised Subset 4. The timing and severity of the FCW system alarms pertaining to a sample of conflicts (Subset 4B) were then validated by applying code generated in Volvo (2005). Each conflict in Subset 4B passed this evaluation.

A component of the safety benefit evaluation consists of judging how much additional time a driver would have had to brake to avoid a crash had an FCW alarm been evoked. This additional time is referred to as the lag time. Since conflicts with lag times of less than 0 s or greater than 15 s were to be discarded, the lag process was performed both prior to simulating the driver responses to the hypothetical FCW alarms (to reduce computational complexity), and then again on the remaining conflicts that had the simulated driver response behavior applied. The conflicts that remained after the lag process was performed on the conflicts that did not have the FCW system effects applied comprised Subset 5. Subset 5 had a total of 1,030 conflicts.

Driver behavior in response to the FCW alarms was then simulated using a Monte Carlo approach. The point in time at which a driver started to brake, as well as the level of deceleration, in response to the alarms generated during a conflict was simulated. The driver perception-response time (PRT) and braking-level distributions used in this simulation were modeled from actual driver behavior data collected during the Volvo (2005) FOT. The simulation modeled the drivers' course of action by selecting their optimum decisions (safest response) to the various alarm levels. The conflicts with the FCW effects applied comprised Subset 6A. The lag process was then applied to Subset 6A, leaving 1,026 conflicts in Subset 6B after those conflicts with lag

times of less than 0 s or greater than 15 s were removed. A visual inspection of 160 conflicts from Subset 6A found that 2 percent of the conflicts were invalid (all invalid events consisted of an LV traveling outside of the FV's lane. This occurred when the road geometry had a slight curvature).

The safety benefits afforded by an FCW system were assessed through three research questions. The methods used to answer each question were based on the methods presented in Battelle (2006) (see Table ES-5 for a list of the modifications). The first research question assessed the degree to which an FCW system prevents heavy-vehicle drivers from encountering RE conflict scenarios. This question was addressed by computing the exposure ratio (ER), which compares the number of RE conflict scenarios encountered with an FCW system to the number of RE conflict scenarios encountered without an FCW system. This study did not find a meaningful reduction in the number of RE conflicts scenarios avoided (i.e., the ERs were approximately equal to one). This result opposed the ERs found in Battelle (2006), in which an ER low of 0.48 for RE conflict scenarios involving the FV traveling at a constant speed was found (Table ES-1). This Battelle (2006) finding suggests that an FCW system could be expected to reduce the number of constant-speed RE conflict scenarios encountered. It should be noted that the high ERs found in the current study are not striking because the vehicles in the DDWS FOT did not have an FCW system to warn drivers they were entering dangerous conditions.

Table ES-1. ER Estimates by Conflict Category

Category	ER$_{\text{Current Study}}$	ER$_{\text{Battelle (2006)}}$
Constant Speed	1.00	0.48*
Decelerating	0.97*	1.10
Lane Change	1.00	0.85

* Indicates statistical significance with 95% confidence.

The second research question assessed the degree to which an FCW system prevents crashes once heavy vehicles have entered RE conflict scenarios. This question was addressed by computing the prevention ratio (PR). The PR compares the mean lag time with an FCW system to the mean lag time without an FCW system. It was found that the PRs showed a meaningful improvement in crash avoidance once drivers entered RE conflict scenarios. This result opposed that found in Battelle (2006), where the PRs were not meaningfully different from 1 (Table ES-2). It should be noted that none of Battelle's PR estimates were statistically significant, whereas all three PR estimates derived in the current study were statistically significant.

Table ES-2. PR Estimates by Conflict Category

Category	PR$_{\text{Current Study}}$	PR$_{\text{Battelle (2006)}}$
Constant Speed	0.69*	1.05
Decelerating	0.83*	0.90
Lane Change	0.74*	0.82

* Indicates statistical significance with 95% confidence.

The third research question assessed how many crashes an FCW system could be expected to prevent given a national deployment across the entire fleet of heavy vehicles. It was addressed by combining the ER and PR estimates into an overall measure, called the crash reduction ratio (CRR) (Table ES-3). It was found that an FCW system was estimated to reduce the number of RE crashes by 21 percent, preventing a total of 4,800 tractor-trailer RE crashes per year (Table ES-4). This result is equivalent to the 21-percent reduction in crashes estimated in Battelle (2006). It should be noted that the safety benefit estimated in the Battelle study was not found to be statistically significant, whereas the safety benefit estimated in the current study was statistically significant.

Table ES-3. CRR Estimates by Conflict Category

Category	$CRR_{Current\ Study}$	$CRR_{Battelle\ (2006)}$
Constant Speed	0.69*	0.51
Decelerating	0.83*	0.99
Lane Change	0.74	0.70

* Indicates statistical significance with 95% confidence.

Table ES-4. Estimate of the Percent Reduction in RE Crashes

Category	$\%R_{Current\ Study}$	$\%R_{Battelle\ (2006)}$
Constant Speed	13%	20%
Decelerating	7%	0%
Lane Change	1%	1%
Total	21%	21%

The implications are as follows: Battelle estimates that a 21-percent safety improvement is attainable by an FCW system that reduces the number of RE conflict scenarios encountered, but does not necessarily help drivers avoid crashes once they enter RE conflict scenarios. In contrast, the current study estimates that the same 21-percent safety improvement is attainable by an FCW system that helps drivers avoid crashes once RE conflict scenarios are encountered. It was not possible to accurately estimate the benefit from helping drivers avoid RE conflict scenarios altogether due to the nature of this study. Since the FCW system effects were simulated using driver behavior observed in RE conflict scenarios and because DDWS FOT drivers did not actually receive FCW alarms, particularly the first five grades of visual alarms offered by the Eaton VORAD FCW system, behavior that may lead to avoiding the RE conflicts altogether was not modeled. Had drivers received such earlier feedback, the number of RE conflicts encountered may have been lower, thus lowering the ER and improving the safety benefit estimate calculated in this study.

Table ES-5. List of Modifications Made to Methods Used in Volvo (2005) and Battelle (2006)

Procedure	Current Study	Volvo (2005) and Battelle (2006)
Trigger RE Events	• Identified trigger time point (and resolved issues pertaining to multiple targets simultaneously tracked) by tracking the target-of-interest across multiple VORAD data streams	• Volvo (2005) used data from first VORAD data stream
Filter RE Events	• Short presence target filter threshold set to 4 s for both stationary and moving targets • Out-of-lane target filter encompassed both stationary and moving vehicles • Combined deceleration level with brake pedal input for driver reaction filter • Lane-change driver reaction filter identified both smooth and aggressive lanes changes	• Short presence target filter threshold set to 1 s for stationary targets and 2 s for moving targets (Volvo (2005), p. 29) • Out-of-lane target filter encompassed only stationary vehicles (Volvo (2005), p. 30) • Deceleration level and brake pedal input considered separately for driver reaction filter (Volvo (2005), p. 30) • Lane-change driver reaction filter identified smooth lane changes (Volvo (2005), Lane Change Algorithm Logic)

Additional Filtration	• Removed RE events in which:
	  o Target was oncoming
	  o LV in the same lane as FV less than 4 s
	  o FV accelerated
	  o FV decelerated before LV appeared
	  o Difference between FV max and min speed < 1.2 m/s.
	  o LV out of lane and no lane change occurred	

Conflict Identification	• KME filter equation used:	• KME filter equation used:

	$$\hat{d}_F = \frac{\hat{V}_{Fo}^2 - \hat{V}_{Lo}^2}{2(\hat{R}(t_{Fb}) - (\hat{V}_{Fo} - \hat{V}_{Lo})t_R)} > d_{F,Threshold}$$	$$\frac{(v_F - v_L)^2}{2(R - (v_F - v_L)t_{R,Threshold})} < a_{F,\,Threshold}$$ (Battelle (2006), page 4-24)
Perform Lag Process	• Combination of numerical and analytical solution. Lag time computed by incrementing t from t_{Fb} onwards in steps of 0.01 s until a real non-negative value was obtained. The t associated with this real non-negative solution was set to be the lag time.	• Determine position of FV and LV. Numerically increase lag time by one frame and simulate LV and FV profiles to determine if a crash occurs. Repeat computations until a crash occurs (Battelle (2006), pp. 4-33)

LIMITATIONS

As with any type of research, several limitations need to be mentioned:

1. Missed RE Conflicts
As part of the DDWS FOT data reduction (unrelated to this particular project), RE conflicts were identified through both parametric and 100-percent visual inspection. Conflicts were categorized as either crashes, near-crashes, or crash-relevant conflicts. A crash was defined as any contact made with an object, either moving or fixed, at any speed in which kinetic energy was measurably transferred or dissipated. A near-crash was defined as any circumstance requiring a rapid, evasive maneuver by the FV or LV to avoid a crash. A crash-relevant conflict was defined as any circumstance that required a crash avoidance response on the part of the FV or LV that was less severe than a rapid evasive maneuver, but greater in severity than a "normal maneuver" to avoid a crash. The DDWS FOT data reduction effort identified 596 RE conflicts (1 RE crash, 26 RE near-crashes, and 569 RE crash-relevant conflicts). Only 7 of the 596 conflicts validated in the DDWS FOT were identified by the current study's conflict identification process (Figure ES-2). Six of these conflicts were identified by KME logic, while one was identified by TTC logic (see Chapter 3 of this report for KME and TTC definitions). All 7 commonly identified conflicts were classified as crash-relevant conflicts in the DDWS FOT visual data reduction. The one valid RE crash and 26 valid RE near-crashes were removed by the filter logic. They were thus not included in the safety benefit evaluation.
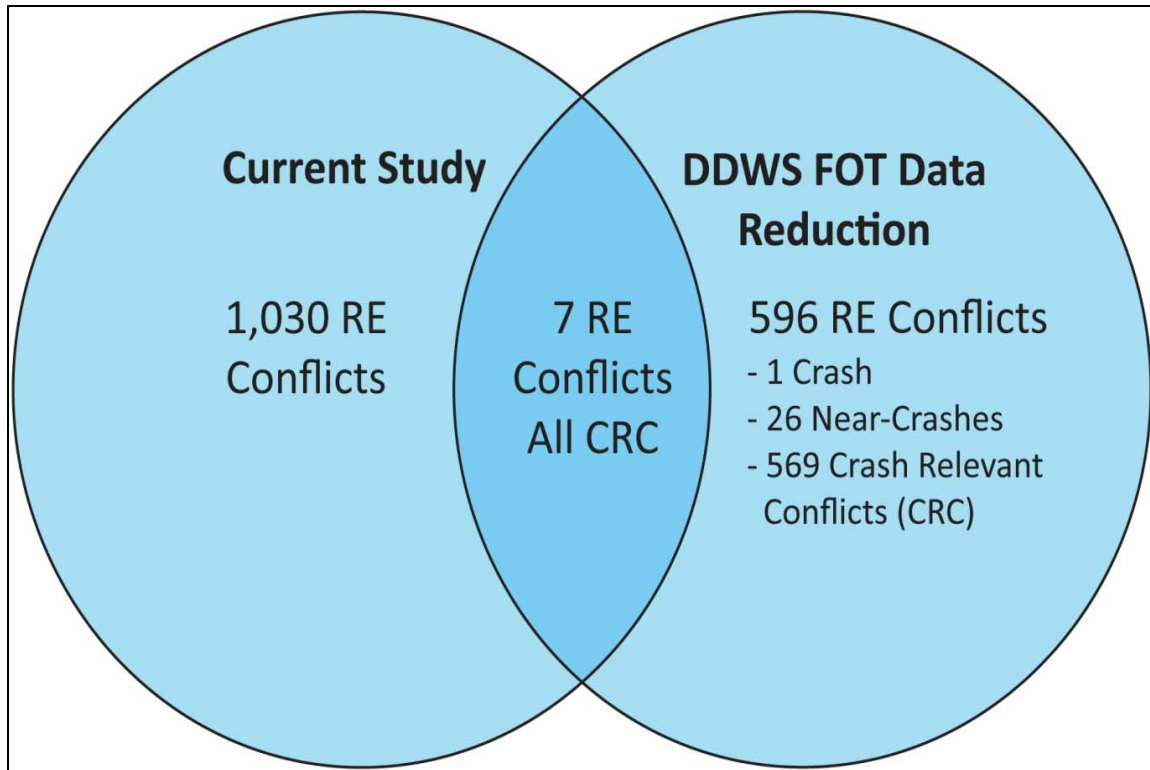
Figure ES-2. Venn Diagram Showing the Number of Conflicts That Coincide Between the Current Study and Those Identified in the DDWS FOT Data Reduction

2. RE Conflicts were Parametrically Identified
A 100-percent visual inspection of each conflict to certify its validity was outside the scope of this study. Visual inspection performed on a sample of conflicts revealed that some non-threatening RE events were not removed through the filtration process. A conflict was considered valid if the LV is located in the FV's lane. Based on the visual sampling, it is estimated that approximately 2 percent of the identified conflicts were not valid.

3. False Alarms
Some concern exists on the impact of false alarms. False alarms, also known as nuisance alarms, are alarms generated when no driver response is required. Drivers' responsiveness to valid FCW alarms may decrease as the number of false alarms increases. This is because drivers may become biased into thinking an FCW alarm is false. The safety benefit estimate does not fully consider the impact of a high false alarm rate on the efficacy of the FCW system. An understanding of how multiple false alarms may bias drivers to ignore credible alerts is needed.

4. FCW System Novelty
The data input to the simulation was based on FOT data collected over the course of three years. The driver behavior observed with the FCW system may not be representative of behavior pertaining to drivers who have adapted to the novelty of the FCW alarms. Novelty effects might be extracted from the data by comparing driver response behavior to the alarms over time. These comparisons may reveal whether the safety benefits observed were owing to a heightened sensitivity to the FCW system during the onset of the study.

ACRONYMS

ACC	Adaptive Cruise Control
CAS	Collision Avoidance System
CDF	Cumulative Density Function
COTR	Contracting Officer's Technical Representative
CRR	Crash Reduction Ratio
DART	Data Analysis and Reduction Tool
DAS	Data Acquisition System
DDWS	Drowsy Driver Warning System
DDWS FOT	Drowsy Driver Warning System Field Operational Test
ECBS	Electronically Controlled Braking System
ER	Exposure Ratio
FCW	Forward Collision Warning
FI	Following Interval
FOT	Field Operational Test
FV	Following Vehicle
GES	General Estimates System
GPS	Global Positioning System
IRB	Institutional Review Board
IVI	Intelligent Vehicle Initiative
KME	Kinematic Motion Event
LV	Lead Vehicle
LVD	Lead-Vehicle Decelerating
LVS/LVCS	Lead-Vehicle Stopped/Constant Speed
NHTSA	National Highway Traffic Safety Administration
PRT	Perception-Response Time
PR	Prevention Ratio
RE	Rear-End
SOW	Statement of Work
SQL	Structured Query Language
SV	Subject Vehicle
TOM	Task Order Manager
TTC	Time-to-Collision
U.S. DOT	United States Department of Transportation
VORAD	Vehicle Onboard RADar
VTTI	Virginia Tech Transportation Institute

TABLE OF CONTENTS

LIST OF FIGURES

LIST OF TABLES

CHAPTER 1. INTRODUCTION

A rear-end conflict occurs when a following vehicle strikes or nearly strikes a vehicle in its forward pathway (termed a leading vehicle, or LV). This study defines RE conflicts to occur when: (1) an FV is required to brake above 0.25 g within 1.5 s to avoid an LV, (2) an FV will strike an LV within 4 s if no driver response is performed, and (3) an FV closely follows an LV with a 0.5 s headway. RE conflicts are the most common type of conflict when two vehicles are involved. A recent analysis of heavy-vehicle – light-vehicle interactions, performed using naturalistic driving data collected while 95 participants drove instrumented commercial heavy vehicles through their daily routes, found that 42 percent of the safety critical events they encountered consisted of RE conflicts (Hickman, Knipling, et al., 2005). It was also found that FVs were predominantly going straight when the RE conflicts developed (observed for 60% of the conflicts), and that the LVs were generally going straight (30%) or decelerating (33%) in the FV's lane prior to the conflict. Hickman et al., 2005, also revealed that the most common reasons for the safety critical events were:

- Inadequate evasive action on the part of the FV driver (14%),
- The FV driver was distracted by an object inside the heavy vehicle cabin (11%),
- The FV driver was distracted by an object outside the heavy vehicle cabin (6%),
- The FV driver misjudged the range to the LV or the LV's speed (6%), and
- The FV was traveling too fast for the road conditions (5%).

Forward Collision Warning systems may mitigate the severity of RE conflicts by alerting drivers to impending RE crashes. By tracking the position of LVs and using algorithms to assess their crash threat, FCW systems stand to warn drivers when their proximity and approach rate to an LV becomes dangerous. It is anticipated that this feedback can cue drivers' attention to the crash threat (particularly when they are distracted) and allow them to brake sooner, reducing their impact speed with the LV or enabling them to avoid the crash altogether.

One technology used to track the position of LVs is the Eaton VORAD system. The Eaton VORAD is a monopulse radar that operates at 24.725 GHz (Eaton VORAD Web site, 2001). It is capable of simultaneously tracking the angular distance of up to 20 targets that lie within its 12-degree beam. Range, speed, and azimuth data can be collected within a 107-meter (350 ft) range. Using Doppler radar, the Eaton VORAD can also determine the absolute speeds of LVs using vehicle speed data from the FV's engine data bus.

The Eaton VORAD FCW system uses vehicular data collected by the VORAD antenna and assesses the crash threat of the tracked targets using the algorithms shown in Table 1. It is worth pointing out that the logic only considers targets as valid if they are tracked in the host vehicle's lane, and if the host vehicle is traveling greater than 10 mph.

Table 1 shows a progression from cautionary to critical alarms as driving conditions become more demanding. With the exception of Alarm Level 2, the first five alarm levels of crash threat are communicated through a visual display, while the last five levels are communicated through an auditory display. This graded alarm feedback assists drivers by clarifying the gap between them and the LVs as well as the relative speed of LVs.

Table 1. FCW Warning Levels. Taken From (Volvo 2005)

Alarm Type	Alarm Level	Alarm Lights Displayed	Unsafe Driving Condition	Audible Tone
None	0	None	None	No
Detect	1	Yellow	LV in our lane, $< \text{Range}_{max}$ from FV vehicle/object	No
Creep	2	Yellow	LV < 4.6 m (15 ft), closing, relative speed < -0.8 km/h (0.5 mph), FV speed < 3.2 km/h (2 mph)	Double Pulse[1]
2 to 3 s	3	Yellow, Orange	LV in same lane, 2 to 3 s following interval, opening/closing, $LV < \text{Range}_{max}$, FV speed > 16 km/h (10 mph)	No
2 s, Opening	4	Yellow, Orange	LV in same lane, 1 to 2 s following interval, LV speed > 101% of FV speed, $LV < \text{Range}_{max}$, FV speed > 16 km/h (10 mph)	No
1 s, Opening	5	Yellow, Orange, Red	LV in same lane, < 1 s following interval, LV speed > 105% of FV speed, $LV < \text{Range}_{max}$, FV speed > 16 km/h (10 mph)	No
2 s, Closing	6	Yellow, Orange, Red	LV in same lane, 1 to 2 s following interval, LV speed < 101% of FV speed, $LV < \text{Range}_{max}$, FV speed > 16 km/h (10 mph)	Single Pulse[1,2,3]
1 s, Closing	7	Yellow, Orange, Red	LV in same lane, < 1 second following interval, LV speed < 105% of FV speed, $LV < \text{Range}_{max}$, FV speed > 16 km/h (10 mph)	Double Pulse[2,3]
Stationary	8	Yellow, Orange, Red	LV < 5.4 km/h (3.4 mph), in same lane, within 3 s and LV range is < 67 m (220 ft) or Range_{max} whichever is smaller, FV speed > 16 km/h (10 mph)	Double Pulse[2,3]
Slow Moving	9	Yellow, Orange, Red	LV in same lane, within 3 s, LV range < 67 m (220 ft) or Range_{max} whichever is smaller, and FV vehicle speed is 25% greater than LV speed, FV speed > 56 km/h (35 mph)	Double Pulse[2,3]
½ s	10	Yellow, Orange, Red	LV in same lane, < 0.5 s following interval, opening/closing, FV speed > 16 km/h (10 mph)	Double Pulse[2,3,4]

Notes:
1. Configurable on or off.
2. Tone disabled in hard turns (< 229 m (750 ft) radius).
3. Tone disabled with brake on.
4. Repeats constantly twice per second.

Audible tones as follows: In steady closing scenarios, tones occur once each, when the LV crosses the threshold into the 2-second and 1-second zones. However, tones reoccur every time the LV transitions from opening to closing if the LV has opened for more than 2 s during a transition cycle. The following intervals can be modified based on the heading knob input.

Tones that are not continuous shall only be sounded when the applicable alarm level is initially entered. Once a tone has been sent, only higher-level alarms shall initiate new tones. The same for lower level tones shall be allowed after 2 s have elapsed since the previous tone was initiated (and the alarm level drops to a lower level than the previous tone).

Volvo's Intelligent Vehicle Initiative program assessed the performance of the Eaton VORAD FCW system (Volvo, 2005). This investigation, which was sponsored by the U.S. Department of Transportation consisted of performing a field operational test on 100 tractors, 50 of which had the Eaton VORAD FCW system as well as other safety features (including adaptive cruise control and an electronically controlled braking system). Data Acquisition Systems recorded driving behavior for three years. An independent evaluation performed by Battelle (2006) found that, on average, drivers using the FCW system adopted following distances 4.6 m (15 ft) longer than drivers without FCW systems, and that the FCW system was the main contributor in reducing RE crash likelihood by 21 percent. However, these results were not found to be statistically significant at a 0.05 level of significance.

The U.S. DOT sponsored an FOT of a drowsy driver warning system conducted by the Virginia Tech Transportation Institute. Naturalistic driving data was collected between May 2004 and September 2005 from 103 volunteer commercial driver participants (Hanowski et al., in press). A database consisting of approximately 46,000 hours of driving data spanning 3.7 million km (2.3 million mi) (equivalent to almost 96 trips around the world or 770 coast-to-coast trips across the United States) was produced. Additionally, all trucks collected range data using the Eaton VORAD antenna. Since both video and parametric driving data were continuously collected, the DDWS dataset offers a repository that can be mined to investigate other driving phenomena.

OBJECTIVES

The objective of the current study is to estimate the safety benefits that may be obtained by deploying an FCW system across the entire national fleet of heavy vehicles. The approach taken involves simulating driver behavior in response to FCW alarms for RE conflicts observed in previously collected naturalistic driving data. The RE conflicts used were identified in the DDWS FOT dataset using an approach similar to the one used to identify conflicts in the Volvo FOT. The Eaton VORAD FCW alarm algorithms were applied to the driving conflicts to determine when an FCW alarm would have been generated. Driver response behavior to the virtual alarms was then generated using a Monte Carlo simulation. The safety benefits were estimated by using the simulated effects of FCW system feedback on driver behavior to answer the following research questions.

RESEARCH QUESTIONS

Research Question 1. How well does an FCW system prevent heavy-vehicle drivers from encountering RE conflict scenarios?

This research question will be answered by comparing the number of RE conflict scenarios encountered given simulated FCW system feedback to the number of RE conflict scenarios encountered in the absence of FCW system feedback.

Research Question 2. How well does an FCW system prevent crashes once heavy vehicles have entered RE conflict scenarios?

The second research question investigates whether FCW alarms can be expected to assist heavy-vehicle drivers avoid RE crashes once they have entered RE conflict scenarios. This research

question will be answered by comparing the probabilities of a crash with the FCW system versus the probabilities without the FCW system, given that an RE conflict occurs. It should be noted that the RE crashes used in this study are simulated using a lag model similar to the one used in Battelle (2006).

Research Question 3. How many crashes can an FCW system be expected to prevent given a national deployment across the entire fleet of heavy vehicles?

The final research question investigates the overall efficacy of the FCW system. This research question will be answered by combining the results from research questions 1 and 2 with the likelihoods associated with various RE conflict types reported in the General Estimates System database.

REPORT OVERVIEW

This document is divided into five chapters: Chapter 1 introduces the concept of an FCW system and states the project objectives, Chapter 2 provides background on how the data in the DDWS FOT database were collected, Chapter 3 presents the project's methods, Chapter 4 shows the study results, and the discussion and concluding remarks are part of Chapter 5. Study limitations and areas of future research are presented as well.

CHAPTER 2. BACKGROUND

The DDWS FOT data collection occurred in a naturalistic driving environment in which data were collected from commercial trucks during normal operations. The participant sample included two different operation types (long-haul and line-haul) and was intended to be representative of the commercial vehicle driver population. Forty-six tractor trailers from three motor carriers were instrumented with data collection equipment developed by VTTI. DAS installed in each tractor continuously collected data whenever the trucks were in motion. The DAS consisted of an encased unit that housed a computer, external hard drive, dynamic sensors, interface with the existing vehicle network, an "incident box," and video cameras. Figure 1 shows an example of the encased unit installed under the passenger seat.

Figure 1. Encased Computer and External Hard Drive Installed Under the Passenger's Seat

Three types of data were collected by the DAS: video, parametric, and audio data. The video and parametric data were continuously recorded, while the audio data were recorded on demand by the driver after encountering an incident. The four video cameras were oriented as follows: (i) forward road scene, (ii) driver's face area, (iii) rearward from the left side of the tractor, and (iv) rearward from the right side of the tractor. Figure 2 is a representation of the area covered by the camera views. Low-level infrared lighting (not visible to the driver) illuminated the vehicle cab to allow the driver's face to be visible at night. No cameras or sensors were mounted on trailers. Therefore, there was no recorded view directly behind the tractor trailer. However, vehicles trailing the instrumented truck could usually be partially seen in the rearward side-view cameras.
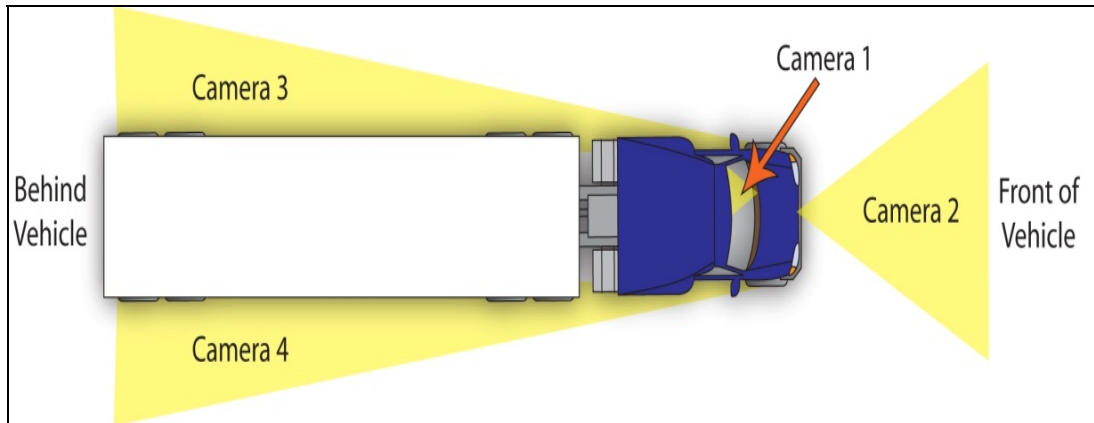
Figure 2. Camera Directions used in DDWS FOT

Figure 3 shows how the recorded images from the four cameras were merged into a single image. A timestamp was also included in the MPG data file but was not displayed on the screen. The video data was recorded at a sampling rate of 30 Hz.
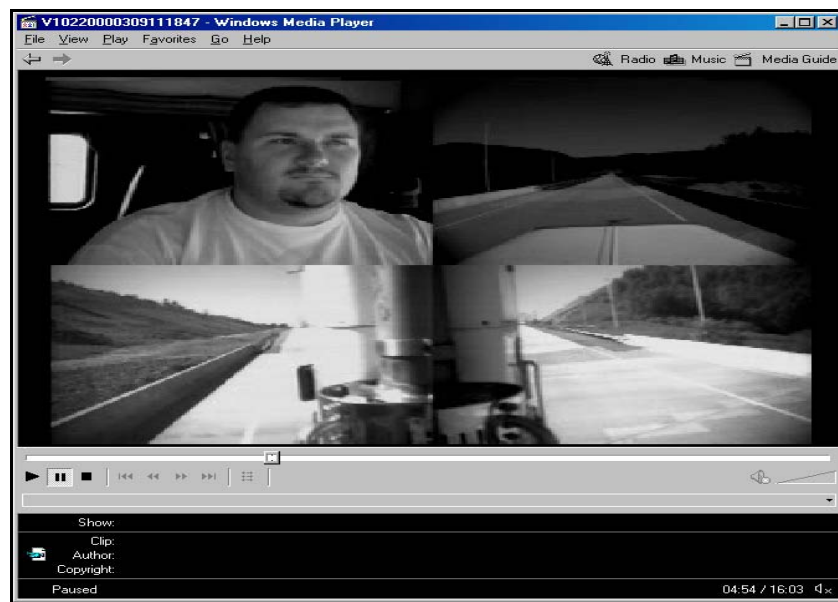
Figure 3. Split-Screen Presentation of the Four Camera Views

Recorded parametric data included basic vehicle motion parameters such as speed, longitudinal acceleration (e.g., indicative of braking levels), and lateral acceleration. Vehicles were also equipped with global positioning system sensors, lane trackers, and forward-looking Eaton VORAD radar units. All parametric data were recorded at a sampling rate of 10 Hz. The audio data were enabled from an "incident box" with a pushbutton and microphone for drivers to make verbal comments about traffic incidents.

The DDWS FOT database consists of approximately 46,000 driving-data hours covering 3.7 million km (2.3 million mi) traveled (equivalent to almost 96 trips around the world or 770 coast-to-coast trips across the United States). There are more than a quarter-million dynamic sensor and

video files in the database (278,900 files total), which are approximately 11.8 TB in size. The data files are stored in binary format and have text headers that contain the data read directly from the instruments on the vehicle. The computations presented in Chapter 3 are only performed when an individual file is opened. To identify RE conflicts, VTTI's DART opens and examines every time point in a data file for the requested criteria to be met. When conditions are met, a unique identifier (trigger ID) is assigned and linked to the file number, start time point, end time point, and trigger type. This is then written to an event database along with information used to control video reduction. No other part of the data file is extracted or stored in the database when this is done. Structured query language is then used to query the data once they are in the database.

CHAPTER 3. METHODS

This chapter details the methods used in this study. Figure 4 illustrates the flow of data through the different steps that were involved in order to appropriately manipulate the data and serves as a reference throughout this document. The rectangles represent processes, while the parallelograms represent data output. The diamonds are decision points. The arrows denote the flow of data from one task to the next.
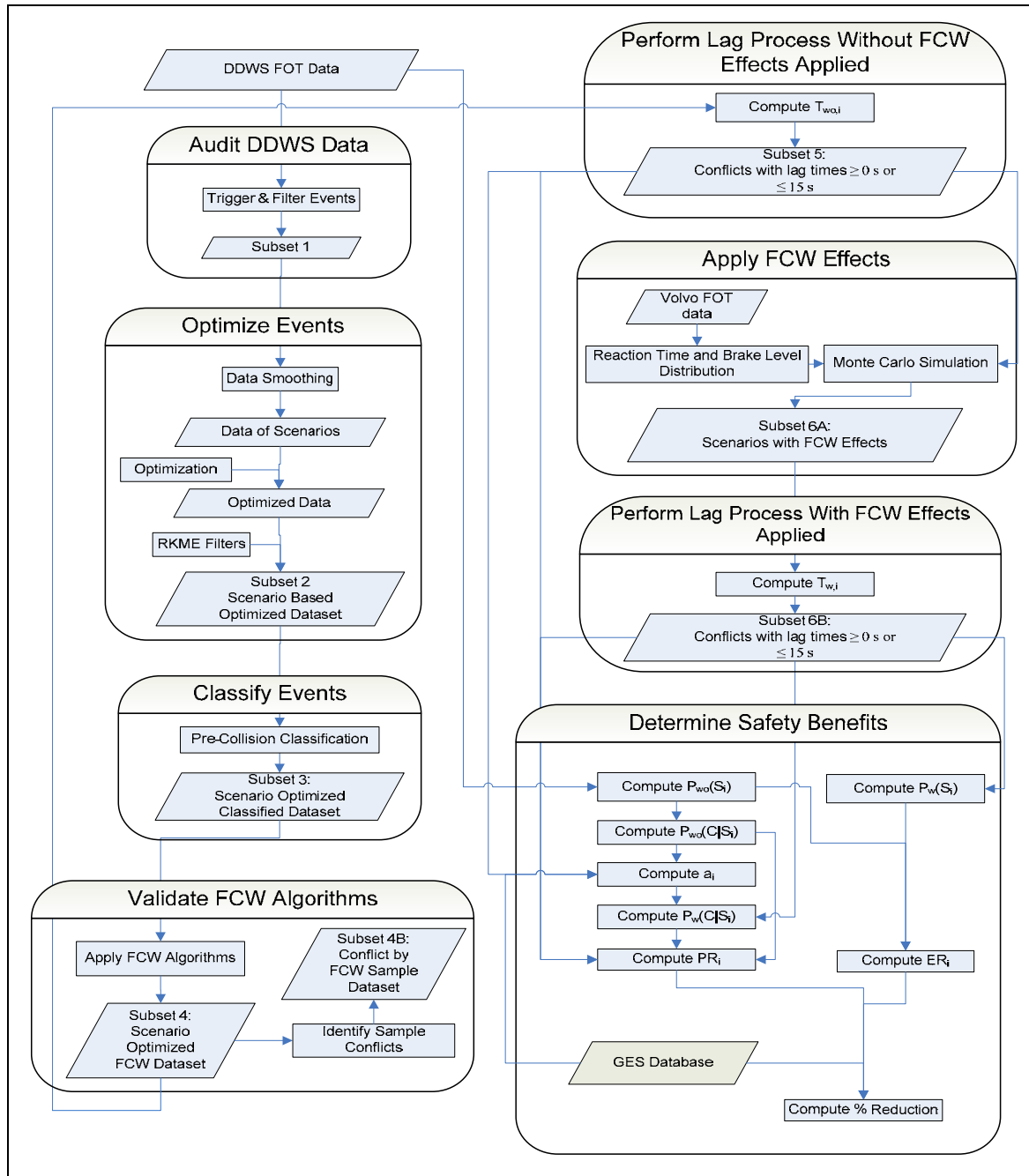
Figure 4. Data Flow for Safety Benefit Analysis

AUDIT DDWS FOT DATA

The scope of this project was limited to studying the RE conflicts the FCW system was designed to identify; specifically, VORAD targets in the same lane as the FV which require collision avoidance action by the FV driver. Conflicts resulting from intersection violations, single-lane road departures, or lane change sideswipes were not considered in this evaluation. Other issues related to FCW systems, such as estimating changes in driver behavior from false alarms, were also out of the project's scope.

One of the first steps taken in this project was to determine whether there was a sufficient amount of RE conflict data to perform a safety benefit evaluation. The DDWS FOT was audited as follows. All potentially valid RE conflicts, termed events, were identified using liberal selection criteria. Events were "triggered" when parametric data thresholds indicative of a conflict were exceeded. These triggered events were then filtered to remove non-threatening events. Since the DDWS FOT dataset includes continuous video footage, a sample of the remaining events was visually inspected to assess the proportion of true RE conflicts. Specifics regarding these tasks are provided below.

Identify Triggered Events

RE events were triggered in the DDWS database using VTTI's DART software to flag the data when specific driving parameters exceeded set thresholds indicative of RE conflicts. The basis of the trigger logic used was developed in Volvo (2005). The following trigger logic was used.

Kinematic Motion Event (KME) Trigger

Definition	Triggers events in which a deceleration greater than 0.25 g is required to avoid a collision with an LV within 1.5 s
Duration	Trigger must persist for seven contiguous time points (0.7 s at 10 Hz sample rate)

The KME trigger identified potentially hazardous driving situations by flagging events in which a large deceleration was required to avoid a collision with an LV in a short amount of time. The following parameters were used in the KME calculation:

- Range (R) and range rate ($\dot{R}$).
- FV and LV velocities (V_F and V_L, respectively)
- FV and LV accelerations[1] (a_F and a_L, respectively)

A KME trigger occurred when a driver had to respond within 1.5 s of the conflict with an action that caused the truck to decelerate at a rate above 0.25 g. Two parallel schemes of the KME

---

[1] LV acceleration was calculated by adding relative acceleration to FV acceleration. Relative acceleration was derived from the VORAD range rate. For each time point, the relative acceleration was calculated using a range rate linear regression that spans between 2 and 17 time points. The selected points began at the current time point, and go out one time point at a time both forward and backwards, summing the number of valid time point values. This process was done until either at least 16 time points were accumulated, or the range of the search reached 16 time points from the original time point.

Trigger Hierarchy

To consistently identify the beginning of an event, when multiple triggers were pointing to the same event, the following hierarchy was applied. KME triggers took precedence, followed by TTC triggers, followed by FI triggers. When an FI trigger was overlapped by a TTC trigger or KME trigger, the FI trigger was deleted. Additionally, when a TTC trigger was overlapped by a KME trigger, the TTC trigger was deleted. For example, the top of Figure 5 shows overlapping KME, TTC, and FI triggers. The bottom of Figure 5 depicts the deletion of the lower priority FI and TTC triggers in grey, and the remaining KME trigger in black.

Furthermore, if a trigger occurred after another trigger in less than 5 s, then the lower priority trigger was deleted. This means that if a KME trigger followed a TTC trigger, then the TTC trigger would be deleted. However, if a trigger followed another trigger of equal importance (e.g., KME followed by a KME), then the second KME trigger would be deleted (Figure 5).

Figure 5. Example of Trigger Hierarchy

Filter Out Non-Threatening Triggered Events

In using liberal selection criteria to identify potential RE events, many triggers pointed to benign events. Benign events included those generated by the FV driving under a bridge, street sign, or by a parked vehicle in an adjacent lane. The next step involved removing these non-threatening events. The following filters were used to remove invalid triggered events: (1) short-presence target, (2) stopped- or oncoming-target-on-curve, (3) out-of-lane target, (4) crossing-lane target, (5) high-lateral-acceleration, (6) target with no driver reaction, and (7) receding target. Each filter is explained below.

Short-Presence Target Filter

Definition	Filters out triggered events that are tracked for a short amount of time by the Eaton VORAD
Criteria	Remove trigger if: A stopped or moving target is present less than 4 s

Volvo (2005) found that triggers were uneventful if the time they were tracked by the Eaton VORAD was short. An example would be when a street sign is picked up by the Eaton VORAD

(Figure 6). Triggered events were considered non-threatening when both stationary and moving (either oncoming or in the same direction) targets were tracked less than 4 s. The filter logic is shown below:

> Upon detecting a triggered event,
> If target presence ≤ 40 time points, then non-threat
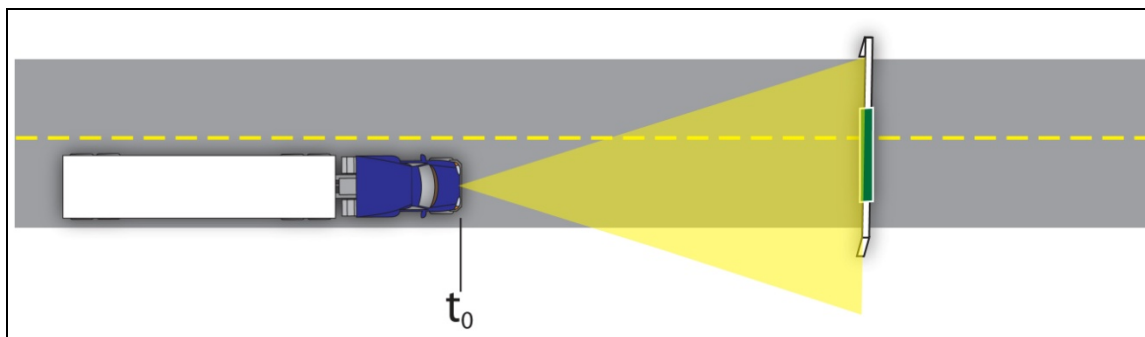
Figure 6. Example of a Short-Presence Target: Eaton VORAD Detecting an Overhanging Street Sign

Stopped- or Oncoming-Target-on-Curve Filter

Definition	Filters out triggered events that are tracked as the FV executes a turn. Removes triggered events that are generated from tracking targets located in the oncoming lane.
Criteria	Stopped or oncoming critical target defined as $V_L < 1.2$ m/s (4 ft/s). (Negative values represent oncoming targets). Curve condition: FV yaw rate > 2 deg/s for > 3 s continuously.

The stopped- or oncoming-target-on-curve filter is designed to remove triggered events that are generated as the FV executes a turn. Figure 7 shows a triggered event generated as the FV approaches a curve as well as when the FV drives through a curve. The rationale behind this filter is that as the FV turns, the Eaton VORAD no longer points down the FV's lane, but rather extends across to oncoming traffic. Targets tracked during such maneuvers can be interpreted by the FCW system as threatening even though they pose no threat, and so must be discarded. Triggered events were filtered out if V_L was less than 1.2 m/s (4 ft/s) and the FV executed a turn (yaw rate > 2 deg/s) for 30 continuous time points starting anywhere from 100 time points before the trigger to 50 time points after the trigger.
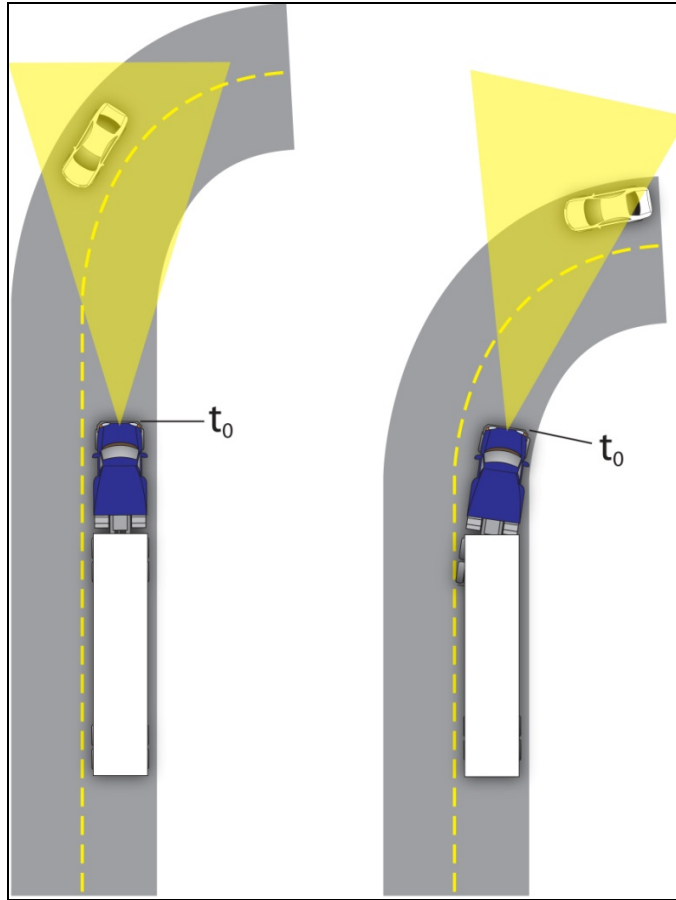
Figure 7. Examples of an Out-of-Lane Target or Oncoming Target on a Curve Being Interpreted as Threatening by the Eaton VORAD

Out-of-Lane Target Filter

Definition	Filters out triggered events that are tracked outside of the FV's lane.
Criteria	Targets are considered out-of-lane when the lateral distance separating them from the projected FV path is greater than 2 ft for all points during critical target presence. Here, the FV width is set at 102 in.

The out-of-lane filter was intended to remove all non-threatening triggered events that arose from the FV passing proximal stationary and moving objects such as parked cars and slower moving vehicles in adjacent lanes (Figure 8). The filter classified a triggered target as out-of-lane if it was more than 2 ft away from the projected FV's path, meaning the right- or left-most edge of the FV. The assumption was that targets greater than 2 ft away from the FV's edge were benign.
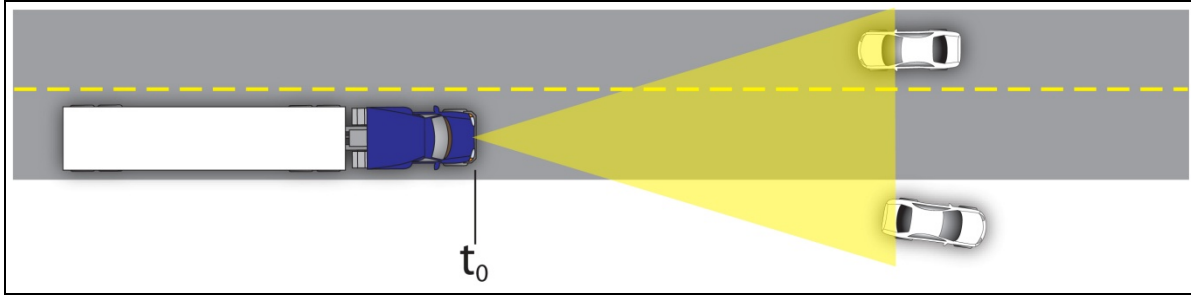
Figure 8. Example of Out-of-Lane Targets: A Parked Vehicle on the Right Shoulder and An Oncoming Vehicle in the Opposite Lane

Crossing-Lane Target Filter

Definition	Filters out triggered events that arose from an object perpendicularly crossing the FV's lane, such as at an intersection.
Criteria	Critical target tracked out of lane for > 0.5 s to one side of the lane at the start of presence, and out of lane for > 0.5 s to other side at the end of presence. Only applies when the target relative speed in the direction of the following vehicle = 0.

The crossing-lane target filter removed triggered events generated from vehicles crossing the FV's lane, such as at an intersection (Figure 9). The filter removed triggered events that were first tracked for more than 0.5 s on one side of the lane and then tracked for 0.5 s out-of-lane on the other side at the end of their presence. Since this filter only removed triggered events when their relative speed was equal to zero, only vehicles traveling exactly at 90 deg to the following vehicle's projected path were removed.
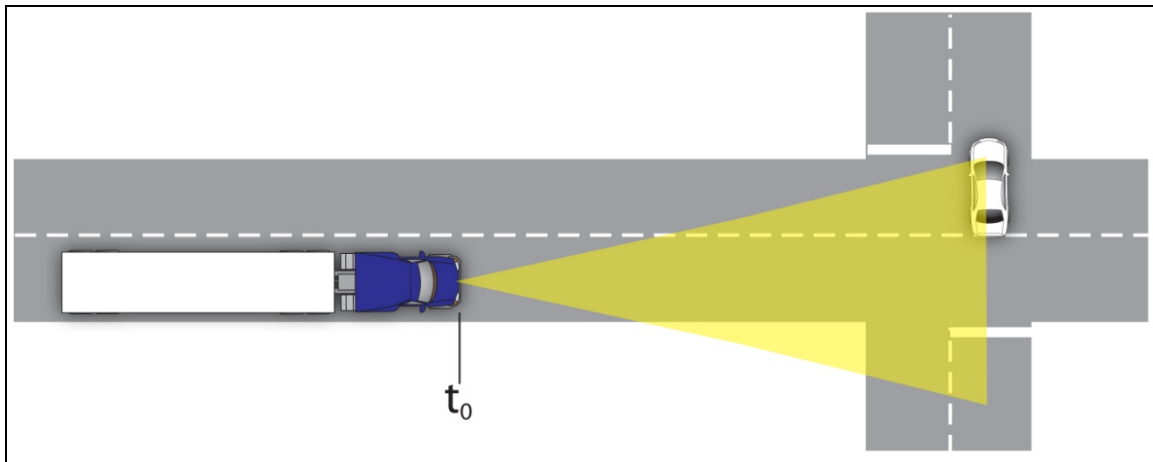
Figure 9. Example of a Crossing-lane Target: A Vehicle Passing Through an Intersection

High-Lateral-Acceleration Filter

Definition	Filters out triggered events when unreasonably high lateral accelerations would have been required by the FV to avoid a target.
Criteria	If the lateral acceleration required to avoid a stopped target exceeds 0.4 g for > 0.5 s during the critical target presence and no collision occurred, then the target is considered to be benign.

The high-lateral-acceleration filter was designed to remove triggered events where unreasonably high lateral accelerations would have been required to avoid a collision with the target. The logic behind this filter is that heavy vehicles are limited with respect to the amount of lateral acceleration they can physically experience when avoiding a target (Figure 10). Therefore, if the calculation based on the triggered event data indicates an FV would have had to perform a steering maneuver generating lateral acceleration > 0.4 g to avoid a stopped LV, but no collision occurred, then the target must have been non-threatening. The algorithm, shown below, functions by: 1) calculating the angle at which the stopped target is located relative to the center of the FV, 2) calculating the radius of the turn that must be executed to avoid the stopped target, and 3) computing the required lateral acceleration using the FV speed.

Required Angle:

_____

where θ_R is the required angle, T_W is half the vehicle width (1.2 m or 4 ft), R is the range, and θ_{Az} is the azimuth angle.

Turn Radius:

_____

Required Lateral Acceleration:

_____

where V_F is the following-vehicle speed and g is the force of gravity (9.81 m/s^2 or 32.2 ft/s^2)
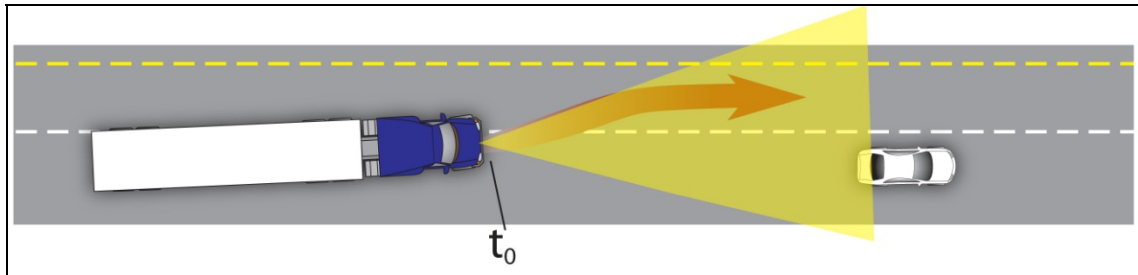
Figure 10. Illustration of a Truck Performing a Reasonable Lateral Acceleration
If the required lateral acceleration was computed to be unreasonable, then the event was non-threatening.

Filter for Target With No Driver Reaction

Definition	Filters out triggered events that are not followed by a driver reaction.
Criteria	Driver reactions considered:
	Service brake application and FV decelerations greater than 0.609
	m/s^2 (2 ft/s^2 or 0.0625 g)
	FV lane change
	This filter is only applied to stopped critical targets.

The filter for a target with no driver reaction assumed that drivers react in some way or another in response to valid RE conflicts. Triggered events that were not followed by a driver reaction within 5 s were considered to be non-threatening. An example would be when the FV drives under a bridge (Figure 11). It should be noted that this filter was only applied to stationary critical targets. This filter was implemented by marking the data if one of two driver reactions occurred. These mark points were then compared to the trigger occurrences. Any triggered event that did not coincide with a driver reaction mark point was then treated as non-threatening and removed.
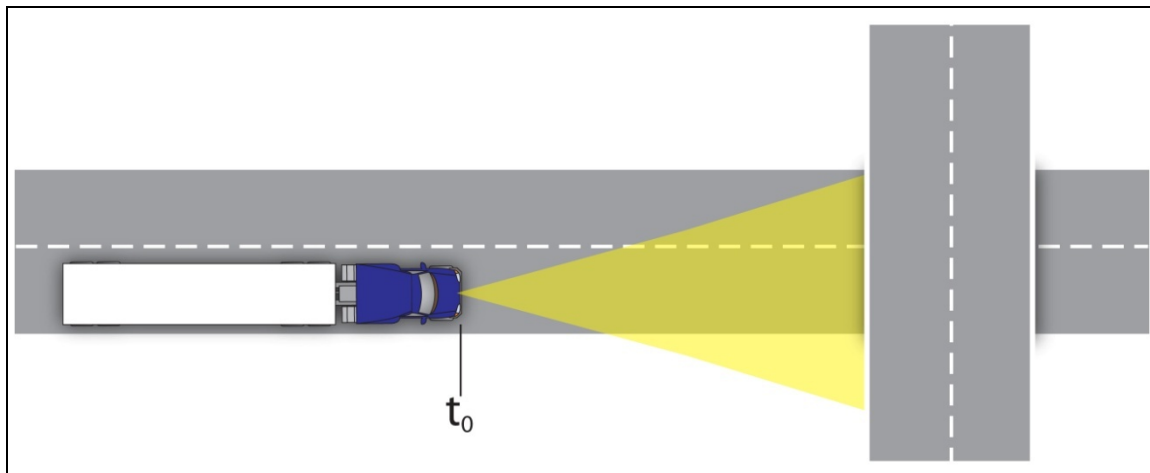
Figure 11. Example of the Eaton VORAD Detecting an Overhanging Bridge
This triggered event would be filtered out since the driver does not react to it.

The two driver reactions that were marked in the data are as follows:

Service Brake Application Combined With FV Deceleration
The data were scanned for brake applications and FV decelerations greater than 0.609 m/s^2 (2 ft/s^2 or 0.0625 g). If these two conditions were met, the previous 5 s worth of data was marked as having a driver reaction. One time point's worth of braking qualified as a service brake application. Additionally, one time point's worth of high deceleration qualified as an FV deceleration. It should be noted that the FV acceleration data was smoothed using a five-point cubic filter to eliminate sensor noise.

Lane Change

The data was scanned for lane changes using the following logic.

1. *Bias Removal*

   A seven-point cubic regression was used to smooth out the noise present in the gyro data. Yaw data were then sorted by value to find the median value. This median value was assumed to be a bias and subtracted from all other yaw values.

2. *Threshold of Yaw Rate Signal*

   Yaw values with a magnitude less than or equal to 0.05 were set to 0.

3. *Sine Wave First Half-Cycle Determination*

   The positive and negative lateral accelerations characteristic of lane changes formulate sine waves. Lane changes were detected by identifying the first half-cycle of the sine wave as follows:

   a. If the current yaw value is not equal to zero, and the previous value is either zero, or has the opposite sign from the current value, then this time point is marked as a zero crossing. The first and last time points of a half-cycle are marked as zero crossings.

   b. If the current value is a zero crossing, then set the largest yaw value in the range between the previous zero crossing and the current zero crossing to be the amplitude of the half-cycle. The amplitude is defined as the minimum value reached for negative half-cycles and the maximum value reached for positive half-cycles. This is accomplished as follows:

      i. If the current value is a zero crossing, set max and min tracking variables to 0

      ii. If the current value is less than minimum, set minimum = current value

      iii. If the current value is greater than maximum, set maximum = current value

4. *Total Time Span of Sine Waves*

   a. This was done using the list of zero crossings and associated yaw data. Each consecutive pair of zero crossings (which defines a sine half-cycle) was examined to see if they exceeded the time threshold of 1.7 s. If the half-cycle had a period greater than 1.7 s, then subsequent points were examined for the second half of the sine wave. The logic used in Volvo (2005) called for a threshold of 1.83 s. This was altered after video data revealed that this threshold was missing aggressive (evasive) lane changes.

   b. The periods of subsequent half-cycles were then examined. In order for a lane change to be considered true, the second half-cycle period had to be at least 1.7 s long. Additionally, if the period of the first half cycle was longer than the second half cycle, then the period of the first half cycle had to be less than 500 percent of the period of the second half cycle. Alternatively, if the period of the second half cycle was greater than the first half cycle, then the period of the second half cycle had to be less than 500 percent of the period of the first half cycle.

   c. The second half cycle period had to begin no more than 0.3 s following the ending of the first half cycle. Additionally, the ending point of the second half cycle had to be within 12 s of the starting point of the first half-cycle.

5. *Sine Wave Amplitudes*
   a. The magnitudes of the sine waves found in the previous step were then examined. For a lane change to be considered true, the first and second halves had to have opposite signs. The magnitude of the first and second half cycles also had to be greater than 1.2 deg/s. Video inspection indicated that this threshold was functional for separating true lane changes from sensor noise. Additionally, if the magnitude of the first half cycle was greater than the magnitude of the second half cycle, then the magnitude of the second half cycle had to be greater than 60 percent of the magnitude of the first half cycle. Alternatively, if the magnitude of the second half cycle was greater than the magnitude of the first half cycle, then the magnitude of the first half cycle had to be greater than 60 percent of the magnitude of the second half cycle.

6. *Wandering in Lane*
   a. If a sine wave did not have at least one half where the amplitude exceeded 0.4 deg/s, then the sine wave was considered to represent normal wandering in the lane, and not a lane change.

Receding-Target Filter

Definition	Filters out triggered events that occur as a critical target is pulling away from the following vehicle.
Criteria	Range rate > 0 ft/s for ≥ 0.5 s after the trigger.

A receding target was defined as a critical target pulling away (positive range rate) from the FV following the triggered time point. Receding targets were typical of LVs closely merging in front of the FV and accelerating away (Figure 12). Receding targets were recorded but were of little interest from a threat and safety standpoint. The criteria used to identify receding targets were as follows:

For each time point during a target's presence, the range rate was checked to see if it was greater than zero. If the current range rate was greater than zero, then the next four time points (a total of five contiguous time points or 0.5 s) were checked to see if the range rate for the tracked target remained above zero. If this condition was met, then the data spanning the 4.5 s prior to the first above-zero range rate time point was marked as a positive range rate. Any triggers that occur during this interval were then marked as non-threats.
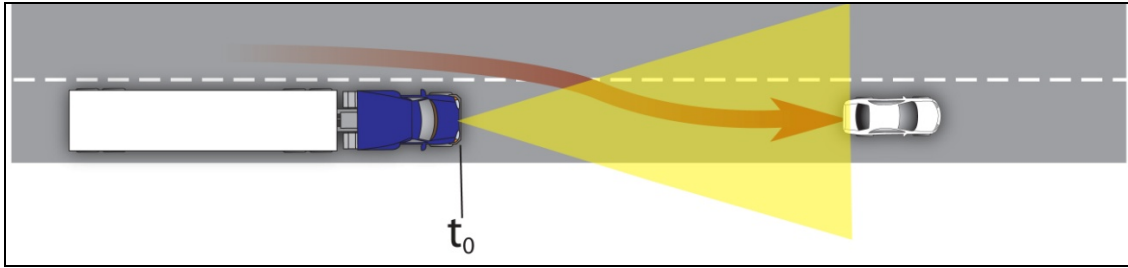
Figure 12. Example of a Receding Target:
A Vehicle Closely Merging in Front of the Truck As It Accelerates Away

Treatment of Continuous Data

The DDWS FOT data were continuously recorded as instrumented vehicles were driven. This was accomplished by storing the data in a compressed binary format. DART was then used to scan this compressed data to both identify and filter triggered events. DART's trigger process flagged events as long as the trigger conditions persisted. Triggers were therefore windows that encompassed the entire time the trigger thresholds were surpassed. Based on the beginning time point of the trigger, 10 s of parametric data before the trigger as well as 5 s of data after the trigger were then expanded from the compressed binary format and stored in a separate database. This database was approximately 7 GB in size.

Target Tracking

The Eaton VORAD system used in the DDWS FOT simultaneously tracked up to seven targets. Since data pertaining to the most threatening target were not grouped in the raw data, VTTI developed algorithms to identify and track the primary target of interest within the VORAD data. This also allowed events in which VORAD data appeared to be missing to be salvaged. Target tracking also served to ensure that the trigger time point was accurate.

Validate a Sample of the Triggered Events

The RE events that remained after filtration formulated Subset 1. The suitability of these events for use in the safety benefit estimate was assessed by visually validating a sample of 300 events (100 KME, 100 TTC, and 100 FI triggered events). Validation involved using video footage of the events to confirm the presence of an RE conflict. Events were marked as invalid if the LV or object was outside of the FV's lane within the 10 s prior to the trigger time point. It was revealed that targets in opposite and adjacent lanes could be parametrically classified as being in the FV's lane when there was a slight curvature to the road. It should be noted that events consisting of an LV slowing down to turn off the road were deemed valid (i.e., a true crash threat), but events identified by a vehicle traveling in an adjacent lane were considered invalid (i.e., a non-threatening event).

IDENTIFY RELEVANT CONFLICTS

Visual inspection revealed that numerous non-threatening events existed in Subset 1. Additional filtration was thus performed to remove these events from the database. The criteria listed below were used. Events that met these criteria were flagged in case they needed to be considered in future analyses.

1. Conflicts in which the target was oncoming. A target was considered to be oncoming when its speed was less than -6 ft/s (-1.83 m/s).
2. Conflicts in which the LV was found to be in the same lane as the FV less than 4 s.
3. Conflicts in which the FV accelerated.
4. Conflicts in which the FV began to decelerate before the LV appeared.
5. Conflicts in which difference between the FV maximum and minimum speed were less than 1.2 m/s.
6. Conflicts in which the LV was out-of-lane at any time and no lane changes occurred during the time history.

Optimization of Events

The remaining RE events were then optimized. Optimization involves approximating the impending RE crash scenarios by constructing an ideal speed profile in which the FV and LV travel at a constant speed before decelerating at a constant deceleration rate to a final speed. An example of an optimized conflict is shown in Figure 13. Specifically, the figure illustrates the optimized speed profiles (termed theoretical) for the LV and FV (designated with the inverted v character $\hat{V}_L$ and $\hat{V}_F$). The optimized profiles are represented as a solid line. The smoothed profiles of the raw data (V_L and V_F) are shown as dotted lines.
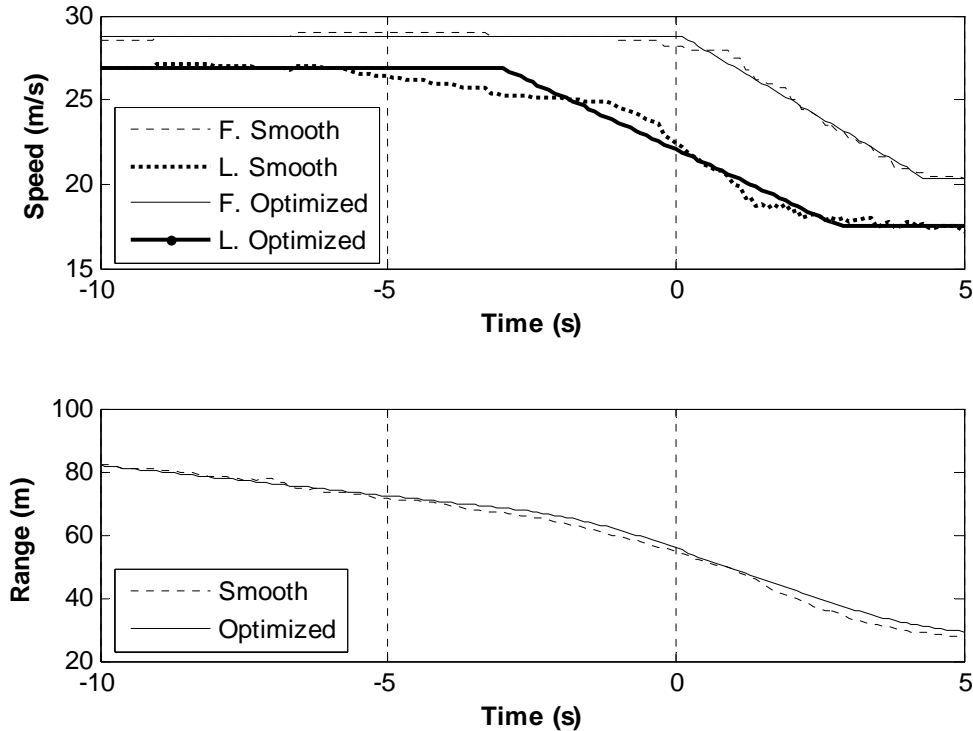
Figure 13. Example Illustration of Optimized LV and FV Profiles

The optimization procedure is based on earlier work done by Martin and Burgett (2001) with some modifications. These modifications include: (a) optimizing eight parameters instead of six;

(b) using a bi-level optimization procedure; and (c) using a custom heuristic optimization tool. The procedure involves applying a bi-level non-linear optimization procedure to estimate eight variables (initial speed, time to start deceleration, deceleration rate, and final speed for both the FV and LV). The first level optimization minimizes the sum of squared error, E, between the observed and estimated speed profile for the FV. The optimization of the FV speed is done first given that the FV speed is directly measured in the field. Since the LV speed is derived from the FV speed, the FV speed is considered to be more accurate. Once the FV speed profile is optimized, the second level of optimization estimates the LV parameters by minimizing the error between the observed and estimated speed profile for the LV.

The bi-level optimization is performed using a custom-developed heuristic procedure. The heuristic is described in Appendix B. The MATLAB code used to perform the heuristic is presented in Appendix C.

Filter by Conflict Severity

The optimized RE events were then screened to identify theoretical RE conflicts. An RE conflict was said to occur when the FV approached an LV in a manner that would result in a crash if one of the vehicles did not change its behavior. RE conflicts were identified using KME filter equations, which are not to be confused with KME0 and KME1 trigger equations. The KME filter equations address two kinematic situations: 1) LV is stopped or traveling at a constant speed (LVS/LVCS), and 2) LV is decelerating (LVD). The derivation of the KME equations is explained in Appendix D.

In the case of the LVS/LVCS, a scenario is considered if the required deceleration exceeds a deceleration level threshold ($d_{F,Threshold}$):

$$\hat{d}_F = \frac{\hat{V}_{Fo}^2 - \hat{V}_{Lo}^2}{2(\hat{R}(t_{Fb}) - (\hat{V}_{Fo} - \hat{V}_{Lo})t_R)} > d_{F,Threshold}, \tag{1}$$

where $\hat{V}_{Fo}$ is the initial velocity of the FV; $\hat{V}_{Lo}$ is the initial velocity of the LV; $\hat{R}(t_{Fb})$ is the range between the FV to the LV at the instant the FV decelerates (t_{Fb}); t_R is the perception-response time of the FV ($t_{Fb} - t_{Lb}$). It should be noted that conflicts in the LVS/LVCS case had a t_{Lb}, but the ensuing deceleration level of the lead vehicle was marginal.

In the case of the LVD, a scenario is considered if the deceleration rate exceeds the deceleration rate threshold as

$$\hat{d}_F = \frac{\hat{V}_{Fo}^2}{\frac{\hat{V}_{Lo}^2}{\hat{d}_L} - 2\hat{V}_{Fo}t_R + 2\hat{R}(t_{Fb})} > \hat{d}_{F, Threshold}, \tag{2}$$

where other variables are as defined earlier and $\hat{d}_L$ is the deceleration level of the LV.
Two example illustrations pertaining to the LVD case are presented in Figure 14. The top graph shows a theoretical crash, while the bottom graph does not. Both the FV and LV have an initial

23

speed of 20 m/s. In the first graph, the LV (thin line) decelerates at a rate of 3 m/s^2 while the FV (thick line) decelerates at a milder rate of 2.25 m/s^2. It should be noted that in both cases the FV comes to a complete stop after the LV stops. The fact that the FV stops later is not an indication that a collision will occur, as was assumed in an earlier study (Battelle, 2006).
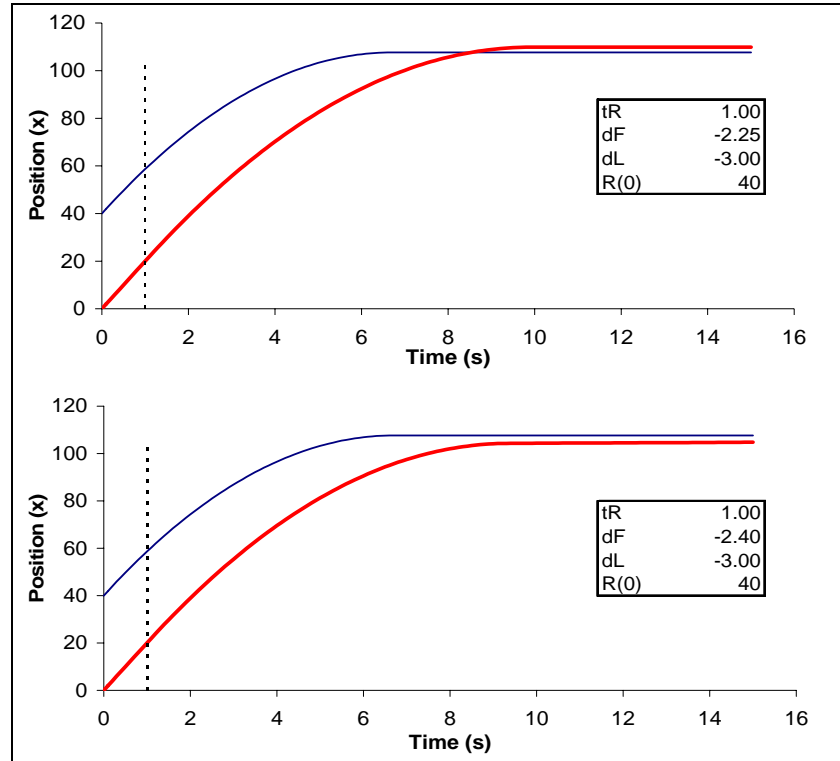
Figure 14. Example Illustration of Two Conflict Scenarios (LV shown as a thin line, while the FV is shown as a thick line)

Theoretical RE conflicts were identified as those optimized RE events that resulted in a crash using the medium-level deceleration thresholds specified in Battelle (2006). The medium-level deceleration threshold was 3 m/s^2 (10 ft/s^2). Scenarios that did not result in a crash were discarded. It should be noted that this study used the actual response time (T_{Fb}-T_{Lb}) instead of the 1.0 s response time used in Battelle (2006). The scenario-based optimized data comprise Subset 2.

Visual Inspection

A second visual inspection was performed on a random sample of sixty conflicts (20 KME, 20 TTC, and 20 FI) to assess their suitability for the FCW algorithm evaluation. A 95-percent confidence interval on the number of visually valid conflicts was made for each trigger type and on all the data combined. The results are presented in Chapter 4.

CLASSIFY CONFLICTS

Conflicts were then classified into one of five pre-collision conflict types developed in Volvo (2005). The five conflict types are shown in Table 2. RE pre-collision conflict types were distinguished using the following operational definitions:

1. *Constant Speed*
   A vehicle was considered to be traveling at constant speed if the absolute value of deceleration was less than or equal to 0.609 m/s^2 (2 ft/s^2) during the period the LV was present. Note: the constant speed condition also included an accelerating vehicle ($0 < a \leq 0.609$ m/s^2 (2 ft/s^2)). The value of 0.609 m/s^2 was selected because this represented the margin of error in the acceleration measurements.

2. *Decelerating*
   A vehicle was considered to be decelerating if its deceleration was greater than 0.609 m/s^2 (2 ft/s^2) at any point during the period the LV was present.

3. *Lane Change*
   A vehicle was considered to be changing lanes if it was traveling at a constant speed and met the lane change criteria specified in the No-Driver-Reaction filter.

4. *Stopped*
   A vehicle was considered to be stopped if the absolute value of its speed was less than 1.218 m/s (4 ft/s) during the period the LV was present. This value was selected because it is equal to the pedestrian speed utilized in the computation of pedestrian green time requirements in the design of signal timings (Highway Capacity Manual, 2000).

Conflicts that did not fit into the above classification were flagged and discarded. The remaining conflicts formulated Subset 3. It should be noted that conflicts were also distinguished by whether or not a lane change was made after the trigger time point. Such instances may be indicative of a driver reaction. These events were eventually included in the safety benefit calculations.

25

Table 2. RE Pre-Collision Conflict Types

Conflict Type	FV Lane Change Prior to Critical Point	FV Speed	LV Speed
1. Closing with constant speed: • No lane change and closing with constant speed • Lane change after closing with constant speed	No	Constant	Constant
2. Closing with both vehicles decelerating: • No lane change and closing with both vehicles decelerating • Lane change after closing with both vehicles decelerating	No	Decelerating	Decelerating
3. Closing preceded by lane change	Yes	Constant	Constant
4. Closing with stopped LV: • No lane change after closing with stopped LV • Lane change after closing with stopped LV	No	Constant or Decelerating	Stopped
5. Closing with decelerating LV: • No lane change and closing with decelerating LV • Lane change after closing with decelerating LV	No	Constant	Decelerating

The following strategy was taken when classifying events. The LV speed was identified first, followed by identification of the FV speed, followed by identification of any FV lane change. If the LV was stopped, the only possible conflict type was number four regardless of what the FV was doing. If the LV speed was constant, possible conflict types were Numbers 1 or 3:
- If the FV speed was constant with no lane change preceding the trigger, the conflict type was Number 1.
- If an FV lane change preceded the trigger, the conflict type was Number 3.

If the LV speed was neither stopped, nor constant, but decelerating, the possible conflict types were Numbers 2 and 5:
- If the FV was decelerating, then the conflict type was Number 2.
- If the FV was traveling at a constant speed, then the conflict type was Number 5.

To facilitate comparisons, Subset 3 was also classified into the three conflict categories used in Battelle (2006) based on FV kinematic considerations. These three categories are shown in Table 3. Category 1 combines Conflict Types 1 and 5. Category 2 combines Conflict Types 2 and 4. Category 3 remains the same as Conflict Type 3.

Table 3. RE Pre-collision Categories

Category	FV Kinematic Condition	Volvo (2005) Conflict Type	
1. Constant Speed: Overtaking at constant speed (1+5)	Constant	1	Overtaking slower LV
		5	Slowing LV
2. Slowing: Overtaking while slowing (2+4)	Decelerating[1]	2	Overtaking while slowing
		4	Stopped LV
3. Lane Change: Changing Lanes (3)	Lane Change	3	Changing lanes

[1]If the LV is stopped, the conflict is placed in this category regardless of the FV behavior.

IMPLEMENT FCW ALGORITHMS

The FCW algorithms cited in Volvo (2005) were then coded using Mathworks' MATLAB numerical computing environment. MATLAB is a high-level language and interactive environment that enables computationally intensive tasks to be performed faster than with traditional programming languages such as C, C++, and Fortran. The FCW algorithms are shown in Table 4. These algorithms were those associated with the last five grades of audible alarms presented by the Eaton VORAD FCW system. Vehicles were considered to be in the FV's lane if the LV's lateral distance to the center of the FV was less than 1.9 m (6.25 ft) (i.e., half of the vehicle width plus a clearance of 0.6 m (2 ft)).

Table 4. Eaton VORAD EVT300 Audible Alarm Types

Alarm Type	Alarm Level	Unsafe Driving Condition	Audible Tone
2 s, Closing	6	LV in same lane, 1 to 2 s following interval, LV speed < 101 percent of FV speed, LV < $Range_{max}$, FV speed > 16 km/h (10 mph)	Single Pulse[1,2,3]
1 s, Closing	7	LV in same lane, < 1 s following interval, LV speed < 105 percent of FV speed, LV < $Range_{max}$, FV speed > 16 km/h (10 mph)	Double Pulse[2,3]
Stationary	8	LV < 5.4 km/h (3.4 mph), in same lane, within 3 s and LV range is < 67 m (220 ft) or $Range_{max}$ whichever is smaller, FV speed > 16 km/h (10 mph)	Double Pulse[2,3]
Slow Moving	9	LV in same lane, within 3 s, LV range < 67 m (220 ft) or $Range_{max}$ whichever is smaller, and FV vehicle speed is 25 percent greater than LV speed, FV speed > 56.3 km/h (35 mph)	Double Pulse[2,3]
½ s	10	LV in same lane, < 0.5 s following interval, opening/closing, FV speed > 16 mph (10 mph)	Double Pulse[2,3,4]

Notes: 1) Configurable on or off; 2) Tone disabled in hard turns (<229m (750 ft) radius); 3) Tone disabled with brake on; 4) Repeats constantly twice per second.

The FCW algorithms were applied to the raw data in Subset 3 to identify the time point at which each of the FCW alarms would have activated if the FV had an FCW system in operation. This dataset is referred to as Subset 4.

The performance of the coded algorithms were compared against the FCW algorithm code used in Volvo (2005). Both the timing and type of alarm generated were compared in this fashion. A limited number of events from Subset 4B were selected for this inspection. One conflict for each alarm severity and conflict type was inspected. This sample constitutes Subset 4.

PERFORM LAG PROCESS

A component of the safety benefit evaluation is estimating the number of RE crashes that could have been prevented had drivers received FCW system feedback. This was accomplished by comparing how close the FVs were to encountering an RE crash when they did not receive the FCW system feedback to how close they were to a crash when they did receive the FCW system feedback. How close they were to a crash was assessed by computing the maximum additional time FVs could have waited to brake before avoiding an RE crash. This additional time is called the lag time. The computation of the lag time assumes that the FV brakes in the same manner as it did during the actual conflict. It also assumes that the FV and LV maintain the same kinematic profiles. This is illustrated in Figure 15. The longer the lag time, the less severe a conflict is considered to be. That is, FVs that could have waited an additional 2 s before applying the brakes to avoid an RE crash were in less threatening circumstances than FVs who could only

28

wait an additional 0.5 s to apply the brakes. An underpinning of this study is that the FCW system feedback can notify FV drivers to brake earlier in response to impending RE conflicts. The lag times for cases in which FCW feedback was provided are thus expected to be longer.
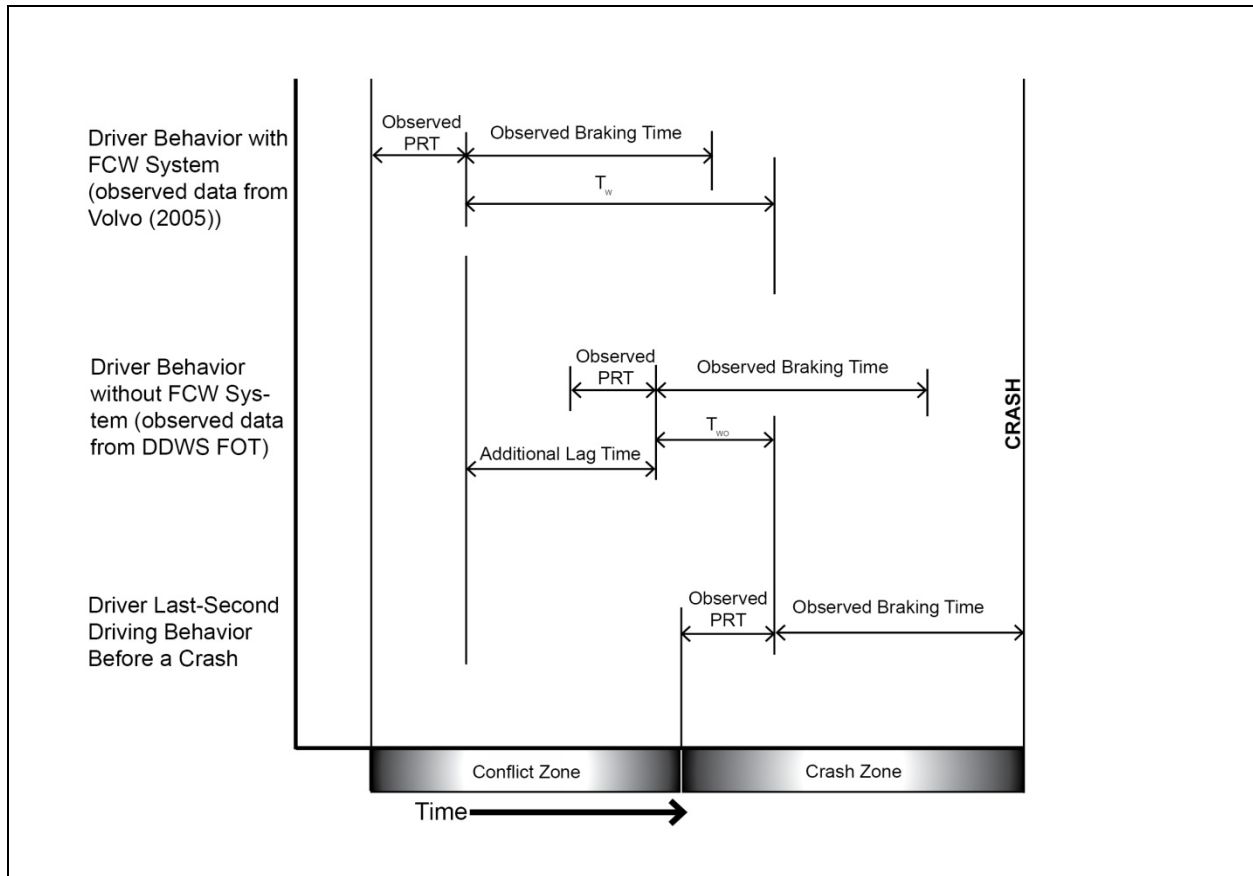
Figure 15. Illustration of Lag Times Computed With and Without the FCW System

The procedure for estimating the lag time was modified from that used in Battelle (2006). The procedure used in Battelle (2006) involved numerically increasing the lag time in steps of 0.17 s and iteratively simulating the LV and FV profiles to see if a crash occurs (range equals zero). The approach taken in the current study, however, combines an analytical approach with this numerical approach. Appendix E details the lag process procedure used and provides computational examples. Appendix F documents the MATLAB code used to compute the lag time.

The analytical component of the lag time computation involved solving for the time in which a collision between the FV and LV occurs. Equation 3 was used for conflicts in the LVS/LVCS category, while Equations 4 and 5 were used for conflicts in the LVD category. For the first step, t_{Fb} is substituted into t and the solution is evaluated. If the solution is not a real non-negative number, then t is incremented by 0.01 s (following the numerical approach specified in Battelle [2006]). The solution is evaluated in an iterative fashion, each time incrementing t by 0.01s until a real non-negative solution is obtained. The sum of the incremented time units that were added to t is the lag time. It should be noted that the most t can be incremented is 15 s. If a real non-negative solution is not found by that point, then the event is discarded.

29

Case 1: LVS/LVCS

$$t = \frac{\left(\hat{V}_{Fo} - \hat{V}_{Lo}\right) \pm \sqrt{\left(\hat{V}_{Fo} - \hat{V}_{Lo}\right)^2 - 2d_F R}}{d_F} \quad . \tag{3}$$

Case 2: LVD - FV decelerates after LV ($t_{Fb} \geq t_{Lb}$)

$$t = \frac{\left(\hat{V}_{Fo} - \hat{V}_L\right) \pm \sqrt{\left(\hat{V}_{Fo} - \hat{V}_L\right)^2 - 2(d_F - d_L)R}}{(d_F - d_L)} \quad . \tag{4}$$

Case 3: LVD - FV decelerates before LV ($t_{Fb} < t_{Lb}$) and $t \leq (t_{Lb}\text{-}t_{Fb})$

$$t = \frac{\left(\hat{V}_{Fo} - \hat{V}_{Lo}\right) \pm \sqrt{\left(\hat{V}_{Fo} - \hat{V}_{Lo}\right)^2 - 2d_F R}}{d_F} \tag{5}$$

Case 4: LVD - FV decelerates before LV ($t_{Fb} < t_{Lb}$) and $t > (t_{Lb}\text{-}t_{Fb})$

$$t = \frac{-\left(\hat{V}_{Lo} - \hat{V}_{Fo} + d_L t'\right) \pm \sqrt{\left(\hat{V}_{Lo} - \hat{V}_{Fo} + d_L t'\right)^2 - 2(d_F - d_L)\left(R - 0.5 d_L t'^2\right)}}{(d_F - d_L)} \tag{6}$$

The MATLAB code used to increase the lag time in increments of 0.01 s is presented in Appendix F. Conflicts that had lag times less than 0 s and greater than 15 s were discarded. This filtration left a total of 1,030 conflicts. This formulated Subset 5.

From here, both the arithmetic and geometric means of the lag times were computed. The arithmetic mean lag time was computed as

$$\overline{T}_{ki} = \frac{\sum_{n_{ki}} T_{kji}}{n_{ki}} \qquad \forall\, k, i \tag{7}$$

while the geometric mean lag time was computed as:

$$\overline{T}_{ki} = \left(\prod_{n_{ki}} T_{kji}\right)^{\frac{1}{n_{ki}}} \qquad \forall k, i \,. \tag{8}$$

Where n_{ki} is a count of valid scenarios that remained. n_{ki} was computed as:

$$n_{ki} = \sum_j J_{kji} \quad \forall\, k, i \,.\; where \; J_{kji} = \begin{cases} 1 & 0 < T_{kji} < 15 \\ 0 & Otherwise \end{cases} \tag{9}$$

It should be noted that the geometric mean was computed in order to compute the confidence limits of the various parameters as will be discussed later.

The next section describes how the FCW effects were applied to the conflicts in Subset 5. The conflicts that had the FCW system effects applied formulated Subset 6A. The lag times were then computed for the conflicts in Subset 6A. Conflicts with lag times less than 0 s and greater than 15 s were discarded. The 1,026 conflicts that remained formulated Subset 6B. The arithmetic and geometric mean lag times of these conflicts were computed.

APPLY FCW EFFECTS

A Monte Carlo simulation approach was used to model driver response behavior to the generated FCW alarms. The Monte Carlo simulation involved randomly selecting driver perception-response time (PRT) and deceleration levels from distributions generated using the Volvo FOT data. Since drivers may not brake as hard or as fast to a moderately severe level-6 alarm compared to an urgent level-10 alarm, driver PRT and braking-level distributions were derived separately for each alarm. The PRT and deceleration levels were extracted from the data by considering all audible alarms that were activated prior to the driver braking. The data were then separated by alarm level. A dependency between PRT and deceleration level was accounted for by developing regression models considering the deceleration level as an explanatory variable and the PRT as a response variable. In developing this relationship, empirical cumulative density functions (CDFs) were constructed for the PRTs for each of the five alarm levels. In order to satisfy least square assumptions, namely normality and homoscedasticity of the error structure, the data were sorted based on their deceleration rate and aggregated into bins of three observations. The average PRT and deceleration level were then computed for each bin. Regression models were then fit to the data. The linear relationship between the driver deceleration level (d) and PRT was of the form

$$d = b_0 + b_1 \times PRT \qquad (10)$$

where b_0 and b_1 are calibrated model constants. A summary of the calibrated model parameters and their level of significance (p-values in parenthesis) is presented in Table 5. In the case of alarms 7 and 10, no statistically significant relationship was found between d and PRT (the model slope was found to be insignificant at an α value of 0.05). Consequently, an independent CDF was developed for the deceleration level using the raw unaggregated deceleration levels for alarms 7 and 10. In the case of alarms 6, 8, and 9, the residual error was tested for normality using a Kolmogrov-Smirnov test and the results indicated that there was insufficient evidence to reject the normality assumption at a 5-percent level of significance. Consequently, a least square approach would be valid for such an analysis.

Table 5. Linear Regression Model Parameter Summary

Alarm	b_0	b_1	Std. Dev.
6	0.0314 ($p < 0.0005$)	0.0095 ($p < 0.0005$)	0.022
7	0.0551 ($p < 0.0005$)	-0.0014 ($p = 0.06$)	--

8	0.0369 ($p < 0.0005$)	0.0313 ($p = 0.0002$)	0.0418
9	0.0486 ($p < 0.0005$)	0.0228 ($p = 0.0004$)	0.0453
10	0.0650 ($p < 0.0005$)	0.0005 ($p = 0.85$)	--

Sample illustrations of driver PRT and deceleration rate CDFs for Alarm Levels 6 and 10 are shown in Figure 16 and Figure 17, respectively. In the case of alarm 6, there is a linear relationship between the driver PRT and deceleration rate. The deceleration rate CDF is thus based on this relationship. Alternatively, in the case of alarm 10, the two CDFs are independent and thus both CDFs are created independently when simulating the FCW system.
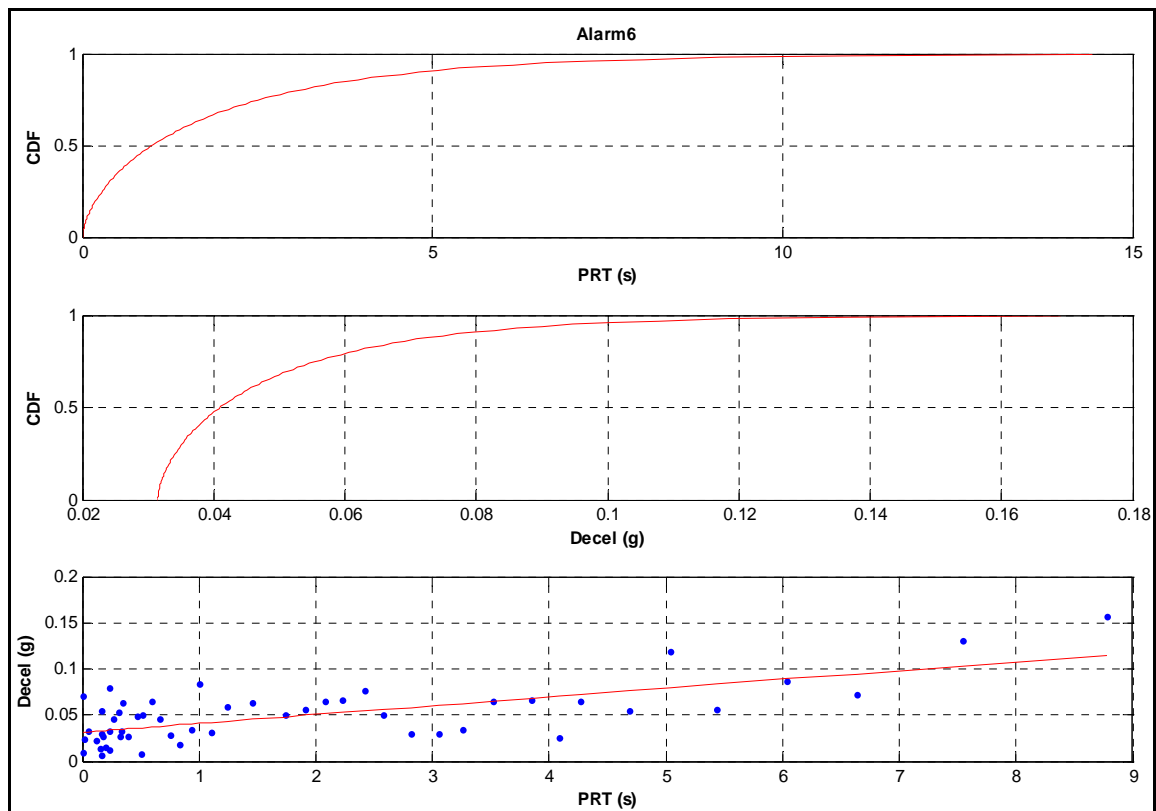
Figure 16. Example Illustration of Driver PRT and Deceleration Distribution for Alarm 6
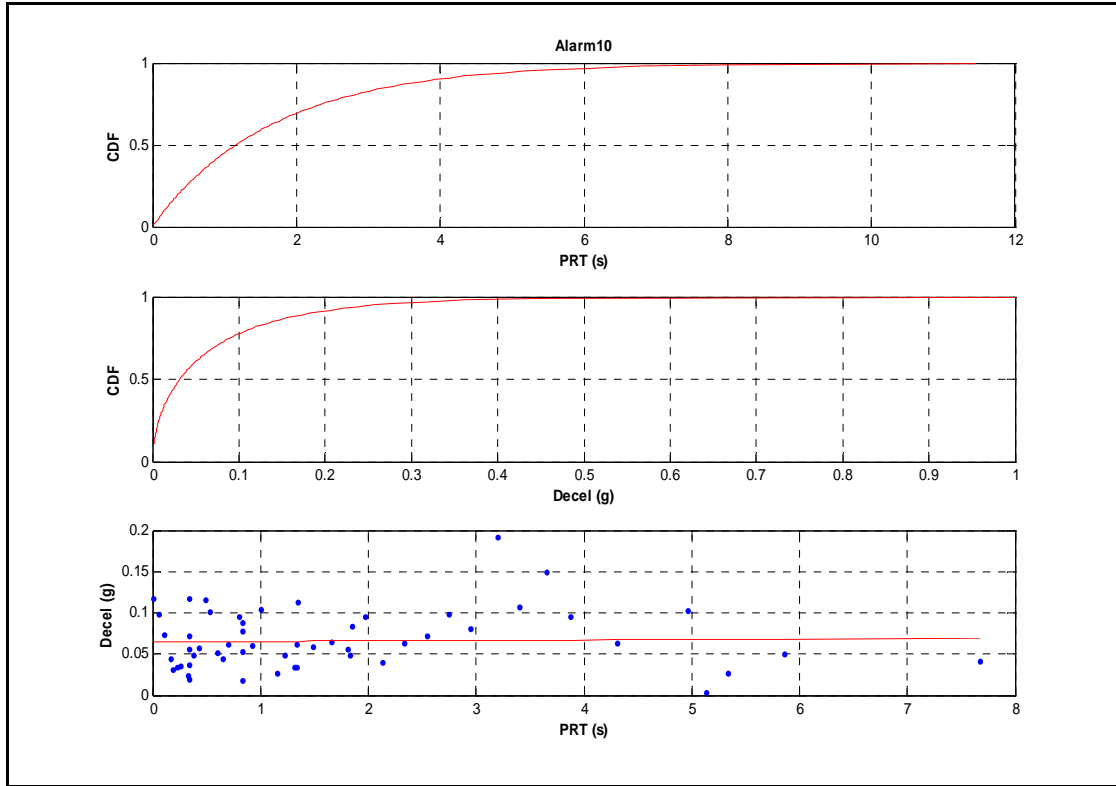
Figure 17. Example Illustration of Driver PRT and Deceleration Distribution for Alarm 10

Drivers' simulated responses to the simulated FCW alarms were then modeled. For a given repetition in the Monte Carlo simulation, a uniformly distributed random number between 0 and 1 was used to select a PRT from the PRT CDF. A corresponding deceleration rate was then selected based on the selected PRT if a regression relationship existed. PRT/braking-level regression relationships for alarms 6, 8, and 9 are shown in Figure 18. It should be noted that a second random number was generated to introduce a normal error about the regression line. The standard deviation of the normal random variable is provided in Table 6. This ensured that the PRT and deceleration levels were consistent with those in the Volvo FOT data. Alarm 8 appears to produce the most significant driver deceleration behavior out of the three alarm levels that had a relationship with PRT. Since PRT and deceleration rates for alarms 7 and 10 were found to be independent, two random numbers between 0 and 1 were generated to select a PRT and deceleration level.
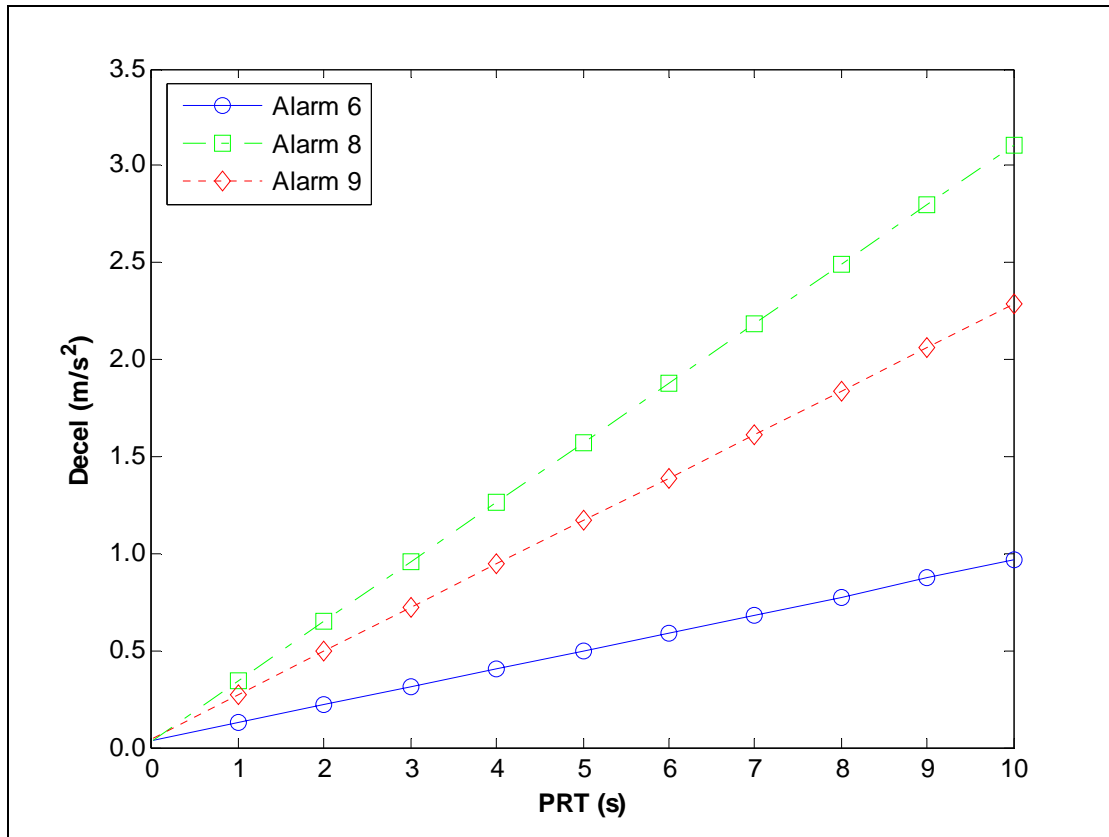
Figure 18. Relationship Between Deceleration Rate and PRT for Alarms 6, 8, and 9

Table 6. The Standard Deviation of Normal Error Introduced About the Regression Line For Alarms 6, 8, and 9

Alarm	Std. Dev.
6	0.0220
8	0.0418
9	0.0453

The Monte Carlo simulation was run twice, each with a different random number seed. A total of up to 100 iterations were performed within each simulation. A valid simulation occurred when a lag time greater than 0 s and less than 15 s was produced. In the event that it was not possible to generate 100 valid events after running 1,000 simulations, the event was excluded (in this case, a total of four events were excluded in the two simulation efforts). A total of 1,026 conflicts remained for the condition with FCW after the Monte Carlo simulation was performed. The resultant data is referred to as Subset 6B.

DETERMINE FCW SAFETY BENEFITS

Estimation of the FCW safety benefits involved comparing driver reaction to a conflict with and without FCW feedback. The safety benefit estimate involved the following steps:

- Compute exposure ratios (ER) for each conflict category.

34

- Compute prevention ratios (PR) for each conflict category.
- Compute the crash reduction ratios (CRR) for each conflict category.
- Compute percent reduction in national crashes.
- Compute the safety benefit (B) by looking at the number of crashes prevented given the deployment of an FCW system across the national fleet of heavy vehicles.

ER is a ratio of exposure to conflicts S_i with and without the FCW system. It is an estimate of how well an FCW system helps drivers avoid entering RE conflict scenarios. It was computed as follows:

$$ER_i = \frac{P_w(S_i)}{P_{wo}(S_i)} = \frac{n_{w,i}}{n_{wo,i}} \qquad \forall\, i \tag{11}$$

where,
- $P_{wo}(S_i)$ is the probability that a driving conflict S_i occurs when the FCW system is not installed
- $P_w(S_i)$ is the probability that a driving conflict S_i occurs when the FCW system is installed
- n_{wo} is the number of conflicts experienced without an FCW system installed
- n_w is the number of conflicts experienced with an FCW system installed

The ER variance was computed using a first order Taylor approximation:

$$Var(ER_i) = Var\left(\frac{P_w(S_i)}{P_{wo}(S_i)}\right) \approx Var(P_w(S_i))\left(\frac{1}{\overline{P}_{wo}(S_i)}\right)^2 + Var(P_{wo}(S_i))\left(\frac{\overline{P}_w(S_i)}{\overline{P}_{wo}(S_i)^2}\right)^2 \qquad \forall\, i \tag{12}$$

where
- $\overline{P}_w(S_i) = \dfrac{N_i}{VMT_w} \,\forall\, i$

- $Var(P_w(S_i)) = \dfrac{N_i}{VMT_w^2} \,\forall\, i$

- N_i is the number of conflicts in category i which occurred in the vehicle miles traveled with (VMT_w) the FCW system.

Similar calculations yield $P_{wo}(S_i)$.

PR is an estimate of the FCW system's efficacy at preventing a crash once drivers have encountered an RE conflict scenario. The PR was computed as follows:

$$PR_i = \frac{P_w(C\,|\,S_i)}{P_{wo}(C\,|\,S_i)} \qquad \forall\, i \tag{13}$$

where,
- $P_{wo}(C|S_i)$ is the probability of an RE crash without the FCW system installed given that a conflict S_i has occurred

- $P_w(C|S_i)$ is the probability of an RE crash with the FCW system installed given that a conflict S_i has occurred

Here, the probability of a crash given that an RE conflict S_i has occurred was computed as follows:

$$P_k(C \mid S_i) = \frac{a_i}{\overline{T}_{ki}}$$ (14)

where k is an index for "with FCW system" or "without FCW system". Equation 14 assumes the probability of a crash is inversely proportional to the mean additional lag time required for a collision to occur. Furthermore, as was done in Battelle (2006), the model constants a_i are assumed to be independent of the fleet characteristics (i.e., the same for FCW and non-FCW trucks).

The model constants were derived as follows:

$$a_i = P_{GES}(C) \times P_{GES}(S_i|C) \times \overline{T}_{wo}$$ (15)

where
- $P_{GES}(C)$ is the probability of a crash obtained from the GES database
- $P_{GES}(S_i|C)$ is the probability of being in a conflict i prior to a crash

Given Equation 15, the PR can thus be computed by dividing the geometric mean lag times pertaining to the "with" and "without" FCW system:

$$PR_i = \frac{P_w(C \mid S_i)}{P_{wo}(C \mid S_i)} = \frac{\overline{T}_{wo,i}}{\overline{T}_{w,i}} \qquad \forall\, i.$$ (16)

The geometric mean was used so that the confidence limits could be computed. The PR variance was computed as follows. Based on Equation 16, the following equation was developed:

$$\ln(PR_i) = \ln(\overline{T}_{wo,i}) - \ln(\overline{T}_{w,i}) \qquad \forall\, i.$$ (17)

Assuming independence between the geometric mean lag times, the variance was computed as:

$$Var(\ln(PR_i)) = Var(\ln(\overline{T}_{wo,i})) + Var(\ln(\overline{T}_{w,i})) \qquad \forall\, i.$$ (18)

Given that $\overline{T}_{w,i}$ and $\overline{T}_{wo,i}$ are geometric means, the natural logarithm of these parameters equals the arithmetic mean of the log-transformed data. Consequently, the variance is equal to the variance of the log-transformed data about the arithmetic mean.

Using a Taylor series approximation the variance of PR_i was computed as:

$$Var(PR_i) = e^{2\ln PR} Var(\ln(PR_i)) \qquad \forall\, i.$$ (19)

The CRR, which is a combined metric of the ER and PR, was computed as:

$$CRR_i = ER_i \times PR_i \qquad \forall\, i.$$ (20)

The CRR variance was computed as:

$$Var(CRR_i) = Var(ER_i PR_i) \approx ER_i^2 \times Var(PR_i) + PR_i^2 \times Var(ER_i) \quad \forall \, i \,. \tag{21}$$

The percent reduction in crashes is obtained by subtracting each CRR from 1 and multiplying them by their respective GES weighting:

$$\text{percent reduction} = \sum_{i=1}^{3} P_{GES}(S_i | C) \times (1 - CRR_i) \tag{22}$$

where, $P_{wo}(S_i|C)$ is the relative frequency that conflict S_i precedes a rear-end crash for a particular fleet without the FCW system (again this is obtained from the GES database).

Assuming independence between the various conflict categories, the variance in the percent reduction in crashes can be calculated as:

$$Var(\% R) = \sum_{i=1}^{3} P_{GES}(S_i | C)^2 Var(CRR_i) \,. \tag{23}$$

Finally, the safety benefit was computed as:

$$B = N_{wo} \times \sum_{i} \left[P_{GES}(S_i | C) \times (1 - CRR_i) \right] , \tag{24}$$

where N_{wo} is the average annual number of RE crashes for tractor trailers without the FCW system. Battelle (2006) reports this number to be 23,300 crashes.

CHAPTER 4. RESULTS

This chapter presents the results obtained for the different tasks completed in order to calculate the safety benefits estimates based on the data collected during the DDWS FOT. It presents the resultant events from the trigger and filter logic used, how the data were inspected, how conflicts were classified, shows theoretical alarms resulting from superimposing the Eaton VORAD algorithm on the DDWS FOT data, and resultant safety benefits. Figure 19 provides an overview of the results chapter by showing the number of conflicts that remained after each step described in the previous chapter.
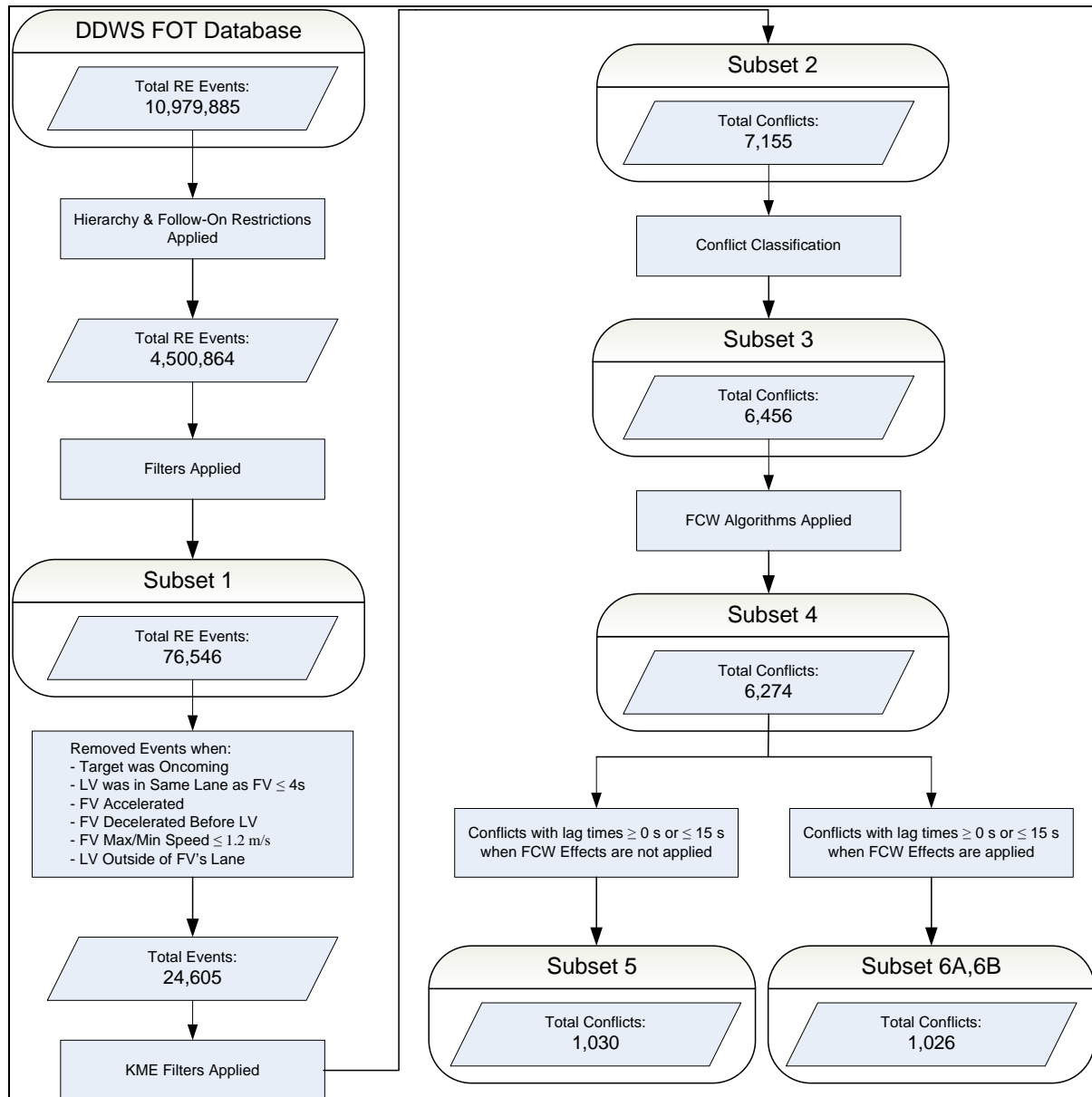
Figure 19. Overview of the Number of Conflicts That Remained After Data Manipulation Was Performed

DDWS FOT DATA AUDIT

The trigger logic identified 10,979,885 events. After applying the trigger hierarchy and follow-on restrictions, there were 4,500,864 triggered events that remained. Table 7 categorizes these events by trigger type. TTC and KME were the predominant trigger types at 50.6 percent and 46.9 percent, respectively.

Table 7. Number of Triggered Events Prior to Filtration

Type	Step 1: Number of Triggered Events	Step 2: Number of Triggered Events After Hierarchy and Follow-On Restriction Is Applied	Percentage (Based on Step 2)	Number of Triggered Events x 1000 per VMT
KME	3,462,818	2,113,039	46.9%	918.7
TTC	7,213,959	2,275,775	50.6%	989.5
FI	303,108	112,050	2.5%	48.7
Total	10,979,885	4,500,864	100.0%	1956.9

Table 8 presents the number of non-threatening triggered events removed through filtration. A large proportion of all of the KME and TTC triggered events were removed by the filtration logic (99.3% and 98.6%, respectively).

Table 8. Number of Non-Threatening Triggered Events Removed by Filtration

Type	Number of Non-Threatening Triggered Events Removed	Percentage Removed	Number of Non-Threatening Triggered Events Removed x 1000 per VMT
KME	2,097,409	99.3%	911.9
TTC	2,243,935	98.6%	975.6
FI	82,974	74.1%	36.1
Total	4,424,318	98.3%	1923.6

A total of 76,546 events remained after the application of the trigger and filter logic. Table 9 categorizes these events by trigger type. TTC and FI were the predominant trigger types at 41.6 percent and 38.0 percent, respectively. These figures equate to 33.3 events per 1,000 VMT (determined using the 2.3 million VMT recorded in the DDWS FOT as the denominator). It should

be noted that this number is greater than the 21.5 events per 1,000 VMT reported in Volvo (2005).

Table 9. Number of Events Identified by Trigger Type (filtered)

Type	Number of Events	Percentage	Number of Conflicts per 1,000 VMT
KME	15,630	20.4%	6.8
TTC	31,840	41.6%	13.8
FI	29,076	38.0%	12.6
Total	76,546	100.0%	33.3

Random visual inspection of the triggered events was iteratively performed during the implementation of the trigger and filter logic to confirm the presence of RE conflicts. This allowed the logic to be refined to capture valid events. After the trigger and filter logic was executed, a visual inspection was performed on 300 of the 76,546 identified events. Table 10 presents estimates for the number of valid events, as well as the lower (p_L) and upper (p_U) bounds for the 95-percent confidence intervals. The visual inspection found that only 67 percent of the data filtered by the algorithms were valid (67% were KME, 41% were TTC, and 94% were FI). At this point it was not possible to say with 95 percent confidence that the dataset was at least 95 percent valid.

Table 10. Point Estimate and 95-Percent Confidence Intervals for the Number of Valid RE Conflicts in the DDWS FOT Database by Trigger Type

Type	Number of Valid Events	$\hat{p}$	$p_L(\alpha = 95\%)$	$p_U(\alpha = 95\%)$
KME	67	0.67	0.6	0.8
TTC	41	0.41	0.3	0.5
FI	94	0.94	0.9	1.0
Total Valid	202	0.67	0.6	0.8

Table 11 presents the classification of the invalid events found in the visual inspection. The invalid events found fall into one of four categories:

1) *Moving Target in Adjacent Lane:* Refers to an LV that was tracked by the Eaton VORAD as being in the same lane as the FV. However, visual inspection revealed that

40

the vehicle was actually located in the adjacent lane. These targets were all moving in the same direction as the FV, but fairly close to it.

2) *Stationary Target in Adjacent Lane:* Refers to a stationary LV that was tracked by the Eaton VORAD as being in the same lane as the FV, but was in reality located in the adjacent lane. An example would be a stopped vehicle on the shoulder of the road.

3) *Oncoming Target:* Refers to an oncoming vehicle that was tracked by the Eaton VORAD as being in the same lane as the FV, but was actually located in the adjacent lane.

4) *Stationary Object:* Refers to an object that was tracked by the Eaton VORAD as being in the same lane as the FV, but was actually located outside of the FV's lane. Examples include road signs, bridges, telephone poles, trees, overhead signs, toll booths, and construction barrels.

Table 11. Classification of Invalid Events

Type	Main Reason for Event to Be Invalid	Number of Invalid Events
KME	Oncoming target	3
	Moving target in adjacent lane	20
	Stationary target in adjacent lane	6
	Stationary object	4
	Total	33
TTC	Oncoming target	34
	Moving target in adjacent lane	16
	Stationary target in adjacent lane	2
	Stationary object	7
	Total	59
FI	Oncoming target	0
	Moving target in adjacent lane	4
	Stationary target in adjacent lane	0
	Stationary object	2
	Total	6

RELEVANT CONFLICTS

The additional filtration performed on the 76,546 triggered events removed 68 percent of these events, leaving a total of 24,605 triggered events. These events were then optimized. The KME filters that were applied removed 71 percent of these events, leaving 7,155 conflicts. Recall that an RE event that passed the KME filter was termed a conflict. Approximately 22 percent of these conflicts were generated by KME triggers, 19 percent were generated by TTC triggers, and 59 percent were generated by FI triggers. A visual inspection of 60 conflicts (20 from each trigger type) was performed afterwards. Table 12 shows the results of the visual inspection.

Table 12. Point Estimate and 95-Percent Confidence Intervals for the Number of Valid Events in the DDWS FOT Database by Trigger Type

Type	Number of Valid Events	$\hat{p}$	$p_L(\alpha = 95\%)$	$p_U(\alpha = 95\%)$
KME	18*	0.90	0.77	1.00
TTC	19*	0.95	0.85	1.00
FI	20	1.00	1.00	1.00
Total	57	0.95	0.85	1.00

*Invalid events consisted of targets in the adjacent lane that were less than the lateral distance threshold.

CONFLICT CLASSIFICATION

Table 13 shows the classification of the identified conflicts by the five pre-collision conflict types. Table 14 classifies the conflicts by the three conflict categories. A total of 699 of the 7,155 conflicts were discarded because they did not fall into any of the five pre-collision conflict types. A total of 6,456 events remained as a result.

Table 13. Frequency Counts of RE Pre-Collision Conflict Types

	Conflict Type	Frequency Count	Percent
1	Closing with constant speed	2,136	34%
	• No lane change and closing with constant speed	2,094	
	• Lane change after closing with constant speed	42	
2	Closing with both vehicles decelerating	1,761	28%
	• No lane change and closing with both vehicles decelerating	1,697	
	• Lane change after closing with both vehicles decelerating	64	
3	Closing preceded by lane change	284	5%
4	Closing with stopped LV	13	0.2%
	• No lane change after closing with stopped LV	13	
	• Lane change after closing with stopped LV	0	
5	Closing with decelerating LV	2,262	36%
	• No lane change and closing with decelerating LV	2,173	
	• Lane change after closing with decelerating LV	89	
	Total	6,456	100%

Table 14. Frequency Counts of RE Pre-Collision Categories

Kinematic Condition of the Following Vehicle	Volvo (2005) Conflict Type		Frequency Count	Percent
Constant Speed	1	Overtaking slower vehicle	4,398	68%
	5	Slowing LV		
Decelerating[1]	2	Overtaking while slowing	1,774	28%
	4	Stopped LV		
Lane Change	3	Changing lanes	284	4%

[1]If the LV is stopped, the conflict is placed in this category regardless of the FV behavior.

FCW ALARMS PRODUCED

The FCW algorithms were applied to the remaining 6,456 conflicts; however, no alarms were generated for 182 of these conflicts (3%). From the resultant 6,274 conflicts that generated one or more alarms a sample set of conflicts were evaluated to validate the algorithm. A total of 22 randomly selected conflicts were evaluated under the five conflict types by the five alarm level matrix (see Table 15). No alarms under the Levels 6, 7, and 10 were available for the conflict type where the FV is closing on a stopped LV (i.e., Type 4). The 22 events were parametrically inspected to ensure that the optimization and classification tasks were successful. The severity and timing of generated alarms were also found to be congruent with those generated by code developed in Volvo (2005).

The outcome of this validation is shown in Table 15. It should be noted that the only event in which an Alarm Level 8 was generated for a conflict type 1 was found to be visually invalid. Additionally, all four of the events in which an Alarm Level 9 was generated for a conflict type 4 were also found to be visually invalid. As such, the file IDs presented in these categories are not exemplary.

Table 15. Outcome of Valid\Invalid FCW Algorithm Sampling

Conflict Type	Alarm Level				
	6 **2 s, Closing**	**7** **1 s, Closing**	**8** **Stationary**	**9** **Slow Moving**	**10** **½ s**
1 Closing with constant speed	valid	valid	invalid	valid	valid
2 Closing with both vehicles decelerating	valid	valid	valid	valid	valid
3 Closing preceded by lane change	valid	valid	valid	valid	valid
4 Closing with stopped LV	*	*	valid	invalid	*
5 Closing with decelerating LV	valid	valid	valid	valid	valid

* This alarm level was not present for the conflict type.

The main goal of this step was to apply the FCW algorithms to the conflicts and identify the types of alarms that were generated. However, in order to describe the conflicts available at this point, several other data of interest are presented. Table 16 is a summary showing which alarm level was generated first for each conflict. Table 17 summarizes the highest urgency alarm that was generated for each conflict. In addition, the number of conflicts where just one alarm type was generated is presented as well (Table 18).

Table 16. Summary of the First Alarm Type That Was Generated per Conflict

	Conflict Type	Alarm 6	Alarm 7	Alarm 8	Alarm 9	Alarm 10	Total
1	Closing with constant speed	1,355	632	1	84	63	2,135
	• No lane change and closing with constant speed	1,327	622	1	82	61	
	• Lane change after closing with constant speed	28	10	0	2	2	
2	Closing with both vehicles decelerating	898	318	167	233	67	1,683
	• No lane change and closing with both vehicles decelerating	865	309	164	221	65	
	• Lane change after closing with both vehicles decelerating	33	9	3	12	2	
3	Closing preceded by lane change	164	48	2	63	2	279
4	Closing with stopped LV	0	0	6	4	0	10
	• No lane change after closing with stopped LV	0	0	6	4	0	
	• Lane change after closing with stopped LV	0	0	0	0	0	
5	Closing with decelerating LV	863	903	22	157	222	2,167
	• No lane change and closing with decelerating LV	831	882	20	139	217	
	• Lane change after closing with decelerating LV	32	21	2	18	5	
	Total	3,280	1,901	198	541	354	6,274

Table 17. Summary of Highest Urgency Alarm Type That Was Generated per Conflict

Conflict Type	Alarm 6	Alarm 7	Alarm 8	Alarm 9	Alarm 10	Total
1 Closing with constant speed	33	32	1	45	2,024	2,135
• No lane change and closing with constant speed	3	22	1	45	2,022	
• Lane change after closing with constant speed	30	10	0	0	2	
2 Closing with both vehicles decelerating	210	135	206	309	823	1,683
• No lane change and closing with both vehicles decelerating	170	124	203	306	821	
• Lane change after closing with both vehicles decelerating	40	11	3	3	2	
3 Closing preceded by lane change	0	15	2	50	212	279
4 Closing with stopped LV	0	0	6	4	0	10
• No lane change after closing with stopped LV	0	0	6	4	0	
• Lane change after closing with stopped LV	0	0	0	0	0	
5 Closing with decelerating LV	190	123	35	241	1,578	2,167
• No lane change and closing with decelerating LV	154	100	33	227	1,575	
• Lane change after closing with decelerating LV	36	23	2	14	3	
Total	433	305	250	649	4,637	6,274

Table 18. Summary of Number of Conflicts That Generated Just One Alarm

Conflict Type	Alarm 6	Alarm 7	Alarm 8	Alarm 9	Alarm 10	Total
1 Closing with constant speed	25	0	0	2	0	27
• No lane change and closing with constant speed	25	0	0	2	0	
• Lane change after closing with constant speed	0	0	0	0	0	
2 Closing with both vehicles decelerating	283	20	134	107	1	545
• No lane change and closing with both vehicles decelerating	276	20	133	102	1	
• Lane change after closing with both vehicles decelerating	7	0	1	5	0	
3 Closing preceded by lane change	15	0	0	6	0	21
4 Closing with stopped lead vehicle	0	0	5	0	0	5
• No lane change after closing with stopped LV	0	0	5	0	0	
• Lane change after closing with stopped LV	0	0	0	0	0	
5 Closing with decelerating LV	257	7	8	50	0	322
• No lane change and closing with decelerating LV	248	7	7	46	0	
• Lane change after closing with decelerating LV	9	0	1	4	0	
Total	580	27	147	165	1	920

FINAL DATASET

A total of 1,030 conflicts remained from the 6,274 conflicts that generated an alarm after those with lag times ≤ 0 s or ≥ 15 s were eliminated. Another visual inspection was performed at this point. A sample of 160 conflicts was visually inspected for validity. Three conflicts were found to be visually invalid. All three involved the detection of an LV in an adjacent lane while the FV was driving in a lane with slight curvature. This minor curvature on the roadway was not perceived by the curve filter, but it was captured by visual inspection of the roadway.

A breakdown of the 1,030 events by each of the five conflict types is summarized in Figure 20. Figure 21 groups these conflicts into the three conflict categories. Figure 22 compares the proportion of conflicts in the final dataset to the proportions observed in GES and the Battelle (2006) study. Compared to GES, the final dataset is similar in that it also had 2 percent of the conflicts fall into Category 3 (FV lane change). However, there was a higher proportion in Cate-

gory 1 (FV constant speed) in the final dataset (69%) compared to 47 percent in GES. Comparing the final dataset to Battelle (2006), the proportion of conflicts in Category 3 was also similar (4% fell into Category 3 in Battelle (2006)). However, there was a higher proportion in Category 1 (FV constant speed) in the final dataset (69%) compared to 44 percent in Battelle (2006).
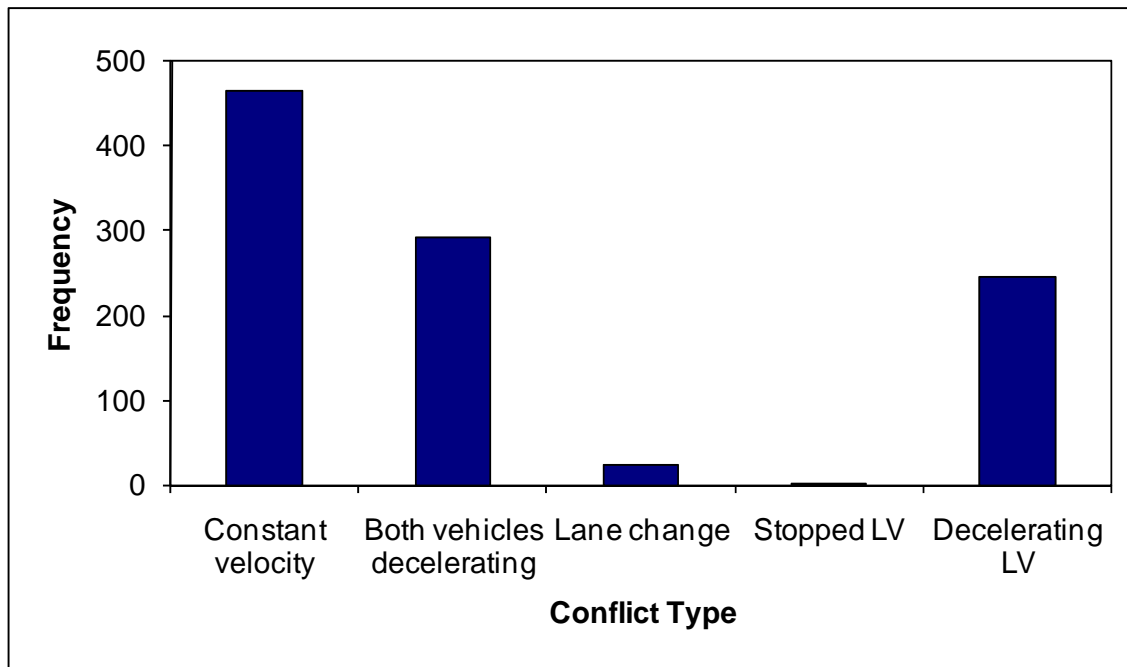
Figure 20. Breakdown of Final Events by Five Conflict Types
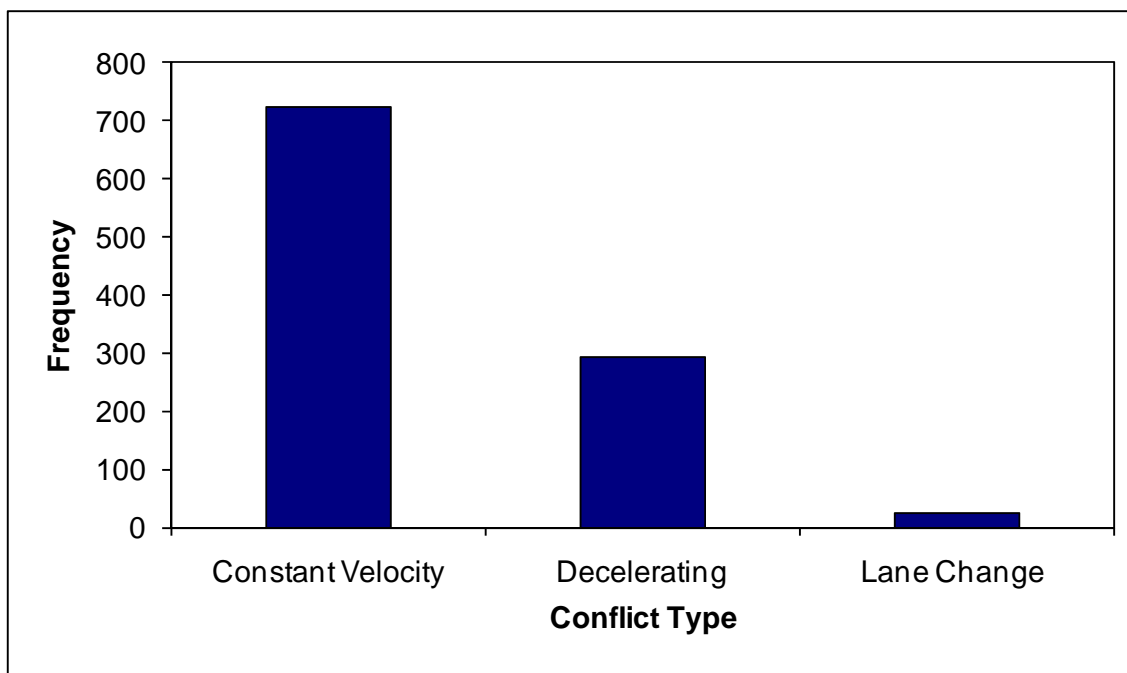
Figure 21. Breakdown of Final Events by Three Conflict Categories
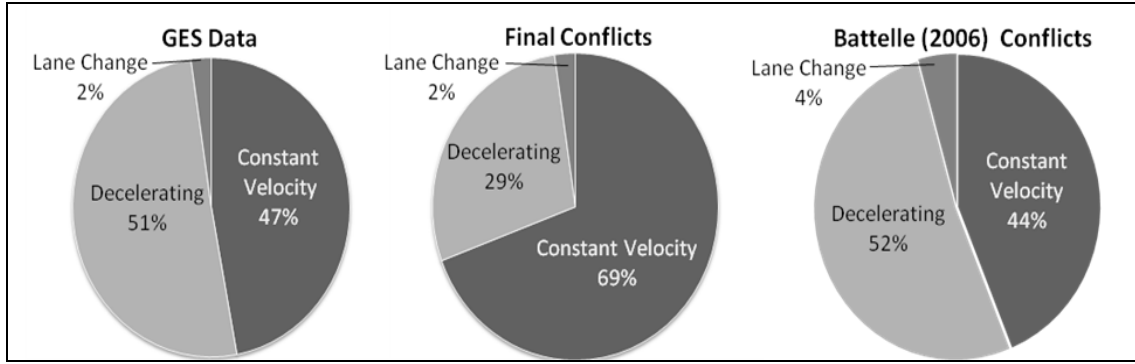
Figure 22. Proportion of the Different Conflict Categories in GES, the Final Dataset, and Battelle (2006)

Table 19 shows the number of conflicts as well as the arithmetic mean and additional lag time available prior to a collision with (T_w) and without (T_{wo}) a theoretical alarm presented for the three conflict categories. It can be seen that by simulating the warning effects of the FCW system, drivers gain an average of 1.43 extra seconds prior to a conflict ($T_w - T_{wo} = 1.43$ s). This additional lag time was illustrated in Figure 15. A t-test revealed that the means for each category differed at the 0.05 level of significance.

Table 19. The Number of Conflicts (N) and Arithmetic Mean Additional Lag Time Available Prior to a Collision (T) With (w) and Without (wo) a Hypothetical FCW System for The Three Conflict Categories

Conflict Category	N_w	T_w (s)	s.e.(s)	N_{wo}	T_{wo} (s)	p-value	Additional Time Afforded by FCW System (s)
Constant Speed	711	7.16	0.002	711	5.34	< 0.001	1.82
Decelerating	291	3.84	0.005	295	3.40	< 0.001	0.44
Lane Change	24	5.62	0.063	24	4.07	< 0.001	1.55
Total	1026			1030			
Average		6.18	0.023		4.75	<0.001	1.43

Figure 23 shows the distribution of lag times for conflicts with and without the FCW system. The two charts illustrate the shift in the lag time to the right (increase in the lag time) as a result of the introduction of the FCW system.
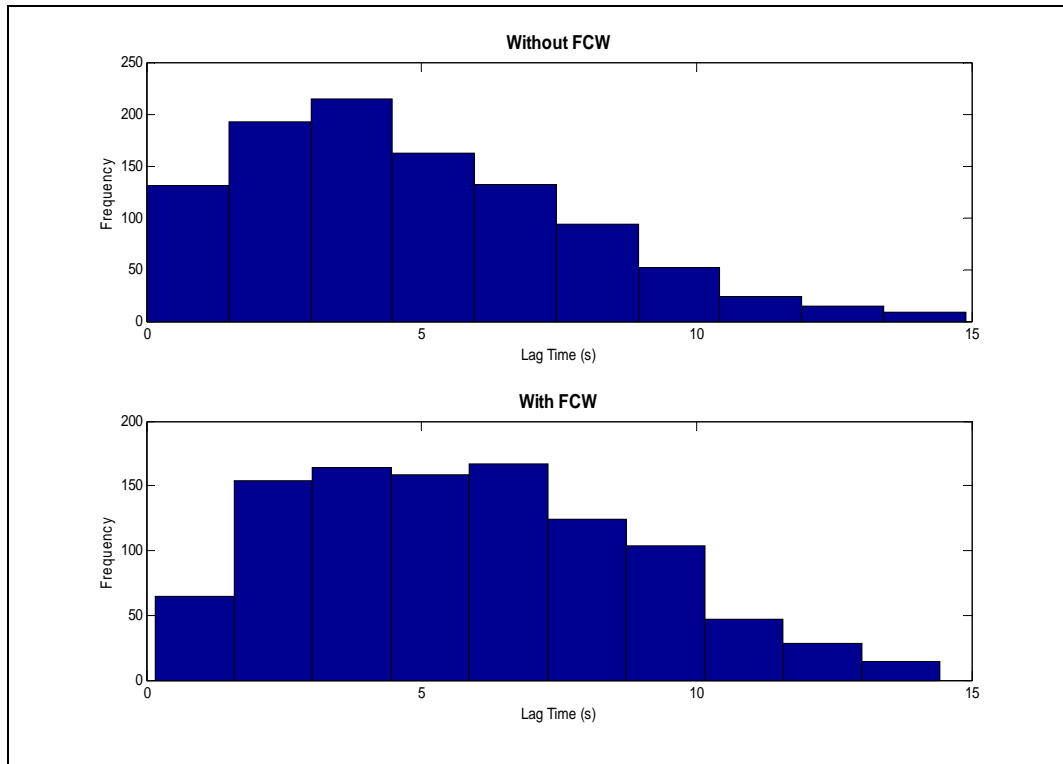
Figure 23. Lag Time Distribution for Conflicts With and Without the FCW System

The Monte Carlo simulation was run on the 1,030 events two times each with a different random number seed. The summary results (average and standard deviation) of the two simulation runs are presented in Table 20. The consistency of the Monte Carlo simulations was tested using a two-sample t-test. A statistical difference between these two runs was not observed.

Table 20. Summary of Monte Carlo Simulation Results for Sample Sizes of 100 Simulations

Conflict Category	Statistics	Run 1	Run 2	p-value
Overall	Arithmetic mean	6.182	6.185	
	Standard deviation	0.048	0.050	0.721
Constant Speed	Arithmetic mean	7.159	7.157	0.816
	Standard deviation	0.064	0.060	
Decelerating	Arithmetic mean	3.841	3.852	
	Standard deviation	0.082	0.092	0.386
Lane Change	Arithmetic mean	5.624	5.660	
	Standard deviation	0.309	0.347	0.435

To inspect the performance of the Monte Carlo simulation, it was run a third time until 150 valid observations were obtained for each conflict. The statistical results are presented in Table 21. A statistical difference between a sample size of 100 and 150 simulations was not found.

Table 21. Summary of Monte Carlo Simulation Results for Sample Sizes of 100 and 150 Simulations

Conflict Category	Statistics	100 Reps	150 Reps	p-value
Overall	Arithmetic mean	6.182	6.181	0.865
	Standard deviation	0.048	0.044	
Constant Speed	Arithmetic mean	7.159	7.157	0.794
	Standard deviation	0.064	0.056	
Decelerating	Arithmetic mean	3.841	3.838	0.774
	Standard deviation	0.082	0.080	
Lane Change	Arithmetic mean	5.624	5.655	0.448
	Standard deviation	0.309	0.321	

FCW SAFETY BENEFITS

The ER, PR, and CRR were used to estimate the safety benefit of the FCW system.

Exposure Ratios

The ER assesses the FCW system's efficacy in helping drivers avoid entering the three RE conflict categories. The ERs and standard error for the three conflict categories are shown in Table 22. ERs less than one suggest that the FCW system helps drivers avoid the driving conflict category. It was expected that the ERs would be approximately equal to 1 since the trucks in the DDWS FOT were not actually instrumented with an FCW system to help drivers avoid driving conflicts. However the ER for the "decelerating" conflict category was computed to be less than 1 owing to a small number of conflicts being discarded due to their lag times being equal to 0 s.

The ERs were all found to be significantly different from 1 except for that pertaining to the lane-change category (p = 0.242).

Table 22. Statistical Analysis of ER

Category	ER_i	s.e.	p-value
Constant Speed	1.000	0.001	1.000
Decelerating	0.986	0.003	< 0.001
Lane Change	1.000	0.043	1.000

Prevention Ratios

The PR indicates whether the FCW system is effective at helping drivers avoid a crash after they enter a driving-conflict situation. Calculation of the PR is the focus of the safety benefits analysis in this study since the task began with identifying conflicts that occurred and then overlaying the FCW algorithm to estimate its effectiveness at preventing crashes. Table 23 shows the probability of a crash with and without the FCW system as well as the model constants a_i. The PRs and s.e. for the three conflict categories are also shown. An asterisk marks those PRs that are signifi-

cantly different from 1 at the 0.05 level of significance. PRs less than 1 suggest that the FCW system helps drivers avoid crashes once they enter one of the three conflict categories.

Table 23. Statistical Analysis of PR

Category	a_i	$P(C|Si)_{wo}$	$P(C|Si)_w$	PR_i	s.e.	p-value
Constant Speed	0.0035	0.0008	0.0006	0.686	0.017	$< 0.001*$
Decelerating	0.0020	0.0009	0.0007	0.837	0.046	$< 0.001*$
Lane Change	0.0001	0	0	0.733	0.102	$0.011*$

*Indicates a statistically significant result

Crash Reduction Ratios

Table 24 presents the CRRs for the three conflict categories. The CRRs were all significant except for that computed for the lane change conflict category.

Table 24. Statistical Analysis of CRR

Category	CRR_i	s.e.	p-value
Constant Speed	0.686	0.031	< 0.001*
Decelerating	0.825	0.062	0.005*
Lane Change	0.733	0.178	0.135

*Indicates a statistically significant result

The overall percent reduction in crashes is shown in Table 25. This estimate was statistically significant ($p < 0.001$). The GES weights used were taken from Battelle (2006).

Table 25. FCW System Efficacy

Category	GES Weight	Efficacy (C_i)
Constant Speed	0.400	31.4%
Decelerating	0.430	17.4%
Lane Change	0.020	26.5%
Total	0.850	20.6%

An FCW system was therefore estimated to provide a 20.6 percent reduction in RE conflicts for applications similar to the long-haul and line-haul truck driving observed in the DDWS FOT. Multiplying this percent reduction by the total annual number of tractor trailer RE crashes ($N_{wo} = 23,300$), an FCW system is estimated to prevent 4,800 RE crashes per year.

CHAPTER 5. DISCUSSION & CONCLUSIONS

DISCUSSION

FCW systems are intended to notify drivers of an impending RE conflict by displaying an alarm when the FV becomes dangerously close to an LV. The Eaton VORAD FCW system uses graded visual and auditory alarms to signal various levels of crash threat to drivers. It is expected that this feedback will modify drivers' behavior to use greater headways, and direct their attention to the forward roadway in threatening situations. Drivers would thus have additional time to perform a collision avoidance maneuver, reducing their impact speed with an LV, or avoiding a collision altogether. This report evaluated the Eaton VORAD FCW algorithm by overlaying its logic on RE conflicts identified in the DDWS FOT dataset.

RE conflicts were parametrically identified using a modification of the logic formulated in Volvo (2005) (see Appendix G for a list of the modifications). First, potential RE events were triggered when: 1) an FV decelerated more than 0.25 g in 1.5 s, 2) an FV had a TTC to an LV less than 4 s, and 3) an FV's FI to an LV was less than 0.5 s. Non-threatening RE events identified through this process were removed using parametric filters. The remaining RE events were then optimized to generate idealized conflict parameters. Hypothetical RE crashes, or conflicts, were said to exist when an FV decelerated more than 3 m/s^2 (10 ft/s^2) to avoid an LV in the same lane. Conflict identification was made under the assumption that drivers do not input a response after the onset of braking. The Eaton VORAD FCW algorithms were then applied to these conflicts. The timing and severity of the FCW alarms were determined. Driver PRTs and deceleration rates for each alarm were modeled using naturalistic driving data collected in Volvo (2005). Driver behavior in response to the FCW alarms was then simulated using a Monte Carlo approach. The number of RE crashes avoided given FCW system feedback, as well as the additional time drivers would have to respond in avoiding a RE crash, was determined from the simulation.

The safety benefits afforded by an FCW system, as determined by answering the three research questions posed in Chapter 1, were computed using a modification of the methods presented in Battelle (2006) (see Appendix G for a list of the modifications).

The first research question, which asked how well an FCW system prevents heavy-vehicle drivers from encountering RE conflict scenarios, was addressed by computing the ER. It was found that the ER did not show a meaningful improvement in RE conflict avoidance. This result contrasted the ER found in Battelle (2006), which Table 26 shows was as low as 0.48 for constant speed RE conflicts. Battelle's (2006) results suggest that an FCW system could be expected to reduce the number of constant-speed RE conflict scenarios encountered. It should be noted that the high ER found in the current study is not surprising because the vehicles in the DDWS FOT did not have an FCW system to warn drivers they were entering dangerous conditions.

Table 26. ER Estimates by Conflict Category

Category	ER_{Current Study}	ER_{Battelle (2006)}
Constant Speed	1.00	0.48*
Decelerating	0.97*	1.10
Lane Change	1.00	0.85

* Indicates statistical significance with 95% confidence.

The second research question, which asked how well an FCW system prevents crashes once heavy vehicles have entered RE conflict scenarios, was addressed by computing the PR. It was found that the PR showed a meaningful improvement in crash avoidance once drivers entered RE conflict scenarios. This result contrasted that found in Battelle (2006), in which Table 27 shows its PR was not meaningfully different from 1. It should be noted that none of Battelle's PR estimates were found to significantly different from 1, whereas all three PR estimates derived in the current study did significantly differ from 1.

Table 27. PR Estimates by Conflict Category

Category	PR_{Current Study}	PR_{Battelle (2006)}
Constant Speed	0.69*	1.05
Decelerating	0.83*	0.90
Lane Change	0.74*	0.82

* Indicates statistical significance with 95% confidence.

The third research question, which asked how many crashes an FCW system could be expected to prevent (given a national deployment across the entire fleet of heavy vehicles) was addressed by combining the ER and PR estimates into an overall measure, or CRR (Table 28). In doing so, it was found that an FCW system was estimated to reduce the number of RE crashes by 21 percent, preventing a total of 4,800 tractor-trailer RE crashes per year (Table 29). This result is equivalent to the 21-percent reduction in crashes estimated in Battelle (2006). However, the benefit estimated in the Battelle study was not found to be statistically significant, whereas the estimate in the current study was found to be statistically significant.

Table 28. CRR Estimates by Conflict Category

Category	CRR_{Current Study}	CRR_{Battelle (2006)}
Constant Speed	0.69*	0.51
Decelerating	0.83*	0.99
Lane Change	0.74	0.70

* Indicates statistical significance with 95% confidence.

Table 29. Estimate of the Percent Reduction in RE Crashes

Category	%R$_{Current Study}$	%R$_{Battelle (2006)}$
Constant Speed	13%	20%
Decelerating	7%	0%
Lane Change	1%	1%
Total	21%	21%

The implications are as follows: Battelle estimates that a 21-percent safety improvement is attainable by an FCW system that reduces the number of RE conflict scenarios encountered, but does not necessarily help drivers avoid crashes once they enter RE conflict scenarios. In contrast, the current study estimates that the same 21-percent safety improvement is attainable by an FCW system that helps drivers avoid crashes once RE conflict scenarios are encountered. It was not possible to accurately estimate the benefit from helping drivers avoid RE conflict scenarios altogether due to the nature of this study. Since the FCW system effects were simulated using driver behaviors observed in RE conflict scenarios and because DDWS FOT drivers did not actually receive FCW alarms, particularly the first five grades of visual alarms offered by the Eaton VORAD FCW system, behavior that may lead to avoiding the RE conflicts altogether was not modeled. Had drivers received such earlier feedback, the number of RE conflicts encountered may be less, thus lowering the ER, and improving the safety benefit estimate calculated in this study.

CONCLUSIONS

The estimated 21-percent reduction in RE crashes is notable. This finding suggests that an FCW system stands to save a significant amount of lives. This is especially true given that RE crashes resulting from heavy vehicles tend to be more catastrophic due to the type of impact these vehicles may cause. For this reason, the amount of damage resulting from heavy-vehicle crashes can also be expected to be considerable. Drivers receiving FCW feedback were estimated to brake earlier. It can therefore be expected that their impact velocities with LVs may be slower, thus reducing the severity of their impact with an LV. By reducing the number of RE crashes, FCW systems also stand to improve traffic flow. This is particularly true since heavy vehicles involved in collisions tend to close off multiple lanes because of their size. The resulting reduction in traffic congestion would also benefit society by reducing the amount of carbon dioxide emissions that result from suboptimal consumption of gasoline and diesel fuel, particularly while idling. For these reasons, FCW systems can prove to be promising.

LIMITATIONS

As with any type of research, several limitations need to be mentioned:

1. *Missed RE Conflicts*

As part of the DDWS FOT data reduction (unrelated to this particular project), RE conflicts were identified through both parametric and 100-percent visual inspection. Conflicts were categorized as either crashes, near-crashes, or crash relevant conflicts. A crash was defined as any contact made with an object, either moving or fixed, at any speed in which kinetic energy was measurably transferred or dissipated. A near-crash was defined as any circumstance requiring a rapid, evasive maneuver by the FV or LV to avoid a crash. A crash-relevant conflict was defined as any circumstance that required a crash avoidance response on the part of the FV or LV that was less severe than a rapid evasive maneuver, but greater in severity than a "normal maneuver" to avoid a crash. The DDWS FOT data reduction effort identified 596 RE conflicts (1 RE crash, 26 RE near-crashes, and 569 RE crash-relevant conflicts). Only 7 of the 596 conflicts validated in the DDWS FOT were identified by the current study's conflict identification process (Figure 24). Six of these conflicts were identified by KME logic, while one was identified by TTC logic. All seven commonly identified conflicts were classified as crash-relevant conflicts in the DDWS FOT visual data reduction. The one valid RE crash and 26 valid RE near-crashes were removed by the filter logic. They were thus not included in the safety benefit evaluation.

Figure 24. Venn Diagram Showing the Number of Conflicts That Coincide Between the Current Study and Those Identified in the DDWS FOT Data Reduction

2. RE Conflicts Were Parametrically Identified

A 100-percent visual inspection of each conflict to certify its validity was outside the scope of this study. Visual inspection performed on a sample of conflicts revealed that some non-threatening RE events were not removed through the filtration process. A conflict was considered valid if the LV was located in the FV's lane. Based on the visual sampling, it is estimated that approximately 2 percent of the identified conflicts are not valid.

3. False Alarms

Some concern exists on the impact of false alarms. False alarms, also known as nuisance alarms, are alarms generated when no driver response is required. Drivers' responsiveness to valid FCW alarms can decrease as the number of false alarms increases. This is because drivers may become biased into thinking an FCW alarm is false. The safety benefit estimate does not adequately consider the implication of a high false alarm rate on the efficacy of the FCW system. An understanding of how multiple false alarms may bias drivers to ignore credible alerts is needed.

4. FCW System Novelty

The data input to the simulation is based on FOT data collected over the course of a year. As such, the driver behavior observed with the FCW system may not be representative of behavior pertaining to drivers who have adapted to the novelty of the FCW alarms. Novelty effects might be studied by comparing driver response behavior to the alarms over time. Such comparisons may reveal whether the safety benefits observed are owing to driver over-reliance on the FCW system at the onset of the study.

FUTURE RESEARCH

Future research should focus on the conflicts that were not identified as they may offer a wealth of insight into the efficacy of an FCW system in preventing or reducing the effects of RE crashes. This can be accomplished by:

- Applying the FCW alarm algorithms to these conflicts and estimating driver PRTs to the theoretical alarms.
- Assessing whether drivers would have avoided these conflicts given their observed level of deceleration.
- Using this knowledge to determine how FCW systems can be improved.
- Providing that the conflicts occur given FCW feedback, the impact speed with FCW feedback could be compared to that when FCW feedback is unavailable. A reduction in impact speed is equally of interest in crash mitigation.

Naturalistic data can offer additional insight into the benefits of an FCW system. Another area of future research could be to investigate what modifications to the trigger and filter logic could be performed to capture the crash/near-crash conflict data that was omitted from this study. Visual inspection could be performed to monitor the performance of the conflict identification logic. The trigger and filter logic could be adjusted in an iterative format. The ability of this logic to accurately identify conflicts may prove to be invaluable.

The current analysis assumes that the crash risk is inversely proportional to the additional lag time in the estimation of the PR. Another area of future research could be to test other measures as explanatory variables. One potential explanatory variable is the shortest TTC for each event. It is proposed that a shifted negative exponential function is used to relate the TTC to the crash risk. Using actual FOT data, these parameters can be calibrated and the crash savings of an FCW system can be compared to the findings of this study. Another approach, which can easily be implemented within microscopic traffic simulation software, is to estimate the TTC over all valid data at a deci-second level of resolution. The hypothesis will then be that a reduction in the TTC results in an incremental increase in the crash risk so that when a vehicle eventually crashes the summation of the incremental crash risks sums up to 1.0 (probability of a crash is 1.0 when a crash occurs). The calibration of the parameters can be computed by analyzing the near and actual crashes from the DDWS FOT database. Subsequently, the model can be applied to the entire 6,456 events to compute the crash risk. Again the study results can be compared to the findings of the study presented in this report. Furthermore, this approach can be easily implemented within microscopic traffic simulation software. The software can also be adjusted to model the car-following behavior associated with an FCW system and, subsequently, the system-wide impacts of an FCW system can be computed for different network configurations, different traffic demands, and different percentages of truck volumes.

REFERENCES

Battelle (2006). Evaluation of the Volvo Intelligent Vehicle Initiative Field Operational Test (No. version 1.2). Washington, DC.

Eaton VORAD Web site (2001). "Eaton VORAD Collision Warning System - EVT-300 Technical Highlights." 2007, from http://path.berkeley.edu/~cychan/Research_and_Presentation/Pedestrian_Detection_TO5 200/Sensors_Information/EVT-300.pdf.

Hanowski, R. J., Blanco, M., Nakata, A., Hickman, J. S., Schaudt, W. A., Fumero, M. C., et al. (in press). *The drowsy driver warning system field operational test, data collection final report* (No. DTNH22-00-C-07007, Task Order 14). Blacksburg, VA: Virginia Tech Transportation Institute.

Hickman, J. S.,Knipling, R. R., et al. (2005). Commercial vehicle data collection & countermeasure assessment project. Phase I: Preliminary analysis of data collected in the drowsy driver warning system field operational test- Task 3: Preliminary analysis of partial countermeasure data. Blacksburg, VA, Virginia Tech Transportation Institute.

Highway Capacity Manual (2000) Transportation Research Board, National Research Council, Washington, DC.

Martin, P.G., & Burgett, A.L. (2001). Rear-End Collision Events: Characterization of Impending Crashes. Proceedings of the 1st Human-Centered Transportation Simulation Conference, The University of Iowa, Iowa City, Iowa, November 4-7, 2001. (ISSN 1538-3288).

Volvo (2005). Volvo Trucks Field Operational Test: Evaluation of Advanced Safety Systems for Heavy Truck Tractors. Washington, DC.

APPENDIX A – KME0 AND KME1 ALGORITHMS

Is lead vehicle constant speed?

$|a_L| \leq a_{L,chk}$?

N

Is lead vehicle decelerating?

$a_L < -a_{L,chk}$?

N → No KME0 Trigger

Y

Y

Lead Vehicle Constant Speed (LVCS)

$$a_{F,req} = \frac{\dot{R}^2}{2(R + \dot{R} * t_{react})}$$

Lead Vehicle Decelerating (LVD)

$$a_{F,req} = \frac{V_F^2}{2\left[\dfrac{V_L^2}{2a_L} + V_F * t_{react} - R\right]}$$

Is following vehicle required deceleration greater than max?

$a_{F,req} < -a_{F,max}$?

N → No KME0 Trigger

Y

KME0 Trigger

Variables:
- V – Velocity
- a – Acceleration
- R – Range
- $\dot{R}$ – Range Rate
- t – Time
- F – Following Vehicle
- L – Lead Vehicle

Constants:
- $a_{L,chk}$ = 0.25 ft/s^2
- $a_{F,max}$ = 8 ft/s^2
- t_{react} = 1.5 sec

Figure 25. Algorithm for KME0

(Taken from Volvo [2005])

Is lead vehicle
accel > threshold?

$a_L > -a_{L,thr}$?

N

Y

LVCS

$$a_{F,req} = \frac{\dot{R}^2}{2(R + \dot{R} * t_{react})}$$

LVD

$$a_{F,req} = \frac{V_F^2}{2\left[-\dfrac{V_L^2}{2a_{L,thr}} + V_F * t_{react} - R\right]}$$

Is following vehicle
required deceleration
greater than max?

$a_{F,req} < -a_{F,max}$?

N

No KME1
Trigger

Y

KME1
Trigger

Variables:

V – Velocity
a – Acceleration
R – Range
$\dot{R}$ – Range Rate
t – Time
F – Following Vehicle
L – Lead Vehicle

Constants:

$a_{L,thr}$ = 6.4 ft/s^2
$a_{F,max}$ = 8 ft/s^2
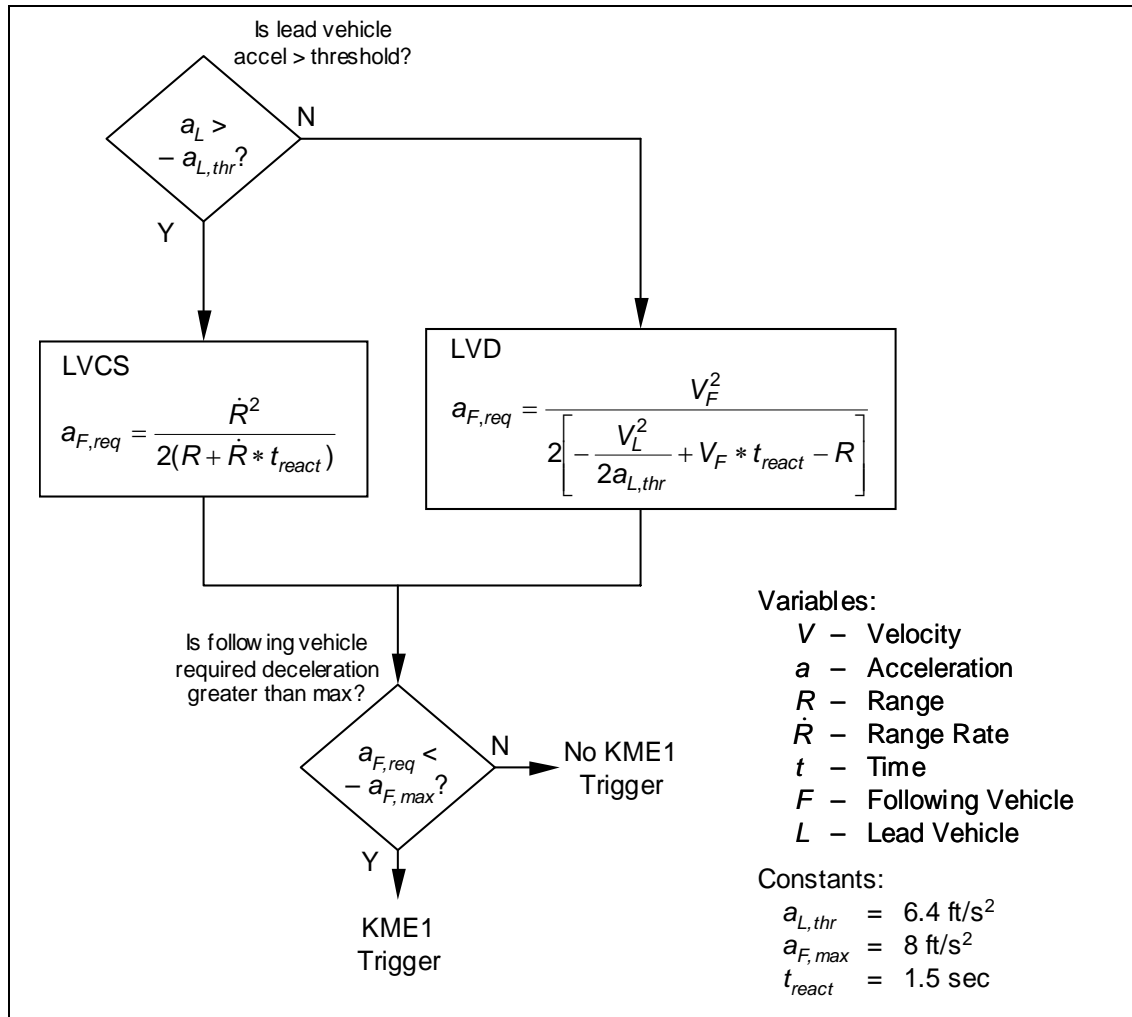t_{react} = 1.5 sec

Figure 26. Algorithm for KME1

(Taken from Volvo [2005]).

APPENDIX B – OPTIMIZATION PROCEDURE

The optimization procedure is based on earlier work done by Martin and Burgett (2001). The procedure involves three steps:

Step 1. Retrieve the three input time histories from the raw (smoothed) data. The raw data variables include V_F, R, and V_L.

Step 2. Express theoretical time-histories as functions of time, t. These variables are distinguished by adding an inverted "v" to each variable (e.g., $\hat{V}_F$ to denote the theoretical speed of the following vehicle). The procedure is summarized as follows. Write the expressions for the times when both vehicles start to decelerate t_{Fb} and t_{Lb}, when they stop decelerating t_{Ff} and t_{Lf}, and then write expressions for the decelerations $\hat{d}_L$ and $\hat{d}_F$ as functions of t, t_{Fb}, t_{Lb}, t_{Ff}, t_{Lf} as

$$t_{Ff} = \frac{(\hat{V}_{Fo} - \hat{V}_{Ff})}{\hat{d}_F} + t_{Fb}, \tag{25}$$

$$t_{Lf} = \frac{(\hat{V}_{Lo} - \hat{V}_{Lf})}{\hat{d}_L} + t_{Lb}, \tag{26}$$

$$\hat{d}_F(t) = \begin{cases} 0; & t < t_{Fb} \\ \hat{d}_F; & t_{Fb} < t < t_{Ff} \\ 0; & t > t_{Ff} \end{cases} \tag{27}$$

$$\hat{d}_L(t) = \begin{cases} 0; & t < t_{Lb} \\ \hat{d}_L; & t_{Lb} < t < t_{Lf} \\ 0; & t > t_{Lf} \end{cases} \tag{28}$$

Where $\hat{V}_{Fo}$ and $\hat{V}_{Lo}$ are the initial theoretical speeds for the FV and LV, respectively and $\hat{V}_{Ff}$ and $\hat{V}_{Lf}$ are the final theoretical speeds for the FV and LV, respectively.

Write the expressions for the theoretical time-histories of velocities $\hat{V}_F$ and $\hat{V}_L$, travel distances $\hat{X}_F$ and $\hat{X}_L$, and range $\hat{R}$ as functions of t, t_{Fb}, t_{Lb}, t_{Ff}, t_{Lf}, and the seven variables.

$$\hat{V}_F(t) = \begin{cases} \hat{V}_{Fo}; & t < t_{Fb} \\ \hat{V}_{Fo} + \hat{d}_F(t_{Fb} - t); & t_{Fb} \le t < t_{Ff} \\ \hat{V}_{Ff}; & t \ge t_{Ff} \end{cases} \tag{29}$$

$$\hat{V}_L(t) = \begin{cases} \hat{V}_{Lo}; & t < t_{Lb} \\ \hat{V}_{Lo} + \hat{d}_L(t_{Lb} - t); & t_{Lb} \le t < t_{Lf} \\ \hat{V}_{Lf}; & t \ge t_{Lf} \end{cases} \tag{30}$$

$$\hat{X}_F(t) = \begin{cases} \hat{V}_{Fo}t; & t < t_{Fb} \\ \hat{V}_{Fo}t + 0.5\,\hat{d}_F(t - t_{Fb})^2; & t_{Fb} \le t < t_{Ff} \\ \hat{V}_{Ff}(t - t_{Ff}); & t \ge t_{Ff} \end{cases} \tag{31}$$

$$\hat{X}_L(t) = \begin{cases} \hat{V}_{Lo}t; & t < t_{Lb} \\ \hat{V}_{Lo}t + 0.5\,\hat{d}_L(t - t_{Lb})^2; & t_{Lb} \le t < t_{Lf} \\ \hat{V}_{Lf}(t - t_{Lf}); & t \ge t_{Lf} \end{cases} \tag{32}$$

$$\hat{R}(t) = \hat{X}_L(t) - \hat{X}_F(t) \tag{33}$$

Step 3. Apply a bi-level non-linear optimization procedure to compute the eight variables (initial speed, time to start deceleration, deceleration rate, and final speed for both the FV and LV). The first optimization minimizes the sum of squared error, E, between the observed and estimated speed profile for the FV as:

$$E = \sum_t \left(\hat{V}_F(t) - V_F(t)\right)^2 \tag{34}$$

This optimization is done first given that the FV speed is directly measured in the field, and the LV speed is computed from the FV speed. Given the higher accuracy of the FV speed, the FV theoretical speed is computed initially. Once the FV speed profile is optimized, the second level of optimization estimates the LV parameters by minimizing the following objective function:

$$E = \sum_t \left(\hat{V}_L(t) - V_L(t)\right)^2 \tag{35}$$

The optimization is subject to constraints (25) through (33).

The bi-level optimization uses a heuristic procedure to compute the optimum objective function and control variables. The first level optimizes the FV parameters, while the second level optimizes the LV parameters. The heuristic, which was written as a MAT-LAB code (Appendix C), operates as follows:

1. Iterate for each of the two vehicles.
2. Iterate over a user-specified number of iterations (which was set at five to balance accuracy and computational speed).

3. Vary the four vehicle parameters ($\hat{V}_{Fo}$, t_{Fb}, $\hat{d}_F$, and $\hat{V}_{Ff}$) simultaneously considering the following:
4. Vary the initial and final speed over the range of speeds observed in a user specified window.
5. Vary the brake time and deceleration level within a user-specified search range.
6. Select the optimum solution and refine the search range for each iteration by either decreasing the search range, fine tuning the search resolution, or a combination of both.
7. Continue the search by refining the search windows until the number of iterations is reached or a solution change is within the user-specified threshold.
8. The optimization may be terminated if t_{Fb} is less than the time at which the LV appeared because it implies that the FV is reacting to a stimulus other than the LV.

APPENDIX C – OPTIMIZATION PROCEDURE MATLAB® CODE

```
function [Tfb,Df,Vfe,Tlb,Dl,Vle,Re,flag1,flag2,Vl_max,Vl_min,Vf_max,Vf_min]=OptProfile(Zero,T,Vf,Vl,R,Lat,LCh,flag)
% This function finds the profile of a vehicle

% ----------------------- Initialize Variables ----------------------
Vdiff = 0; % Maximum allowed difference in the follower vehicle speed profile
nrow1 = 20;  % Number of rows to be considered in computing the initial speed
nrow2 = 40;  % Number of rows to be considered in computing the final speed
nrow3 = 75;  % Number or rows to be considered in computing the time to brake
Dmax = 8;  % Maximum deceleration rate considered
niter = 5; % Number of iterations
% --------------------------------------------------------------------

flag1=0;
flag2=0;%no lane change
FL=0;
r1 = min(find(Vl>0 | Vl<0)):1:max(find(Vl>0 | Vl<0));
Vl_max=max(find(Vl>0 | Vl<0));;
Vl_min=min(find(Vl>0 | Vl<0));;
r2 = 1:1:max(find(Vf>=0));
Vf_max=max(find(Vf>=0)); Vf_min=min(find(Vf>=0));
r=r1;
Re=NaN(151,1); Vfe=[]; Vle=[];
Vf1=Vf(r2);

if(length(r)>40) % Only include scenarios with more than 4 seconds of data
    Later=Lat(min(r):max(r)); % Only use data where lead vehicle is present
    OutofLn = find(Later<-1.905 | Later>1.905);%Out of Lane
    Vl = Vl(min(r):max(r)); % Only use data where lead vehicle is present
```

```matlab
R = R(min(r):max(r));      % Only use data where lead vehicle is present
T = T(min(r):max(r));      % Only use data where lead vehicle is present
af = ([Vf1(2:end);Vf1(end)]-Vf1(1:end))/0.1;
al = ([Vl(2:length(r));Vl(length(r))]-Vl(1:length(r)))/0.1;
if(max(al)>8 |min(al)<-8)
   flag1=5;
end

if(max(af)>8 |min(af)<-8)
   flag1=4;
end
if(flag1==0)
    if(max(Vf1)-min(Vf1)>=Vdiff)  % Exclude scenarios where the following vehicle does not change speed
       if(length(find(LCh(r)>0))>0)%Lane change occurs
           flag2=1;
       end

       if(flag2==1)
          if(min(find(LCh(r)>0))<Zero)%Lane change prior to Critical Point
            flag2=2;
          else
            flag2=10;%Lane change after Critical Point
          end

       end

       if(length(OutofLn)>0& flag2==0)
           flag1=3; %Out of lane and No Lane change

       end
    else
```

```matlab
            flag1=2;%this is not imposed
          end
          if(Vl<-1.83)
              flag1=2;%On coming Targets <-6ft/s
          end
      end

  else
     flag1=1;
end
% Optimize the vehicle speed profiles independently using a heuristic approach
if(flag1==0)
 for i=2:-1:1
  E = 10000;
  if(i==1); r=r1; else; r=r2; end
  if(i==1)
     V0min = min(Vl(1:round(nrow1))); V0max = max(Vl(1:round(nrow1)));
     Vfmin = min(Vl(length(r)-nrow2+1:length(r)));Vfmax = max(Vl(length(r)-nrow2+1:length(r)));
     Tbmin = 1; Tbmax = min(length(r),nrow3); V=Vl;
  else
     V0min = min(Vf1(1:nrow1*2)); V0max = max(Vf1(1:nrow1*2));
     Vfmin = min(Vf1(length(r)-nrow2+1:end));Vfmax = max(Vf1(length(r)-nrow2+1:end));
     Tbmin = 1; Tbmax = min(length(r),nrow3); V=Vf1;
  end
  for it=1:niter
     V0 = (V0max+V0min)/2; Vx = (Vfmax+Vfmin)/2;
     V0min = V0 - (V0max-V0min)/2;
     V0max = V0 + (V0max-V0min)/2;
     for v1 = linspace(V0max,V0min,7);
        Vfmin = Vx - (Vfmax-Vfmin)/2;
        Vfmax = Vx + (Vfmax-Vfmin)/2;
```

```
for v2 = linspace(Vfmax,Vfmin,7);
  step1 = niter-it+1;
  if(it>1); Tbmin=round(max((Tb-nrow3/2/it),1)); Tbmax=round(min(length(r),Tb+nrow3/2/it)); end
  for v3 = Tbmin:step1:Tbmax;
   step2 = 1/it;
   if(it==1)
     D1=0; D2=Dmax;
    else
     D1=min(D+Dmax/it,D-Dmax/it); D2=max(D+Dmax/it,D-Dmax/it);
     if(v2<=v1);
       D1=max(D1,0); D2=min(D2,9.81);
      else
       D1=max(D1,-9.81); D2=min(D2,0);
      end
    end
   for v4 = D1:step2:D2;
     if(v4>=0)
       temp = [ones(1,v3)*v1 max(v1 - v4*(0.1:0.1:(length(r)-v3)/10),v2)]';
      else
       temp = [ones(1,v3)*v1 min(v1 - v4*(0.1:0.1:(length(r)-v3)/10),v2)]';
      end
     if(i==1)
       Ecalc = sum((V - temp).^2);
      else
       Ecalc = sum((V - temp).^2);
      end
     if(Ecalc<E)
       E = Ecalc; V0=v1; Vx=v2; Tb=v3; D=v4;
       if(i==1)
         Dl=v4; Tlb=v3/10; Vle=temp';
        else
```

```
                Df=v4; Tfb=v3/10; Vfe=temp';
            end
          if(E==0.0);break;end
        end
       if(E==0.0);break;end
     end
    if(E==0.0);break;end
   end
   if(E==0.0);break;end
  end
  if(E==0.0);break;end
 end
 if(E==0.0);break;end
 end
end
R(min(r):max(r))=R;
R(1:min(r)-1)=NaN;
R(max(r)+1:151)=NaN;
Vl(min(r):max(r))=Vl;
Vl(1:min(r)-1)=NaN;
Vl(max(r)+1:151)=NaN;
Vle(min(r):max(r))=Vle;
Vle(1:min(r)-1)=NaN;
Vle(max(r)+1:151)=NaN;
if(length(Vfe)<151)
 Vfe(min(r2):max(r2))=Vfe;
 Vfe(1:min(r2)-1)=NaN;
 Vfe(max(r2)+1:151)=NaN;
 end

end
```

```
% Discard events that have a Tfb< time at which lead vehicle appears
if(flag1==0)
   if(Tfb*10<=min(r) & min(r)>=1)
      flag1=4;
   end
   if(Tfb*10>max(r) & min(r)>=1)
      flag1=4;
   end
end

% Compute the estimated range for valid events and parameters for non-valid events
if(flag1==0)
 Re(min(r)) = R(min(r));
 for i=min(r)+1:max(r)
  Re(i)=Re(i-1)+(Vle(i-1)-Vfe(i-1))*0.1;
 end
else
   Tfb=NaN; Df=NaN; Vfe=NaN(151,1); Tlb=NaN; Dl=NaN; Vle=NaN(151,1); Re=NaN(151,1);
end
```

function [Tfb,Df,Vfe,Tlb,Dl,Vle,Re,flag1,flag2,Vl_max,Vl_min,Vf_max,Vf_min]=OptProfile(Zero,T,Vf,Vl,R,Lat,LCh,flag)
% This function optimizes finds the profile of a vehicle

% ----------------------- Initialize Variables ----------------------

```
Vdiff = 0;   % Maximum allowed difference in the follower vehicle speed profile
nrow1 = 20;  % Number of rows to be considered in computing the initial speed
nrow2 = 40;  % Number of rows to be considered in computing the final speed
nrow3 = 75;  % Number or rows to be considered in computing the time to brake
Dmax = 8;    % Maximum deceleration rate considered
niter = 5;   % Number of iterations
% -----------------------------------------------------------------------

flag1=0;
flag2=0;%no lane change
FL=0;
r1 = min(find(Vl>0 | Vl<0)):1:max(find(Vl>0 | Vl<0));
Vl_max=max(find(Vl>0 | Vl<0));;
Vl_min=min(find(Vl>0 | Vl<0));;
r2 = 1:1:max(find(Vf>=0));
Vf_max=max(find(Vf>=0)); Vf_min=min(find(Vf>=0));
r=r1;
Re=NaN(151,1); Vfe=[]; Vle=[];
Vf1=Vf(r2);

if(length(r)>40)   % Only include scenarios with more than 4 seconds of data
    Later=Lat(min(r):max(r)); % Only use data where lead vehicle is present
    OutofLn = find(Later<-1.905 | Later>1.905);%Out of Lane
    Vl = Vl(min(r):max(r));   % Only use data where lead vehicle is present

    R = R(min(r):max(r));     % Only use data where lead vehicle is present
    T = T(min(r):max(r));     % Only use data where lead vehicle is present
    af = ([Vf1(2:end);Vf1(end)]-Vf1(1:end))/0.1;
    al = ([Vl(2:length(r));Vl(length(r))]-Vl(1:length(r)))/0.1;
    if(max(al)>8 |min(al)<-8)
      flag1=5;
```

75

```matlab
        end

   if(max(af)>8 |min(af)<-8)
       flag1=4;
   end
   if(flag1==0)
        if(max(Vf1)-min(Vf1)>=Vdiff)  % Exclude scenarios where the following vehicle does not change speed
           if(length(find(LCh(r)>0))>0)%Lane change occurs
                flag2=1;
           end

           if(flag2==1)
              if(min(find(LCh(r)>0))<Zero)%Lane change prior to Critical Point
                 flag2=2;
              else
                 flag2=10;%Lane change after Critical Point
              end

           end

           if(length(OutofLn)>0& flag2==0)
                flag1=3; %Out of lane and No Lane change

           end
        else
           flag1=2;%this is not imposed
        end
        if(Vl<-1.83)
           flag1=2;%On coming Targets <-6ft/s
        end
    end
```

```
    else
        flag1=1;
end
% Optimize the vehicle speed profiles independently using a heuristic approach
if(flag1==0)
  for i=2:-1:1
    E = 10000;
    if(i==1); r=r1; else; r=r2; end
    if(i==1)
        V0min = min(Vl(1:round(nrow1))); V0max = max(Vl(1:round(nrow1)));
        Vfmin = min(Vl(length(r)-nrow2+1:length(r)));Vfmax = max(Vl(length(r)-nrow2+1:length(r)));
        Tbmin = 1; Tbmax = min(length(r),nrow3); V=Vl;
    else
        V0min = min(Vf1(1:nrow1*2)); V0max = max(Vf1(1:nrow1*2));
        Vfmin = min(Vf1(length(r)-nrow2+1:end));Vfmax = max(Vf1(length(r)-nrow2+1:end));
        Tbmin = 1; Tbmax = min(length(r),nrow3); V=Vf1;
    end
    for it=1:niter
        V0 = (V0max+V0min)/2; Vx = (Vfmax+Vfmin)/2;
        V0min = V0 - (V0max-V0min)/2;
        V0max = V0 + (V0max-V0min)/2;
        for v1 = linspace(V0max,V0min,7);
            Vfmin = Vx - (Vfmax-Vfmin)/2;
            Vfmax = Vx + (Vfmax-Vfmin)/2;
            for v2 = linspace(Vfmax,Vfmin,7);
                step1 = niter-it+1;
                if(it>1); Tbmin=round(max((Tb-nrow3/2/it),1)); Tbmax=round(min(length(r),Tb+nrow3/2/it)); end
                for v3 = Tbmin:step1:Tbmax;
                    step2 = 1/it;
                    if(it==1)
```

```
    D1=0; D2=Dmax;
else
    D1=min(D+Dmax/it,D-Dmax/it); D2=max(D+Dmax/it,D-Dmax/it);
    if(v2<=v1);
        D1=max(D1,0); D2=min(D2,9.81);
    else
        D1=max(D1,-9.81); D2=min(D2,0);
    end
end
for v4 = D1:step2:D2;
    if(v4>=0)
        temp = [ones(1,v3)*v1 max(v1 - v4*(0.1:0.1:(length(r)-v3)/10),v2)]';
    else
        temp = [ones(1,v3)*v1 min(v1 - v4*(0.1:0.1:(length(r)-v3)/10),v2)]';
    end
    if(i==1)
        Ecalc = sum((V - temp).^2);
    else
        Ecalc = sum((V - temp).^2);
    end
    if(Ecalc<E)
        E = Ecalc; V0=v1; Vx=v2; Tb=v3; D=v4;
        if(i==1)
            Dl=v4; Tlb=v3/10; Vle=temp';
        else
            Df=v4; Tfb=v3/10; Vfe=temp';
        end
        if(E==0.0);break;end
    end
    if(E==0.0);break;end
end
```

```
        if(E==0.0);break;end
      end
      if(E==0.0);break;end
    end
    if(E==0.0);break;end
  end
  if(E==0.0);break;end
  end
  end
R(min(r):max(r))=R;
R(1:min(r)-1)=NaN;
R(max(r)+1:151)=NaN;
Vl(min(r):max(r))=Vl;
Vl(1:min(r)-1)=NaN;
Vl(max(r)+1:151)=NaN;
Vle(min(r):max(r))=Vle;
Vle(1:min(r)-1)=NaN;
Vle(max(r)+1:151)=NaN;
if(length(Vfe)<151)
 Vfe(min(r2):max(r2))=Vfe;
 Vfe(1:min(r2)-1)=NaN;
 Vfe(max(r2)+1:151)=NaN;
 end

end


% Discard events that have a Tfb< time at which lead vehicle appears
if(flag1==0)
   if(Tfb*10<=min(r) & min(r)>=1)
      flag1=4;
```

```
        end
      if(Tfb*10>max(r) & min(r)>=1)
         flag1=4;
      end
end

% Compute the estimated range for valid events and parameters for non-valid events
if(flag1==0)
  Re(min(r)) = R(min(r));
  for i=min(r)+1:max(r)
    Re(i)=Re(i-1)+(Vle(i-1)-Vfe(i-1))*0.1;
  end
else
   Tfb=NaN; Df=NaN; Vfe=NaN(151,1); Tlb=NaN; Dl=NaN; Vle=NaN(151,1); Re=NaN(151,1);
end
```

APPENDIX D – FILTER BY CONFLICT SEVERITY

The optimized RE events were then screened to identify theoretical RE conflicts. An RE conflict was said to occur when the FV approached an LV in a manner that would result in a crash if one of the vehicles did not change its behavior. RE conflicts were identified using KME filter equations, which are not to be confused with KME0 and KME1 trigger equations. The KME filter equations address two kinematic situations: 1) LV is stopped or traveling at a constant speed (LVS/LVCS), and 2) LV is decelerating (LVD). The derivation of the KME equations is shown below.

Case 1: LVS/LVCS

Assuming that the FV decelerates at a constant rate from its theoretical initial speed ($\hat{V}_{Fo}$) to the theoretical speed of the LV ($\hat{V}_{Lo}$) then the distance traveled during this deceleration maneuver can be computed as:

$$\hat{a} = \hat{V}\frac{d\hat{V}}{dx} \quad \Rightarrow \quad \hat{a}\int_0^{\hat{x}} dx = \int_{\hat{V}_{Fo}}^{\hat{V}_{Lo}} \hat{V}d\hat{V} \quad \Rightarrow \quad -\hat{a}\hat{x} = \frac{\hat{V}_{Fo}^2 - \hat{V}_{Lo}^2}{2} \quad \Rightarrow \quad \hat{x} = \frac{\hat{V}_{Fo}^2 - \hat{V}_{Lo}^2}{-2\hat{a}} = \frac{\hat{V}_{Fo}^2 - \hat{V}_{Lo}^2}{2\hat{d}_F}$$

(36)

Consequently, solving for the deceleration rate in the case of the LVS/LVCS equation for a travel distance equal to the R and considering a lag time (t_R), the deceleration level should be less than the FV deceleration rate threshold ($d_{F,Threshold}$) for a collision to occur as:

$$\hat{d}_F = \frac{\hat{V}_{Fo}^2 - \hat{V}_{Lo}^2}{2(\hat{R}(t_{Fb}) - (\hat{V}_{Fo} - \hat{V}_{Lo})t_R)} > d_{F,Threshold}$$

(37)

Here $\hat{R}(t_{Fb})$ indicates the theoretical range between the two vehicles at the start of the FV deceleration (the distance from the front bumper of the FV to the rear bumper of the LV).

Case 2: LVD

In the case that the LV is decelerating, the distance traveled by the LV during the FV driver's perception-response time (PRT) ($x_{L,R}$) can be computed as:

$$x_{L,R} = \frac{\hat{V}_{Lo}^2 - (\hat{V}_{Lo}^2 - \hat{d}_L t_R)^2}{2\hat{d}_L} = \hat{V}_{Lo}t_R - \frac{\hat{d}_L t_R^2}{2}.$$

(38)

The distance traveled in the same time by the FV can be computed as:

$$x_{F,R} = \hat{V}_{Fo}t_R.$$

(39)

Consequently, the range after the conclusion of the PRT can be estimated as:

$$\hat{R}(t_R) = \hat{R}(t_{Fb}) + x_{L,R} - x_{F,R} = \hat{R}(t_{Fb}) + (\hat{V}_{Lo} - \hat{V}_{Fo})t_R - \frac{\hat{d}_L t_R^2}{2}. \tag{40}$$

In order to ensure that the vehicles do not collide, the position of the LV should always be ahead of the position of the FV. A collision occurs when their positions are equal or when the range equals zero. Consequently, the right-hand side of Equation 40 should be greater than zero and thus the driver response time should satisfy Equation 41 in order to avoid a collision.

$$t_R < \frac{-(\hat{V}_{Fo} - \hat{V}_{Lo}) + \sqrt{(\hat{V}_{Fo} - \hat{V}_{Lo})^2 + 2\hat{d}_L \hat{R}(t_{Fb})}}{\hat{d}_L} \tag{41}$$

In addition to Equation 41, the profiles of the vehicles should be such that they do not intersect over the entire deceleration maneuver. In order to ensure that no collisions occur, the position of the LV when it stops ($x_{L,s}$) can be computed as:

$$x_{L,s} = \hat{R}(t_{Fb}) + \frac{\hat{V}_{Lo}^2}{2\hat{d}_L}. \tag{42}$$

Similarly, the position of the FV when it stops can be computed as:

$$x_{F,s} = \hat{V}_{Fo}t_R + \frac{\hat{V}_{Fo}^2}{2\hat{d}_F}. \tag{43}$$

As was done earlier, in order to avoid a potential collision, Equation 44 must hold.

$$\frac{\hat{V}_{Fo}^2}{2\hat{d}_L} < \frac{\hat{V}_{Lo}^2}{2\hat{d}_L} - \hat{V}_{Fo}t_R + \hat{R}(t_{Fb}) \tag{44}$$

Manipulating Equation 44, the deceleration rate of the FV has to satisfy Equation 45.

$$\hat{d}_F = \frac{\hat{V}_{Fo}^2}{\frac{\hat{V}_{Lo}^2}{\hat{d}_L} - 2\hat{V}_{Fo}t_R + 2\hat{R}(t_{Fb})} > d_{F,Threshold} \tag{45}$$

APPENDIX E – METHODS FOR COMPUTING LAG TIME

A component of the safety benefit evaluation is predicting the number of RE crashes that can be prevented if drivers receive feedback from an FCW system. This estimate is performed by comparing the additional time before braking (increasing t_{Fb}) that results in a crash between the subject and lead vehicle without the FCW system feedback to that after receiving the FCW feedback. This brake lag time that results in a crash is referred to as the lag time.

Lag times were computed using an iterative analytical procedure that computed the time at which a collision occurred. This time was determined by first inputting the time the FV began to brake, t_{Fb}, into the lag time equation and solving it. If the solution was not a real, non-negative number, then the t_{FB} was incremented in steps of 0.01 s until a real non-negative solution was achieved (i.e., a collision occurred). The sum of the incremental time units to the original t_{Fb} was then stored as the lag time for that conflict. If a lag time exceeded 15 s, then a crash was not said to occur and the conflict was discarded. Conflicts with lag times less than 0 s were also discarded.

The estimation of t was computed analytically for each of the three conflict categories, by distinguishing between LVS/LVCS and LVD events.

In the case of LVS/LVCS events, t is computed by tracking the position of both the LV and FV from t_{Fb} onwards until both positions coincide. The position of the LV is computed as $x_L(t) = R + \hat{V}_{Lo}t$ while the position of the FV is computed as $x_F(t) = 0 + \hat{V}_{Fo}t - 0.5d_F t^2$, where t is measured from the instant the FV starts decelerating (t_{Fb}). A crash occurs when $x_L(t) - x_F(t) = 0$, or when $0.5d_F t^2 + \left(\hat{V}_{Fo} - \hat{V}_{Lo}\right)t + R = 0$. Here R is the range at t_{Fb}.

Solving for the t becomes:

$$t = \frac{\left(\hat{V}_{Fo} - \hat{V}_{Lo}\right) \pm \sqrt{\left(\hat{V}_{Fo} - \hat{V}_{Lo}\right)^2 - 2d_F R}}{d_F} \quad . \tag{46}$$

A sample calculation is presented below. Note that the t is increased in increments of 0.1 s for purposes of brevity. The following values are used for this example.

$R_0 = 14.6553$ m, $\hat{V}_{F0} = 30.5278$ m/s, $\hat{V}_{L0} = 29.3289$ m/s, $d_F = 0.25$ m/s^2, $\Delta t = 0.0$ s.

The range (R) is calculated as
$$R = R_0 - \Delta t\left(\hat{V}_{F0} - \hat{V}_{L0}\right) \tag{47}$$

Using equation 47, $R = 14.6553$ m. The quantity under the radical in equation 21 denoted by Q is negative (-5.89032) as shown in Table 30, hence Δt is incremented by 0.1 s and the calculation is repeated until a nonnegative quantity under the radical is obtained. In this example this occurs at $\Delta t = 9.9$ s.

The two solutions of equation 46, denoted by t_1 and t_2 are:

$$t_1 = \frac{\left(\hat{V}_{Fo} - \hat{V}_{Lo}\right) - \sqrt{\left(\hat{V}_{Fo} - \hat{V}_{Lo}\right)^2 - 2d_F R}}{d_F} = 0.358578$$

$$t_2 = \frac{\left(\hat{V}_{Fo} - \hat{V}_{Lo}\right) + \sqrt{\left(\hat{V}_{Fo} - \hat{V}_{Lo}\right)^2 - 2d_F R}}{d_F} = 2.039182$$

The selected t is the minimum of the two solutions. If t is non-negative and not infinity, then lead time is equal to Δt, which in this example is 9.9 s. Otherwise, Δt is incremented and the calculation is repeated until either a valid solution is obtained or Δt becomes 15s.

Table 30. Example Computation of Lag Time

Δt	Q	t_1	t_2	t
0	-5.89032	IMG*	IMG	IMG
0.1	-5.83038	IMG	IMG	IMG
0.2	-5.77044	IMG	IMG	IMG
0.3	-5.71049	IMG	IMG	IMG
0.4	-5.65055	IMG	IMG	IMG
0.5	-5.5906	IMG	IMG	IMG
0.6	-5.53066	IMG	IMG	IMG
⋮	⋮	⋮	⋮	⋮
9.4	-0.25559	IMG	IMG	IMG
9.5	-0.19564	IMG	IMG	IMG
9.6	-0.1357	IMG	IMG	IMG
9.7	-0.07576	IMG	IMG	IMG
9.8	-0.01581	IMG	IMG	IMG
9.9	0.044132	0.358578	2.039182	0.358578
* IMG: Imaginary number.				

In the case of LVD, there are two possible situations. The first situation is when the FV decelerates after the LV ($t_{Fb} \geq t_{Lb}$), while the second situation occurs when the FV decelerates before the LV ($t_{Fb} < t_{Lb}$).

Case 1: FV decelerates after LV ($t_{Fb} \geq t_{Lb}$)
The speed of the LV at t_{Fb} can be computed as $\hat{V}_L = \hat{V}_{Lo} - d_L\left(t_{Fb} - t_{Lb}\right)$. Furthermore, the position of the LV and FV can be computed as
$x_L(t) = R + \hat{V}_L t - 0.5 d_L t^2$, and
$x_F(t) = 0 + \hat{V}_{Fo} t - 0.5 d_F t^2$.

A crash will occurs when $x_L(t) = x_F(t)$ $x_L(t) - x_F(t) = 0$ or when
$0.5(d_F - d_L)t^2 + \left(\hat{V}_L - \hat{V}_{Fo}\right)t + R = 0$.

Solving for t, we can compute the time at which a collision occurs as

$$t = \frac{\left(\hat{V}_{Fo} - \hat{V}_L\right) \pm \sqrt{\left(\hat{V}_{Fo} - \hat{V}_L\right)^2 - 2\left(d_F - d_L\right)R}}{\left(d_F - d_L\right)} \quad . \tag{48}$$

Case 2: FV decelerates before LV ($t_{Fb} < t_{Lb}$)

In solving for the time at which a collision would occur one should consider two potential solutions. The first solution computes t if it is less than the time at which the LV decelerates (i.e., $t \le t_{Lb}\text{-}t_{Fb}$). In this case the solution is identical to the LVS/LVCS solution that was provided in Equation 46. The second solution considers when t occurs after the LV starts decelerating (i.e., $t > t_{Lb}\text{-}t_{Fb}$). In this case we assume $t' = t_{Lb}\text{-}t_{Fb}$ and compute the position of the LV and FV as:

$x_L(t) = R + \hat{V}_{Lo}t' + \hat{V}_{Lo}\left(t - t'\right) - 0.5d_L\left(t - t'\right)^2$, and

$x_F(t) = 0 + \hat{V}_{Fo}t - 0.5d_F t^2$.

A crash will occur when $X_F(t) - x_L(t) = 0$, or when

$0.5(d_F - d_L)t^2 + \left(\hat{V}_{Lo} - \hat{V}_{Fo} + d_L t'\right)t + R - 0.5d_L t'^2 = 0$.

Solving for t we can compute the time at which a collision will occur as:

$$t = \frac{-\left(\hat{V}_{Lo} - \hat{V}_{Fo} + d_L t'\right) \pm \sqrt{\left(\hat{V}_{Lo} - \hat{V}_{Fo} + d_L t'\right)^2 - 2\left(d_F - d_L\right)\left(R - 0.5d_L t'^2\right)}}{\left(d_F - d_L\right)} \tag{49}$$

The solution to Equation 49 is valid if it is real and greater than t'.

An example computation is shown below. The following values are used for this example.

$R_0 = 73.9323$ m, $\hat{V}_{F0} = 22.4597$ m/s, $\hat{V}_{L0} = 17.5220$ m/s, $d_F = 1.00$ m/s^2, $d_L = 1.6667$ m/s^2, $\Delta t = 0.0$ s, $t_{Lb} = 7.1$ s, $t_{Fb} = 5.8$ s.

The quantity under the radical of equation 49, $Q = 103.7192$ m/s.
Calculating, t_1, t_2, and t as explained before we obtain:

$t_1 = 11.1198$ s
$t_2 = -19.4330$ s
$t = 11.1198$ s
$t_{Lb}\text{-}t_{Fb} = 1.3$ s
Note that in this case $t > t_{Lb}\text{-}t_{Fb}$. The lead time in this case is zero.

APPENDIX F – MATLAB CODE FOR CALCULATION OF LAG TIME

```matlab
function [Valid,d]=AddLag4(d)

d(find(abs(d(:,6)-d(:,7))<1.2),9)=0; % Set acceleration equal to zero if speed difference is only 1.2 m/s
d(find(abs(d(:,10)-d(:,11))<1.2),13)=0; % Set acceleration equal to zero if speed difference is only 1.2 m/s
d(find(d(:,9)<0),9)=0; d(find(d(:,13)<0),13)=0; % Set acceleration observations as zero
d(find(d(:,7)<0),7)=0; d(find(d(:,11)<0),11)=0; % Set negative speeds as zero
d=d(find(d(:,9)>0),:); % remove observations where following vehicle does not decelerate
d(:,5)=abs(d(:,5)); % set categories to absolute values

r1=find(d(:,13)>=0 & d(:,13)<=0); % Identify LVCS/LVS events
r2=find(d(:,13)>0); % Identify LVD events

dt=zeros(length(d),1);
tstep=0.01; min_diff=0;

% LVCS/LVS
for i=1:length(r1),
    event=r1(i);
    for ltime=0:tstep:15,
        ttc1=[];ttc2=[];ttc=[];
        R=d(event,14)-ltime*(d(event,6)-d(event,10));
        if((d(event,6)-d(event,10))^2>=2*d(event,9)*R),
            ttc1=(d(event,6)-d(event,10))-sqrt((d(event,6)-d(event,10))^2-2*d(event,9)*R)/d(event,9);
            ttc2=(d(event,6)-d(event,10))+sqrt((d(event,6)-d(event,10))^2-2*d(event,9)*R)/d(event,9);
            if(ttc1<0 & ttc2>0); ttc1=ttc2; end; ttc=min(ttc1,ttc2);
            if(ttc>=0 & ttc<Inf); dt(event)=ltime; break; end
        end
    end
```

```
end

% LVD
for i=1:length(r2),


   event=r2(i);

   R=d(event,14); Tfb=d(event,8); Tlb=d(event,12);
   for ltime=0:tstep:15,
      ttc1=[];ttc2=[];ttc=[];
      Tfb=d(event,8)+ltime;
      if(Tfb>=Tlb) % Following vehicle decelerates after lead vehicle
         Vl=d(event,10)-d(event,13)*(Tfb-Tlb);
         R=R-d(event,6)*tstep+Vl*tstep;
         b1=Vl-d(event,6);
         b2=2*(d(event,9)-d(event,13))*R;
         if(d(event,9)==d(event,13)); dt(event)=-R/b1; break; end
         if(b1^2>=b2),
            d_diff=d(event,9)-d(event,13); if(d_diff==0); d_diff=min_diff; end
            ttc1=(-b1-sqrt(b1^2-b2))/d_diff;
            ttc2=(-b1+sqrt(b1^2-b2))/d_diff;
            if(ttc1<0 & ttc2>0); ttc1=ttc2; end;
            if(ttc1>0 & ttc2<0); ttc2=ttc1; end;
            ttc=min(ttc1,ttc2);
            if(ttc>=0 & ttc<Inf); dt(event)=ltime; break; end
         end
      else% Lead vehicle decelerates after following vehicle
         % Collision occurs before lead starts braking
         Vl=d(event,10);%Vl0
         R=R-d(event,6)*tstep+Vl*tstep;%R(i)=R(i-1)-Vf0*tstep+Vl*tstep
```

```
        b1=d(event,10)-d(event,6); %b1=Vl0-Vf0
        b2=2*R*d(event,9);%b2=2*R*Df
        if(b1^2>=b2),
           ttc1=(-b1-sqrt(b1^2-b2))/d(event,9);
           ttc2=(-b1+sqrt(b1^2-b2))/d(event,9);
           if(ttc1<0 & ttc2>0); ttc1=ttc2; end; ttc=min(ttc1,ttc2);
           if(ttc>=0 & ttc<=(Tlb-Tfb)); break; end
        end
        % Collision occurs after lead starts braking
         b1=d(event,10)-d(event,6)+d(event,13)*(Tlb-Tfb);
         b2=2*(d(event,9)-d(event,13))*(R-0.5*d(event,13)*(Tlb-Tfb)^2);

        if(d(event,9)==d(event,13)); dt(event)=-(R-d(event,6)*Tfb-0.5*d(event,13)*Tlb^2)/b1; break; end
        if(b1^2>=b2),
           d_diff=d(event,9)-d(event,13); if(d_diff==0); d_diff=min_diff; end
           ttc1=(-b1-sqrt(b1^2-b2))/d_diff;
           ttc2=(-b1+sqrt(b1^2-b2))/d_diff;
           if(ttc1<(Tlb-Tfb) & ttc2>(Tlb-Tfb)); ttc1=ttc2; end;
           if(ttc1>(Tlb-Tfb) & ttc2<(Tlb-Tfb)); ttc2=ttc1; end;
           ttc=min(ttc1,ttc2);
           if(ttc>=0 & ttc<Inf & ttc>(Tlb-Tfb)); dt(event)=ltime; break; end
        end
     end
  end
  dt(event)=ltime;
end
d(:,18)=dt;
Valid=find(dt>0&dt<15);
```

APPENDIX G – MODIFICATIONS TO VOLVO AND BATTELLE METHODS

Table 31. Modifications to Volvo (2005) and Battelle (2006) Methods

Procedure	Current Study	Volvo (2005) and Battelle (2006)
Trigger RE Events	• Identified trigger time point (and resolved issues pertaining to multiple targets simultaneously tracked) by tracking the target-of-interest across multiple VORAD data streams	• Used data from first VORAD data stream
Filter RE Events	• Short presence target filter threshold set to 4 s for both stationary and moving targets • Out-of-lane target filter encompassed both stationary and moving vehicles • Combined deceleration level with brake pedal input for driver reaction filter • Lane change driver reaction filter identified both smooth and aggressive lanes changes	• Short presence target filter threshold set to 1 s for stationary targets and 2 s for moving targets (Volvo (2005), page 29) • Out-of-lane target filter encompassed only stationary vehicles (Volvo (2005), page 30) • Deceleration level and brake pedal input considered separately for driver reaction filter (Volvo (2005), page 30) • Lane change driver reaction filter identified smooth lanes changes (Volvo (2005), Lane Change Algorithm Logic)

Additional Filtration	• Removed RE events in which:
	  ○ Target was oncoming
	  ○ LV in the same lane as FV less than 4 seconds
	  ○ FV accelerated
	  ○ FV decelerated before LV appeared
	  ○ Difference between FV max and min speed < 1.2 m/s.
	  ○ LV out of lane and no lane changes occurred	

Conflict Identification	• KME filter equation used: $$\hat{d}_F = \frac{\hat{V}_{Fo}^2 - \hat{V}_{Lo}^2}{2(\hat{R}(t_{Fb}) - (\hat{V}_{Fo} - \hat{V}_{Lo})t_R)} > d_{F,Threshold}$$	• KME filter equation used: $$\frac{(v_F - v_L)^2}{2(R - (v_F - v_L)t_{R,Threshold})} < a_{F,Threshold}$$

		(Battelle [2006], page 4-24)
Perform Lag Process	• Combination of numerical and analytical solution. Lag time computed by incrementing t from t_{Fb} onwards in steps of 0.01 s until a real non-negative value was obtained. The t associated with this real non-negative solution was set to be the lag time.	• Determine position of FV and LV. Numerically increased lag time by one frame and simulate lead and following vehicle profiles to determine if a crash occurs. Repeat computations until a crash occurs (Battelle (2006), page 4-33)

Alt Text for *Safety Benefit Evaluation of a Forward Collision Warning System Final Report*

Cover Figure. Photo. The photo depicts an impending rear-end collision between a tractor-trailer and passenger vehicle. The photo shows the driver's view from the driver's seat of a tractor-trailer. The rear of the passenger vehicle in front of the tractor-trailer is visible in the same lane just ahead of the tractor-trailer. The reflection of the passenger vehicle is visible on the hood of the truck. Both vehicles are in the right lane of an undivided two-way road with double lines separating lanes. The A-pillar is visible along with a partial section of the steering wheel. End of Cover Figure.

Figure ES-1. Data flow for safety benefits analysis. Flow chart. This flow chart helps depict the process in which existing drowsy driver data is analyzed and interpreted. There are eight different tasks listed in the flowchart, with specific steps listed under each task. The tasks, starting from top-left and going to bottom-right, are as follows: "Audit DDWS Data," "Optimize Events," "Classify Events," "Validate FCW Algorithms," "Perform Lag Process Without FCW Effects Applied," "Apply FCW Effects," "Perform Lag Process With FCW Effects Applied," and "Determine Safety Benefits". Exact steps and processes are linked together with blue arrowed lines. The overall flow of this chart starts from the "Drowsy Driver FOT Data" box in the top-left and ends at the "GES Database" box, located in the bottom-right. End of Figure ES-1.

Figure ES-2. Venn diagram showing the number of conflicts that coincide between the current study and those identified in the DDWS FOT data reduction. Venn Diagram. This Venn diagram compares data reduction results for the current study and compares them to DDWS FOT visual data reduction. The current study resulted in 1,030 rear-end conflicts. The DDWS FOT visual data reduction process resulted in 596 rear-end conflicts. These 596 conflicts consisted of 1 crash, 26 near crashes, and 569 crash relevant conflicts. There were a total of seven similar rear-end conflicts determined by both the current study and DDWS FOT visual data reduction, all of which were crash relevant conflicts. End of Figure ES-2.

Figure 1. Encased computer and external hard drive installed under the passenger's seat. Photo. The side profile of the passenger seat of a truck is visible with the seat facing right, toward the windshield. The encased computer and external hard drive are installed underneath it. The encasement for the computer is black. The external hard drive and other components are affixed to the top of the encased computer. Together, the centered encased computer and external hard drive usurp approximately 75 percent of the area underneath the passenger seat. Also visible are wires from the device curling from behind the passenger seat towards the passenger side door, where they are tucked underneath the floor board. End of Figure 1.

Figure 2. Camera directions used in DDWS FOT. Diagram. This is a schematic top view of a truck. The areas covered by the four video cameras mounted on the truck are illustrated. Camera 1 points at the drivers face. Camera 2 points down the forward roadway. Cameras 3 is mounted on the left side of the truck near the front-left fender. It points straight back, covering the area to the left of the truck. Camera 4 is mounted in a similar fashion on the front-right of the truck. No cameras were mounted on the back of the trailer, leaving a blind spot in this area. It should be noted, however, that vehicles in the distant rear were captured by cameras 3 and 4. End of Figure 2.

Figure 3. Split-screen presentation of the four camera views. Photo. The photo shows the recorded images of the 4 cameras arranged in a 2 by 2 matrix to form a single image. The top left image shows the driver's face and upper torso. This view includes the driver's entire face, neck and shoulders. The driver appears to be alert and squinting slightly. The top right image shows the driver's view of the forward road scene, which is an undivided, two-way road. The bottom-right image shows the rearward view from the driver's side of the tractor which pictures a partial strip of the roadway in view, the roadside, surrounding environment, and partial road behind the truck. The bottom left image shows the rearward view from the passenger's side of the tractor which shows the shoulder, the roadside, the surrounding environment, and partial lane behind the truck. End Figure 3.

Figure 4. Data flow for safety benefit analysis. Flow chart. This flow chart helps depict the process in which existing drowsy driver data is analyzed and interpreted. There are eight different tasks listed in the flowchart, with specific steps listed under each task. The tasks, starting from top-left and going to bottom-right, are as follows: "Audit DDWS Data," "Optimize Events," "Classify Events," "Validate FCW Algorithms," "Perform Lag Process Without FCW Effects Applied," "Apply FCW Effects," "Perform Lag Process With FCW Effects Applied," and "Determine Safety Benefits". Exact steps and processes are linked together with blue arrowed lines. The overall flow of this chart starts from the "Drowsy Driver FOT Data" box in the top-left and ends at the "GES Database" box, located in the bottom-right. This is the same figure as Figure ES-1. End of Figure 4.

Figure 5. Example of trigger hierarchy. This figure shows the hierarchy of the three types of triggers: KME, TTC, and FI, as a function of time. The triggers are listed on the y-axis, and time is on the x-axis. The axes are unitless and are present to show the relationship of the triggers as time passes. The graph shows that KME triggers have the highest importance, followed by TTC, and then FI. It also shows the lower priority TTC and FI triggers being deleted if overlapped by a higher priority KME trigger. End of Figure 5.

Figure 6. Example of a short-presence target: Eaton VORAD detecting an overhanging street sign. Diagram. This diagram shows VORAD's detection capabilities when a vehicle is approaching an overhanging street sign. The diagram is a computer-generated bird's eye view image of a tractor-trailer in the right lane of a two-lane highway, travelling from left to right. The two lanes are separated by a dotted yellow line. The trailer is approaching an overhanging street sign located above the highway directly in front of the vehicle. The sign hangs over both highway lanes and is mounted at both shoulders. The area covered by VORAD is represented in the shape of a triangle. The area tracked by VORAD extends from the center front of the truck represented by the pointed and narrow end of the triangle. The base end of the triangle contains the overhead street sign. The triangle containing the street sign is an example of VORAD detecting the sign as a possible conflict. This scenario is an example of an uneventful trigger since the street sign was picked up by VORAD for a very short period of time. End of Figure 6.

Figure 7. Examples of an out-of-lane target or oncoming target on a curve being interpreted as threatening by VORAD. Two diagrams. The diagrams show VORAD's detection capabilities. Both diagrams show computer-generated images of a tractor trailer in the right lane approaching a curve that bends towards the right. On this curve is an oncoming automobile in the adjacent lane.   The first diagram shows a tractor-trailer traveling straight and its VORAD detecting the oncoming vehicle. This is an example of how a VORAD target can be non-threatening when the FV is travelling straight. In the second diagram, the FV is in the curve and its VORAD is detecting the oncoming vehicle. This is an example of how a VORAD target can be non-threatening when the FV is in a curve. End of Figure 7.

Figure 8. Example of out-of-lane targets: a parked vehicle on the right shoulder and an oncoming vehicle in the opposing lane. Diagram. This diagram shows VORAD's detection capabilities when a vehicle is approaching both an oncoming vehicle in an opposing lane and a vehicle parked on the right shoulder. Similar to Figure 6, this is a computer generated bird's eye view of a tractor-trailer travelling from left to right on a two lane road. The two lanes are separated by a yellow dashed line. The area covered by VORAD is represented in the shape of a triangle. The area tracked by VORAD extends from the center front of the trailer represented by the pointed and narrow end of the triangle. The base end of the triangle contains two white vehicles; one in the opposing lane, and one on the right shoulder. The vehicle in the opposing lane is travelling from right to left, and the vehicle on the right shoulder is parked, facing right. The yellow triangle that contains both vehicles signifies that the VORAD system has detected both vehicles as possible conflicts. End of Figure 8.

Figure 9. Example of a crossing-lane target: a vehicle passing through and intersection. Diagram. This diagram shows VORAD's detection capabilities when a vehicle is passing through an intersection which a tractor-trailer is about to enter. In the figure, a tractor-trailer, travelling left to right, is approaching an intersection in which a vehicle is passing through. The vehicle is travelling from the bottom of the diagram to the top, and is expected to clear the intersection by the time the tractor-trailer gets there. The right-of-way at the intersection is given to the lanes running horizontally along the diagram, while the lanes running vertically are required to stop before passing through. The area covered by VORAD is represented in the shape of a triangle. The area tracked by VORAD extends from the center front of the trailer represented by the pointed and narrow end of the triangle. The base end of the triangle covers the vehicle as it passes through the intersection. This scenario is an example of the crossing-lane target filter End of Figure 9.

Figure 10. Illustration of a truck performing a reasonable lateral acceleration. If the required lateral acceleration was computed to be unreasonable, then the event was non-threatening. Diagram. This diagram shows VORAD's detection capabilities when a tractor-trailer is beginning to pass a lead vehicle, which is a white car. The lead vehicle is travelling in the right lane of a two-lane highway. The trailer is in the process of switching lanes from the right lane to the left in an attempt to pass the lead vehicle. The area covered by VORAD is represented in the shape of a yellow triangle. The area tracked by VORAD extends from the center front of the trailer represented by the pointed and narrow end of the triangle. The base end of the triangle contains the lead vehicle. A red arrow is visible inside the triangle representing the trailer's intended path. The objective of the diagram is to show an example of acceptable lateral acceleration as it passes the lead vehicle. End of Figure 10.

Figure 11. Example of the Eaton VORAD detecting an overhanging bridge. This triggered event would be filtered out since the driver does not react to it. Diagram. This diagram shows VORAD's detection capabilities when a tractor-trailer is approaching an overhanging bridge. The trailer is travelling from left to right in the right lane of a two lane highway. An overhanging bridge is present in front of the trailer. The bridge is a two lane highway running from the bottom of the diagram to the top. The lanes in the bridge are separated by a white dotted line. The area covered by VORAD is represented in the shape of a yellow triangle. The area tracked by VORAD extends from the center front of the trailer represented by the pointed and narrow end of the triangle. The base end of the triangle contains the overhanging bridge. This diagram provides a visual example of VORAD detecting an overhanging bridge, which will be filtered out. End of Figure 11.

Figure 12. Example of a receding target: a vehicle closely merging in front of the truck as it accelerates away. Diagram. This diagram shows VOARD's detection capabilities when a white passenger vehicle has recently passed a tractor-trailer, and is accelerating away. The vehicle is an example of a receding target. Both vehicles in the diagram are travelling from left to right on a two lane highway. The two lanes are separated by a dotted white line. The lead vehicle passed the trailer in the left lane, and has just merged back into the right lane. The area covered by VORAD is represented in the shape of a yellow triangle. The area tracked by VORAD extends from the center front of the trailer represented by the pointed and narrow end of the triangle. The base end of the triangle intersects with the rear-end of the passenger vehicle. A red arrow is present to signify the path of the lead vehicle as it passed the trailer. This diagram gives a visual example of a receding target as it accelerates away from the trailer. End of Figure 12.

Figure 13. Example illustration of optimized LV and FV profiles. Two Line graphs. This is a set of two line graphs aligned vertically; top and bottom. The top graph shows a plot of Time, in seconds, on the x-axis, and Speed, in meters per second, on the y-axis. The range on the x axis is -10 to 5 seconds in increments of 5. The range on the y-axis is 15 to 30 seconds in increments of 5. There are a total of four lines on the top graph: a thin solid line, a thin dotted line, a thick solid line, and a thick dotted line. The graph key indicates that the thin solid line represents "F Optimized," the thin dotted line represents "F. Smooth," the thick solid line represents "L. Optimized," and the thick dotted line represents "L. Smooth". Both thin lines start at Time = -10 seconds and Speed approximately 29 meters per second. The speed remains constant until Time = 0 seconds, then linearly decreases to 20 meters per second until Time = 4 seconds; speed then remains constant until Time = 5 seconds. Both thick lines start at Time = -10 seconds and Speed approximately 27 meters per second. The speed remains constant until Time = -3 seconds, then linearly decreases to approximately 17 meters per second until Time = 3 seconds; speed then remains constant until Time = 5 seconds. The bottom graph shows a plot of Time, in seconds, on the x-axis and Range in meters on the y-axis. The range on the x-axis is -10 seconds to 5 seconds in increments of 5. The range on the y-axis is 20 meters to 100 meters in increments of 20. Two lines, one solid and the other dotted, exist on the graph. The solid line represents optimized range. The dotted line represents smoothed range and tends to follow the optimized line. Both lines begin at Range approximately 82 meters and Time = -10 seconds. Range decreases somewhat linearly as a function of time throughout the graph. An initial decrease results in a convex curve, while another decrease results in a concave curve. End of Figure 8.

Figure 14. Example illustration of two conflict scenarios (LV shown as a thin line, while the FV is shown as a thick line). Two Line graphs. This is a set of two line graphs aligned vertically; top and bottom. The graphs show a plot of Time, in seconds, on the x-axis and Position, represented by x, on the y-axis. The x-axis range on both graphs is 0 to 16 seconds in increments of 2, and the y-axis range on both graphs is 0 to 120 in increments of 20. Both graphs have two lines each: a thin blue line representing the lead vehicle, and a thick red line representing the following vehicle. The top graph depicts a collision between the two vehicles, while the bottom graph shows a near miss. The two lines in this graph intersect at Time approximately = 8 seconds, meaning that there was some type of collision involving the two vehicles at this time. The bottom graph depicts a very similar plot as the first, except that the two lines come close together but never intersect; representing a near miss. End of Figure 9.

Figure 15. Illustration of lag times computed with and without the FCW system. Temporal Graph with time along the x-axis. A crash is denoted at the end of the graph on the right. The y-axis presents three categories: 1) driver behavior with the FCW system 2) driver behavior without the FCW system, and 3) driver last second behavior prior to a crash. For each of the three categories, the PRT and time required

to decelerate the vehicle are grouped. The time grouping for category 1 (FCW driver behavior) shows the events taking place much earlier than the occurrence of the crash. The time grouping for category 2 (Non-FCW driver behavior) shows the events taking place just before the occurrence of the crash. The time grouping for category 3 (last second driver behavior) shows the events taking place at the crash. The elapsed time, or lag time, from group 1 to group 3, as well as the elapsed time from group 2 to group 3, is shown. The additional lag time, which is the time from the onset of braking for group 1 to the onset of braking for group 2, is also shown. End of Figure 15.

Figure 16. Example illustration of driver PRT and deceleration distribution for Alarm 6. Three Line graphs. This is a set of three line graphs, aligned vertically. The objective of these graphs is to represent deceleration rate as a function of Perceived Response Time (PRT) for an alarm level of 6. The graphs show the cumulative distribution function (CDF) of PRT, in seconds, the CDF of deceleration rate, g, and deceleration rate (g) as a function of PRT, in seconds, from top to bottom, respectively. The top graph's x-axis (PRT) ranges from 0 to 15 s in increments of 5 seconds, while the y-axis (CDF) ranges from 0 to 1 in increments of 0.5. The red line showing this relationship starts at 0 and increases in a concave manner until the CDF reaches 1 at approximately time = 10 seconds. The middle graph shows the CDF of deceleration rate. The y-axis (CDF) is identical to that of the top graph, and the range of the x-axis (deceleration) is 0.02 g to 0.18 g in increments of 0.02 g. The red line depicting this function increases in a concave manner until the CDF reaches 1, a similar trend to the top graph. The bottom graph shows the relationship between PRT (in seconds), and deceleration rate (in gravitational constant, g). The y-axis (deceleration rate) range is 0 g to 0.2 g in increments of 0.05 g, while the x-axis (PRT) range is 0 s to 9 s in increments of 1 s. This graph is a combination of a scatter plot and line graph. Several blue dots are plotted on the graph as observed from the Volvo FOT data. The solid red line represents a line of best fit for the blue dots, which is linear and increases at a constant rate. End of Figure 16.

Figure 17. Example illustration of driver PRT and deceleration distribution for Alarm 10. Three line graphs. This is a set of three line graphs, aligned vertically. The objective of these graphs is to represent deceleration rate as a function of PRT for an alarm level of 10. The top graph shows the CDF of Perceived Response Time, PRT, in seconds. The middle graph shows the CDF of deceleration rate, in gravitational constant, g. The bottom graph shows the deceleration rate, in g, as a function of PRT, in seconds. The top graph's x-axis (PRT) ranges from 0 to 12 in increments of 2. The graph's y-axis (CDF) ranges from 0 s to 1 s in increments of 0.5 s. The red line showing this relationship starts at [0, 0] and increases in a concave manner until the CDF reaches 1 at approximately t = 7 s. The middle graph shows the CDF of the deceleration rate. The y-axis (CDF) is identical to that of the top graph, and the range of the x-axis (deceleration) ranges from 0 g to 1 g in increments of 0.1 g. The red line depicting this function begins at [0,0] and increases in a concave manner until the CDF reaches 1, a similar trend to the top graph. The bottom graph shows the relationship between PRT, in seconds, and deceleration rate, in gravitational constant, g. The y-axis (deceleration rate) range is from 0 g to 0.2 g with increments of 0.05 g, while the x-axis (PRT) ranges from 0 s to 8 s in increments of 1 s. This graph is a combination of a scatter plot and line graph. Several blue dots are plotted on the graph as observed from the Volvo FOT data. The solid red line represents a line of best fit for the blue dots. The line of best fit in this case is a horizontal line with slope = 0 at deceleration rate approximately = 0.06 g throughout the entire time interval. End of Figure 17.

Figure 18. Relationship between deceleration rate and PRT for Alarms 6, 8, and 9. Line graph. This line graph shows PRT, in seconds, on the x-axis and deceleration rate, in meters per second squared, on the y-axis. The x-axis runs from 0 s to 10 s in increments of 1 s. The y-axis ranges from 0.0 to 3.5 meters per second squared in increments of 0.5. Three lines are present on the graph. A solid blue line represents

alarm 6, a red dotted line represents alarm 9, and a green dotted line represents alarm 8. All three lines start at [0,0] and increase linearly at different rates. The green line (alarm 8) increases at the highest rate, followed by the red line (alarm 9), and the blue line (alarm 6), respectively. The green line increases linearly until it reaches an end point of PRT = 10 seconds, deceleration approximately = 3.1 meters per second squared. The red line reaches an end point of PRT = 10 seconds, deceleration approximately = 2.35 meters per second squared. The blue line reaches an end point of PRT = 10 seconds, deceleration approximately = 1.0 meters per second squared. In summary, the graph shows that alarm 8 results in the highest deceleration rate, while alarm 6 results in the lowest. End of Figure 18.

Figure 19. Overview of the number of conflicts that remained after data manipulation was performed. Flow chart. This flow chart provides an overview of the results chapter by showing the number of conflicts that remained after each of the steps described in the methods chapter. Originally, there were 10,979,885 triggers. These reduced to 4,500,864 triggers after the trigger hierarchy and follow-on restrictions were applied. The filters were then applied to these triggers, leaving 76,546 RE events in Subset 1. Owing to the high rate of non-threatening triggered events, additional filtration was performed. This included removing events in which (1) target was oncoming, (2) LV was in the same lane as the FV for less than or equal to 4 s, (3) FV accelerated, (4) FV decelerated before the LV, (5) the difference between the FV's maximum and minimum speed was less than or equal to 1.2 m/s, and (6) the LV was outside of the FV's lane. A total of 24,605 events remained after this additional filtration. The KME filters were then applied to these events, leaving 7,155 events in Subset 2. These conflicts were then classified. Those that did not meet the classification scheme were discarded, leaving 6,456 conflicts in subset 3. The FCW algorithms were then applied, leaving 6,274 conflicts. The lag process was performed. Conflicts with lag times less than 0 s or greater than 15 s were discarded. A total of 1,030 conflicts remained after the lag process was performed on the conflicts that did not have the FCW system effects applied. This comprised Subset 5. The conflicts with the FCW effects applied comprised Subset 6A. The lag process was applied to Subset 6A, leaving 1,026 conflicts in Subset 6B after those conflicts with lag times less than 0 s or greater than 15 s were removed. End of Figure 19.

Figure 20. Breakdown of final events by five conflict types. Bar chart. Figure 20 shows a breakdown of the 1,030 events by each of the five conflict types. There were 470 conflicts in the "Constant Velocity" category. There were 296 conflicts in the "Both Vehicles Decelerating" category. There were 25 conflicts in the "Lane Change" category. There were three conflicts in the "Stopped LV" category. There were 250 conflicts in the "Decelerating LV" category. End of Figure 20.

Figure 21. Breakdown of final events by three conflict categories. Bar Chart. Figure 21 groups the conflicts into the three conflict categories. There were 720 conflicts in the "Constant Velocity" category. There were 299 conflicts in the "Decelerating" category. There were 25 conflicts in the "Lane Change" category. End of Figure 21.

Figure 22. Proportion of the different conflict categories in GES, the final dataset, and Battelle (2006). Pie Chart. Figure 22 shows three pie charts that compare the proportion of conflicts in the final dataset to the proportions observed in GES and the Battelle (2006) study. Compared to GES, the final dataset is similar in that it also had 2 percent of the conflicts fall into Category 3 (FV lane change). However, there was a higher proportion in Category 1 (FV constant speed) in the final dataset (69 percent) compared to 47 percent in GES. Comparing the final dataset to Battelle (2006), the proportion of conflicts in Category 3 was also similar (4% fell into Category 3 in Battelle (2006)). However, there was a higher proportion in

Category 1 (FV constant speed) in the final dataset (69 percent) compared to 44 percent in Battelle (2006). End of Figure 22.

Figure 23. Lag time distribution for conflicts with and without the FCW system. Histogram. Figure 23 shows the distribution of lag times for conflicts with and without the FCW system through two histograms. The top histogram bins the lag times observed without the FCW system. The distribution is skewed to the left, with the mean centered on 4.75 s. The bottom histogram bins the lag times observed with the FCW system. The distribution is also skewed to the left, but not as much. Although the average was 6.18 s, the frequency counts in the bins from 2 to 7 seconds indicated that these lag times were equally likely. Comparing the two histograms, the shift in the lag time to the right (increase in the lag time) as a result of the introduction of the FCW system can be observed. End of Figure 23.

Figure 24. Venn diagram showing the number of conflicts that coincide between the current study and those identified in the DDWS FOT data reduction. Venn Diagram. This Venn diagram compares data reduction results for the current study and compares them to DDWS FOT visual data reduction. The current study resulted in 1,030 rear-end conflicts. The DDWS FOT visual data reduction process resulted in 596 rear-end conflicts. These 596 conflicts consisted of 1 crash, 26 near crashes, and 569 crash relevant conflicts. There were a total of seven similar rear-end conflicts determined by both the current study and DDWS FOT visual data reduction, all of which were crash-relevant conflicts. End of Figure 24.

Figure 25. Algorithm for KME0 (Taken from Volvo (2005)). Flow chart. Shows the process and steps to take in order to determine if a KME0 trigger event has occurred. The flow chart contains a total of three decision diamonds, and two calculation rectangles. The first step, located on the top-left of the flow chart, is to determine if the lead vehicle is at constant speed. If the lead vehicle acceleration is less than or equal to 0.25 feet per second squared, then the answer is yes and the flowchart flows down to calculate following vehicle acceleration. If the condition is false and the lead vehicle speed is not constant, then the flowchart flows to the right, reaching an additional decision diamond to see if the lead vehicle is decelerating. To test this, the acceleration of the lead vehicle must be less than -0.25 feet per second squared. If this condition is true, the flowchart flows down to calculate the following vehicle acceleration. If the condition is false, then there is no KME0 Trigger. At this point, depending on the first two decisions, the following vehicle required deceleration is calculated. The final decision for this flow chart is to determine whether or not the following vehicle required deceleration is less than -8 feet per second squared. If this condition is true, then a KME0 trigger exists; however if it is false, then no KME0 trigger exists. End of Figure 25.

Figure 26. Algorithm for KME1. (Taken from Volvo [2005]). Flow chart. This flowchart shows the process and steps to take in order to determine if a KME1 trigger event has occurred. The flowchart contains a total of two decision diamonds and two calculation boxes. The first step is a decision diamond to determine if the lead vehicle acceleration is greater than the given threshold. If the lead vehicle acceleration is greater than -6.4 feet per second squared, then the following vehicle required deceleration is calculated using the LVCS formula. If the condition is false, then the following vehicle required deceleration is calculated using the LVD formula. Once this acceleration has been calculated, the next decision box decides whether or not the following vehicle required deceleration is greater than the maximum following vehicle deceleration. If the calculated acceleration is less than -8 feet per second squared, then a KME1 trigger exists. If it is greater than this number, then no KME1 trigger is present. End of Figure 26.